SM-46429

FLOW SEPARATION IN HIGH SPEED FLIGHT

A REVIEW OF THE STATE-OF-THE-ART

MISSILE & SPACE SYSTEMS DIVISION
DOUGLAS AIRCRAFT COMPANY, INC.
SANTA MONICA CALIFORNIA

DOUGLAS

FLOW SEPARATION IN HIGH SPEED FLIGHT

A REVIEW OF THE STATE-OF-THE-ART

DOUGLAS REPORT SM-46429
APRIL 1965

PREPARED BY: J.E. WUERER
THOR AERO/THERMODYNAMICS SECTION

PREPARED BY: F.I. CLAYTON
THOR AERO/THERMODYNAMICS SECTION

PREPARED FOR GENERAL USE AS A
NON-CONTRACTURAL REQUIREMENT

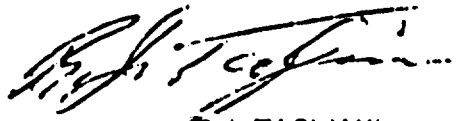

APPROVED BY: R.J. TAGLIANI
CHIEF, AERO/THERMODYNAMICS BRANCH
FLIGHT MECHANICS DEPARTMENT

DOUGLAS MISSILE & SPACE SYSTEMS DIVISION

ABSTRACT

A physical explanation is given of the two types of flow separation classified herein as boundary layer separation and breakaway separation. A short discussion of the fluid dynamic complexity of the problem is presented. Such characteristics of separated flows as the pertinent descriptive parameters, state of flow, length of separated region, compression process, flow steadiness, and three-dimensional effects are discussed. The effects of flow separation on the pressure, skin friction and heat transfer distribution are described, and a review of semi-empirical methods for calculating the critical overall pressure rise, the geometry of the separated region, and the heat transfer at reattachment is presented.

DESCRIPTORS

1. Boundary Layer
2. Separation
3. Reattachment
4. Pressure
5. Heat Transfer
6. Skin Friction
7. Flow
8. Supersonic

ACKNOWLEDGMENT

The authors would like to express their gratitude to D. E. Lapedes for his thought provoking suggestions concerning the technical content and his comments on organizing the material in this report.

TABLE OF CONTENTS

TABLE OF CONTENTS (Continued)

TABLE OF CONTENTS (Continued)

LIST OF FIGURES

LIST OF FIGURES (Continued)

NOMENCLATURE

SYMBOL	DEFINITION	UNITS
C_f	Skin friction coefficient	N.D.[a]
C_p	Pressure coefficient	N.D.
h	Heat transfer coefficient	BTU/ft^2-sec-$^\circ$R
H	Step height or cavity depth	Inches
K, Q, N	Constants	N.D.
	Length	Inches
L	Cavity length	Inches
M	Mach number	N.D.
p	Pressure	Lb/in^2
Δp	Pressure difference	Lb/in^2
u	Velocity	Ft/sec
u_*	Velocity ratio $\frac{u}{u_e}$ along the dividing streamline	N.D.
R	Reattachment point	N.D.
R_D	Reynolds number based on diameter	N.D.
R/	Unit Reynolds number	Ft^{-1}
R_x	Reynolds number based on running length x	N.D.
R_y	Reynolds number based on coordinate y	N.D.
S	Separation Point	N.D.
St	Stanton number	N.D.
T	Temperature	$^\circ$R
TR	Onset of transition	N.D.
x	Coordinate parallel to surface and flow direction	Inches
y	Coordinate perpendicular to surface	Inches
z	Coordinate parallel to surface and perpendicular to flow direction	Inches
α	Flow deflection angle	Degrees
γ	Ratio of specific heats	N.D.
δ	Boundary layer thickness	Inches
δ^*	Boundary layer displacement thickness	Inches
δ_s	Mixing or free shear layer thickness	Inches
θ	Wall deflection angle	Degrees

a Non-dimensional

NOMENCLATURE (Continued)

SYMBOL	DEFINITIONS	UNITS
ρ	Density	Lb_m/ft^3
τ	Shear stress	Lb/in^2
μ	Absolute viscosity	$Lb\text{-}sec/ft^2$

SUBSCRIPTS

f	Final
o	Just prior to pressure rise
w	Wall conditions
e	Conditions at edge of boundary layer
p or plat	Plateau value
crit	Critical value
sep	Value at separation or throughout separated region (for heat transfer)
pk	Peak value
max	Maximum value
∞	Free stream conditions
1	Conditions after incident shock
2	Conditions after reflected shock
ref	Reference conditions
lam	Laminar
turb	Turbulent
t	Total conditions
r	Recovery conditions
b	Base conditions
f.p.	Flat plate value
D	Diameter
exp	Experimental value

SUPERSCRIPTS

'	Values downstream of recompression
-	Mean value

FLOW SEPARATION IN HIGH SPEED FLIGHT

1. INTRODUCTION

Flow separation is a phenomenon which has hindered or limited the development of many devices which depend upon the dynamics of fluids for successful operation. This problem has been particularly significant to the aircraft and aerospace industries. In low speed flight the principal effect of flow separation is to cause drastic changes in vehicle flight characteristics, due to the sudden modification of the pressure distribution. High speed supersonic flight has posed certain new problems associated with separation. Not only does the possibility of undesirable shifts in aerodynamic loading exist, but large local increases in aerodynamic heating have been noted in regions of flow reattachment. In addition, self induced fluctuations in pressure due to unstable flow may occur.

This report is the result of an effort to review the present state of the art concerning the effects of flow separation on both the general flow field structure and on aerodynamic heating. However, before considering these specific areas, it is helpful, if not necessary, to understand certain basic characteristics of separated flows. First, a qualitative description of the flow in separated regions is given and the influences of certain parameters are discussed. Secondly, those aspects of the flow thought to be critical specifically to the problem of aerodynamic heating are defined. The present discussion is appropriately limited to the case of high speed (supersonic and hypersonic) flow, since most critical problems are limited to this regime.

The plan of this report is as follows. First, in section 2, the conditions under which a flow may separate and the sequence of events leading to separation are defined in terms of fundamental flow properties, such as the distribution of momentum in the boundary layer, pressure gradients, and wall shear. The discussion is extended to briefly cover pertinent analytical ideas. Next, the general physical characteristics of separated flows are outlined in section 3. These introductory

concepts lay the groundwork for the major discussion which is divided into three parts, namely: (1) pressure distribution, which is interrelated with the overall geometry of the separated flow region, in section 4; (2) skin friction, in section 5; and (3) heat transfer distribution, in section 6. A summary of the important features of separated flows and conclusive remarks are made in section 7.

2. FLOW SEPARATION PHENOMENON

We may define two broad classes of conditions under which flow separation may be initiated. The first class is associated with the separation of a boundary layer flowing against an adverse pressure gradient. This case has been studied in some detail and the conditions necessary for its occurrence are fairly well understood, at least for two-dimensional and axisymmetric configurations. This case shall be termed, for the purposes of the present discussion, "boundary layer separation". The second class of separation is associated with flows past bluff bodies and sharp convex corners. Here, the flow may separate even though the streamwise pressure gradient is favorable. This flow shall be called "breakaway separation". Less is understood about the mechanism underlying this latter type of flow; however, it is an important problem since it may occur with conventional aerodynamic shapes. Because of the somewhat different conditions giving rise to these two classes of flows they will be discussed independently.

2.1 Boundary Layer Separation

Separation of a two-dimensional boundary layer has been studied ever since it was first explained by Prandtl[1*] in 1904. At present, the underlying principles of the phenomena may be supposed known. On the other hand, it is only quite recently that general three-dimensional separation has been seriously investigated. Much less is known about the criterion necessary for its occurrence.

2.1.1 Two-Dimensional Separation

2.1.1.1 Two-Dimensional Separation - Physical Phenomena

If we consider the two-dimensional flow of a viscous fluid over a body, the fluid near the surface (the boundary layer) is retarded owing to skin friction effects. The velocity of the fluid in the boundary layer varies from zero at the wall to approximately the inviscid value at the outer edge. If no other forces are acting to further retard this flow,

---

* Superscripts denote references listed in Section 8.

the slope of the velocity profile $\frac{\partial u}{\partial y}$ is positive at the wall and gradually approaches zero at the edge of the boundary layer, as illustrated in figure 1-a. However, if in addition to wall shear, the flow encounters an upstream directed force, the flow is further impeded. If the kinetic energy of the fluid is continuously depleted doing work against this force, the flux of oncoming fluid momentum will eventually be balanced by the force and the flow will be brought to rest. This balancing condition will be experienced first by the very low momentum fluid within the boundary layer and nearest the wall. Downstream of this region the acting force will cause the fluid near the wall to flow in the upstream direction, creating a backflow. The original oncoming boundary layer will then separate where the forward and backward moving flows meet.

The normal velocity gradient at the wall, $\frac{\partial u}{\partial y}\Big)_w$, must be positive when the fluid next to the wall moves with the stream and negative when the fluid in this region flows against the stream. It follows that where the two flows meet $\frac{\partial u}{\partial y}\Big)_w = 0$; consequently, the wall shear stress, $\tau_w = \mu \frac{\partial u}{\partial y}\Big)_w$, also vanishes. This point on the wall which divides these two regions of flow, point S in figure 1-b, is defined as the separation point.

In most fluid dynamic situations, the force giving rise to separation is an adverse pressure gradient, i.e., the pressure is increasing in the downstream direction. The remainder of this report shall deal specifically with this most common case. However, it should be kept in mind that any force field, for example that created by the interaction of a moving, conducting fluid in an electromagnetic field[2], could give rise to the phenomenon of separation.

In a supersonic flow, an adverse pressure gradient may be generated by the aerodynamic shape of the body, for example a compression corner, or by an external source such as an impinging shock wave. In

BOUNDARY LAYER VELOCITY PROFILES

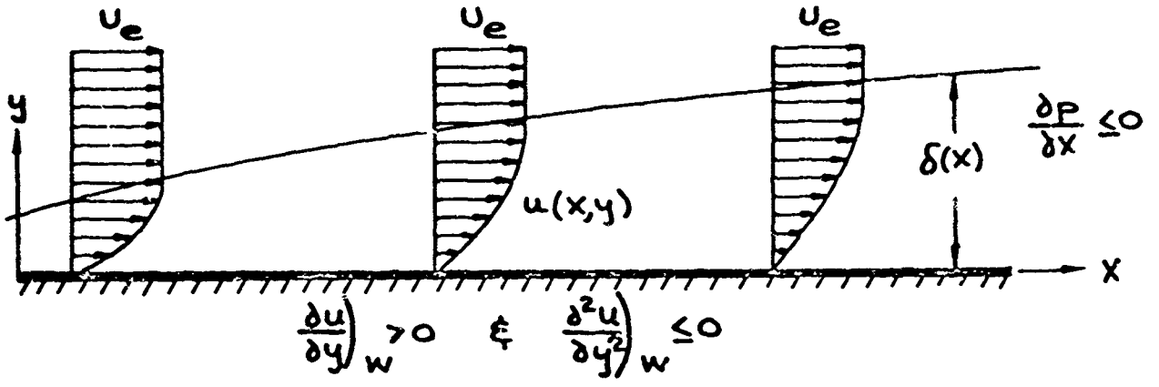

BOUNDARY LAYER ON A SURFACE –
EITHER FAVORABLE OR NO PRESSURE GRADIENT
(a)

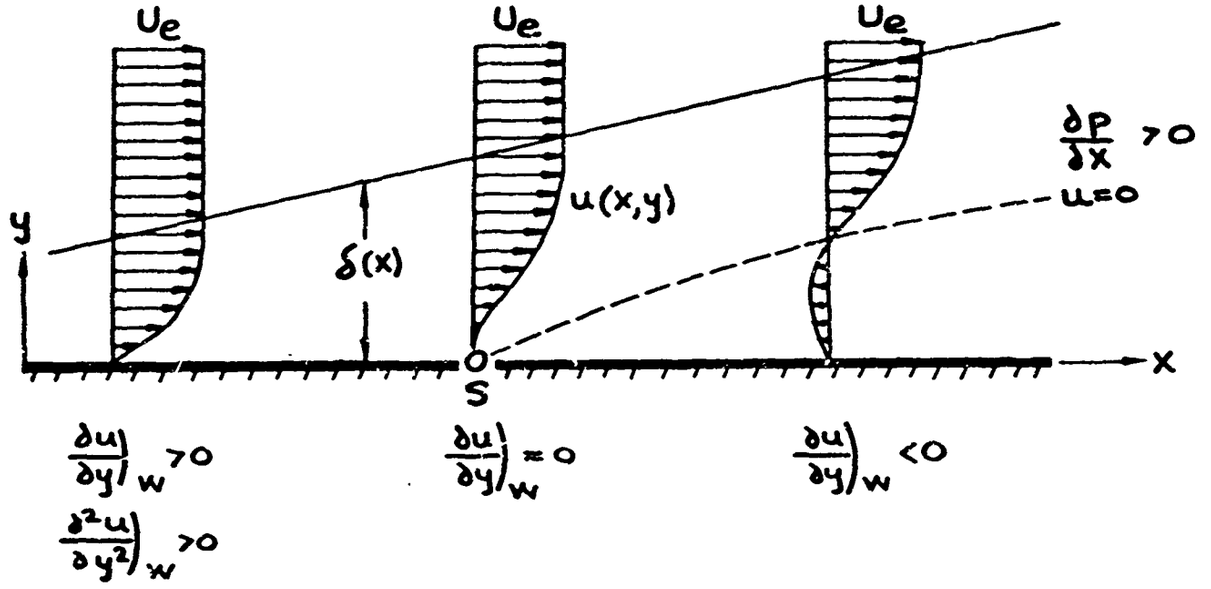

BOUNDARY LAYER ON A SURFACE–
ADVERSE PRESSURE GRADIENT SEPARATION AT POINT S
(b)

FIGURE 1

each case, the supersonic flow experiences a pressure rise across a shock wave. Since in a supersonic flow the body moves faster than the pressure disturbance it creates, the disturbance cannot propagate upstream of the body. The shock wave, which is the front of the pressure rise, is the forward boundary of that region of fluid influenced by the body. Ideally, then, the shock wave represents a discontinuous rise in pressure. However, in any real process a true discontinuity cannot be sustained, and experience shows that in the region of a shock wave, very steep pressure gradients exist, i.e. the rise in pressure takes place over a very short distance. If the shock wave extended throughout the entire flow field, separation would be very localized since the adverse pressure gradient would exist only over a very narrow region (the thickness of the shock wave front). Unfortunately, this is not the case. There is always a region in that part of the boundary layer nearest the wall where the flow is subsonic. In this region, pressure waves will propagate upstream of the disturbance (thus eliminating the formation of a shock wave) because these disturbances are moving faster than the fluid. This allows the pressure gradient to spread over a much longer distance in the low momentum portion of the boundary layer. Experiments have shown that such disturbances may be propagated sizeable distances upstream, of the order of 10 to 100 boundary layer thicknesses.[3] In addition to this streamwise pressure gradient, a normal pressure gradient will also exist since the supersonic flow field outside of the boundary layer and ahead of the shock wave persists at a lower pressure. The process by which this pressure field is established through the subsonic portion of the boundary layer is called "pressure diffusion".

If separation occurs, the streamlines in the external flow will be deflected. For the case of a compression corner, illustrated in figure 2, the effect of separation is to alter the flow geometry such that the supersonic flow will be compressed in two stages through

FLOW SEPARATION IN VISCOUS CORNER FLOW

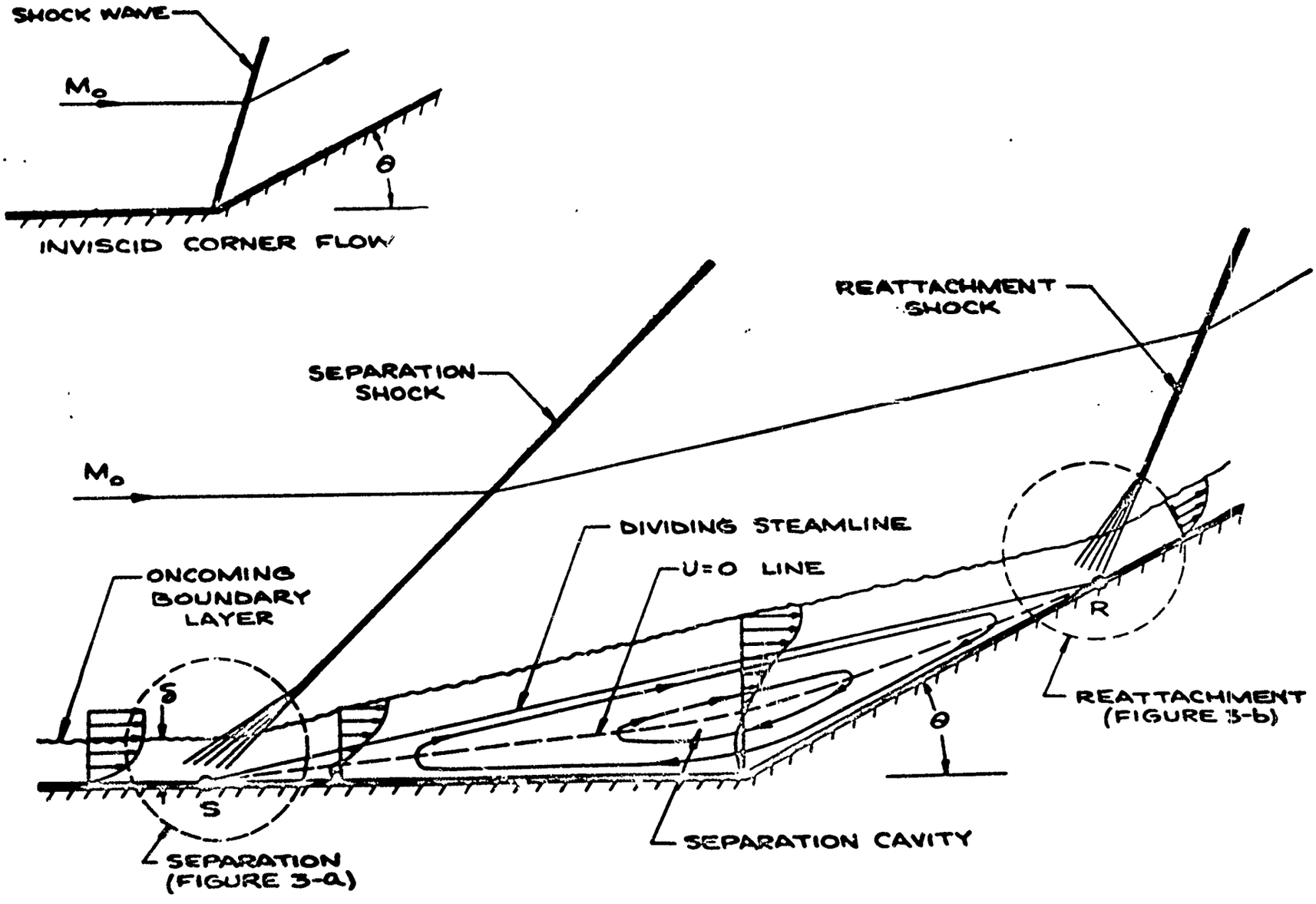

FIGURE 2

two weaker shock waves instead of one stronger shock wave.* The pressure rise in the inviscid flow field is identical to that experienced by the boundary layer. Since separation reduces the initial pressure rise because the initial deflection of the inviscid flow becomes smaller, and since the mechanism of separation (a boundary layer phenomenon) is dependent upon the magnitude of this pressure rise, it can be seen that the external inviscid flow and the viscous separated flow are interdependent through a pressure interaction. An equilibrium between the two flow fields determines the final nature of the flow.

Separated flows frequently reattach on the body, figure 2. At reattachment, the supersonic flow is compressed to its final value, i.e., that value corresponding to the local slope of the body at that point. That fluid with sufficient momentum to proceed against the reattachment pressure rise continues downstream after reattachment, while that having insufficient momentum is reversed back into the separated region. The nature of the pressure rise and local flow at both separation and reattachment are shown in figure 3.

In a steady flow, the dividing streamline at separation must also be the dividing streamline at reattachment. If this were not so, continuity conditions could not be satisfied, i.e., fluid would either be continuously injected into or continuously removed from the cavity region. Thus, ideally the fluid in the separation cavity is a constant mass merely being circulated. The viscous fluid layer outside the dividing streamline behaves much the same as a continuance of the original boundary layer. At the dividing streamline, however, the velocity does not go to zero as it would at a solid wall, since momentum is transferred (by the mechanism of viscous shear) from the external stream through the outer viscous layer into the inner viscous region (separated region). It is this continuous transfer of momentum which sustains the motion of the entrained fluid.

---

* The terminology of "weaker" and "stronger" used here refers to the strength of the pressure rise across the wave. It is not to be confused with the terminology used to differentiate between the two solutions of the inviscid flow expression relating freestream Mach number, flow deflection angle, and shock wave angle.

FLOW CHARACTERISTICS AT SEPARATION AND REATTACHMENT

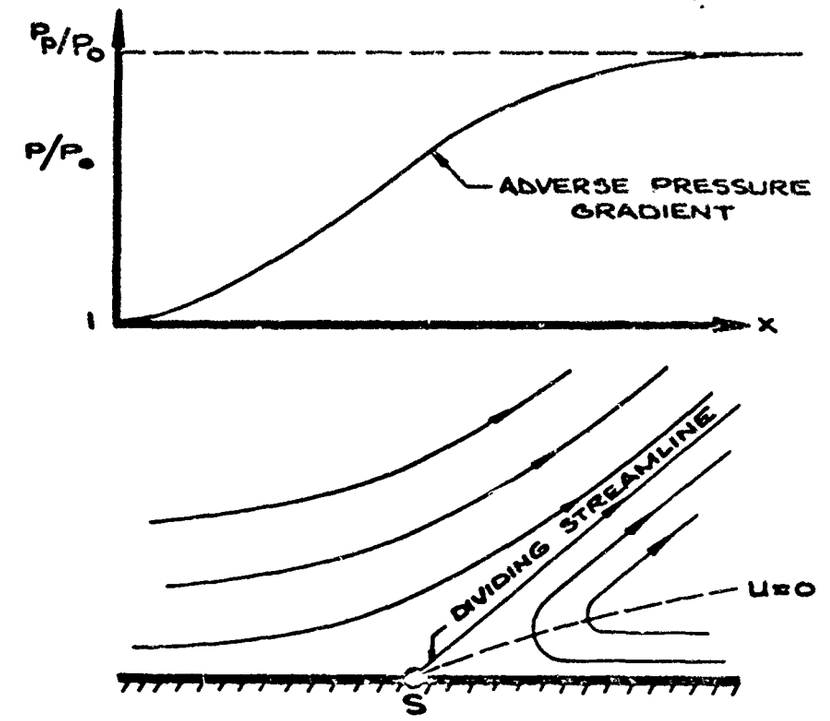

(a) FLOW FIELD AT SEPARATION

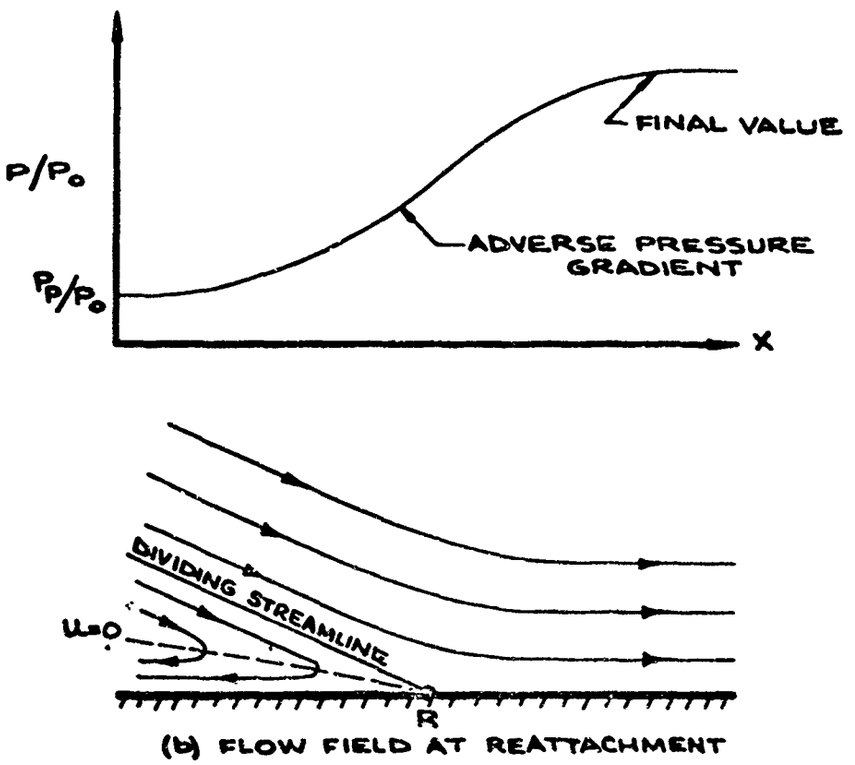

(b) FLOW FIELD AT REATTACHMENT

FIGURE 3

The foregoing arguments apply, at least in principle, whether the boundary layer is laminar or turbulent. The major difference is that turbulent flows are not truly steady. Therefore, as is customary, time average quantities may be applied to describe the flow. For example, in turbulent flow, considerable mass exchange may take place between the separation region and the external viscous flow. This theoretically invalidates the existence of a physical dividing streamline. However, the net time average mass exchange must still be zero for equilibrium conditions.

In summary, if a flow encounters a sufficient adverse pressure rise to bring the low momentum fluid in the boundary layer to rest and establish a region of back flow downstream of this point, the oncoming boundary layer will separate. The onset of separation will deflect the external stream, changing the flow geometry and, hence, the pressure distribution. Since the pressure distribution in the external stream, in turn, affects the location of separation, the two flows (external inviscid stream and viscous flow region) interact until an equilibrium state is reached. The dividing streamline separating the external stream from the separated region may be thought of as the new effective body shape sensed by the supersonic flow. The outer edge of the viscous flow region displays velocity profiles very similar to those for an attached boundary layer. However, profile characteristics change markedly in the innermost portion of the viscous flow region (the separation region) where velocities are further reduced, velocity gradients are small, and a region of reverse flow exists. Separated flows may reattach. At reattachment some boundary layer of finite thickness exists and tends to develop in a normal manner downstream.

2.1.1.2 Two-Dimensional Separation - Analytical Approaches

Serious analytical difficulties are encountered in treating the problem of separated boundary layers. Generally speaking, the boundary layer equations are valid only for attached flows. In the vicinity of separation, two of the assumptions critical to their development are no longer valid:

a. Near separation, significant pressure gradients exist in the direction normal to the local surface.

b. Downstream of separation, the thickness of the viscous flow region increases significantly, hence, the boundary layer thickness (including the separated region) may no longer be negligible compared to a representative body dimension.

In principle, then, separated flow requires the re-examination of the complete and very complex equations of viscous fluid motion (the Navier-Stokes equations) to determine if any simplifying assumptions can be made. Unfortunately, the flow geometries and boundary conditions of separated and reattaching flows are so complicated that no generalized simplifications have been found. Hence, at least for the present, an exact solution of the problem does not seem feasible.

Several attempts have been made to develop approximate analytical solutions to the problem of separation; (references 4, 5, 6, 7, 8, and 9) however, progress has been slow and limited primarily to laminar flows. Of these attempts, the more elaborate method of Lees and Reeves[9] appears to be the most general and promising. This method consists of an approximate solution to the momentum boundary layer equation, and in many respects is similar to methods developed for attached flows.[10,11] Separated flows, however, differ basically from attached flows in that they have a strong pressure interaction with the external flow and that the velocity profiles display a region of reversed flow. Therefore, specific correlation parameters which have been used for attached flow solutions which assume that the velocity profile is a function only of the streamwise pressure gradient outside of the boundary layer are not directly applicable to the present case. The approach taken is to seek a simultaneous solution to the zeroth and first moments of the boundary layer momentum equation, i.e., the momentum integral and energy integral boundary layer equation. Using this technique, the

momentum equation itself need not be satisfied at the surface. Thus, more restrictive parameters used in the attached flow solutions may be replaced by a velocity profile parameter which is related to the shear stress at the wall. This latter dependency posesses a significant physical meaning for the problem of separated flows. The method is capable of producing velocity profiles with reversed flow even for the limiting case of zero free stream velocity gradient. The effects of heat transfer are included in the analysis.

2.1.2 Three-Dimensional Separation

Thus far, the concepts discussed have applied primarily to two-dimensional flows. No serious qualitative complication is introduced in the consideration of boundary layer separation in axially symmetric flows. Instead of the locus of points describing separation from the surface being a line, it is now a circle around the body perpendicular to its axis of symmetry.

For general three-dimensional flows, the problem of boundary layer separation is much more complex and remains relatively unanalyzed. Much of the significant work to date is reported in references 12 through 18. The principal difference between two-dimensional and general three-dimensional flows may be described as follows. In a two-dimensional flow, the fluid in the boundary layer is generally forced into the external flow if the pressure gradient is sufficiently strong, thus causing separation from the wall; however, in three-dimensional cases, the fluid particles can escape sideways along the wall. Hence, the definition of separation is beset with considerable complexity. Maskell[13] suggests that the problem be viewed from the standpoint of limiting streamlines, i.e., the streamlines of fluid particles that pass infinitely close to the surface. If separation exists, two distinct sets of limiting streamlines lie on the surface, one representing forward flow and the other, reversed flow. The locus of separation points is then the boundary between these two sets of limiting streamlines and the flow field is divided into two regions by a stream surface starting at the body, as illustrated in figure 4.

SEPARATION IN THREE-DIMENSIONAL FLOW

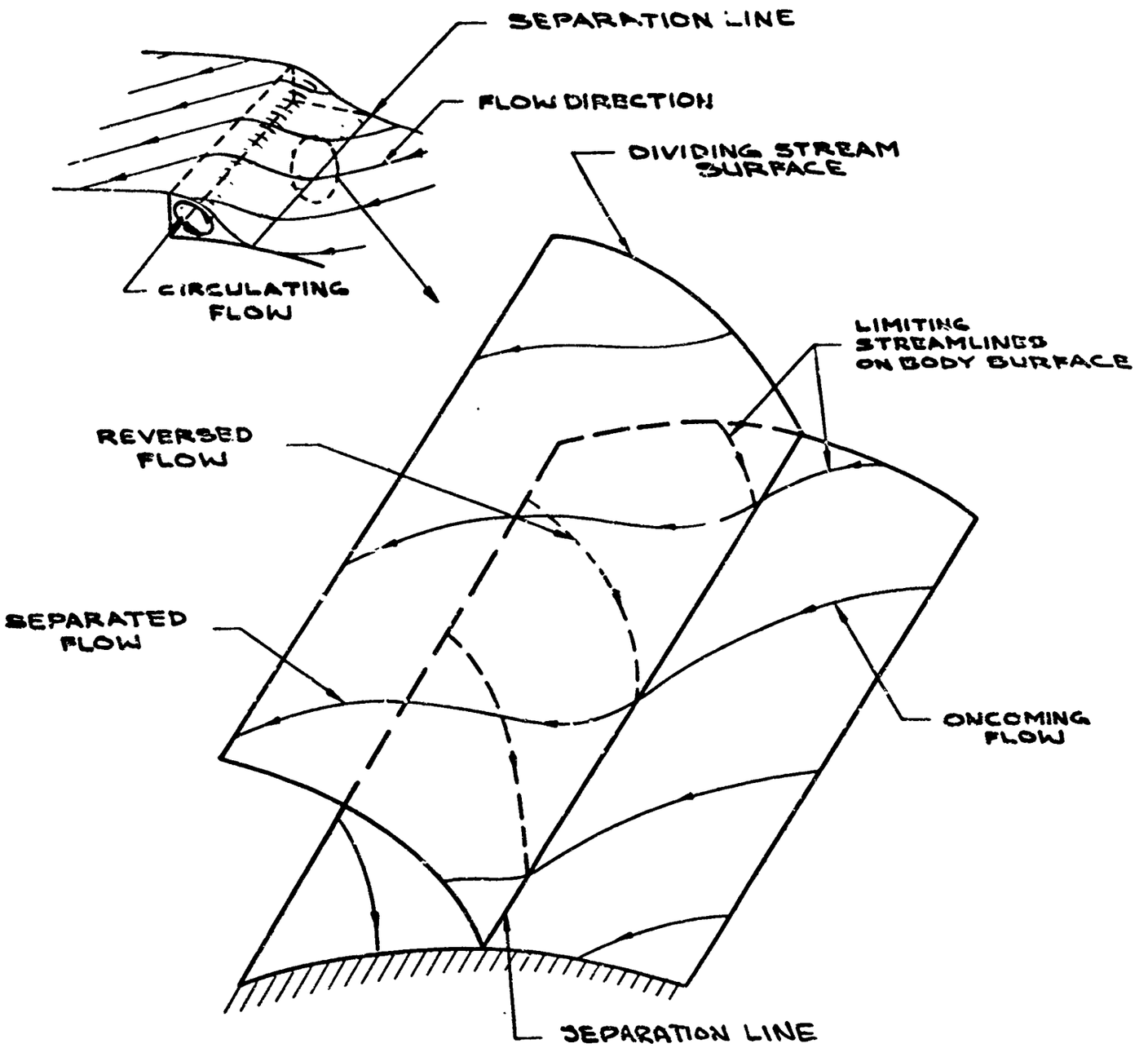

FIGURE 4

2.2 Breakaway Separation

In certain instances, the flow may separate even though the inviscid streamwise pressure gradient is favorable. This type of flow we have already defined as breakaway separation. Some examples are illustrated in figure 5.

In the inviscid sense, breakaway separation in a supersonic flow may be related to the maximum turning angle for the flow, i.e., that angle through which the flow becomes completely expanded. Ideally, an evacuated region results when the geometric angle exceeds this value. At low supersonic Mach numbers the maximum turning angle is quite large, e.g., for a two-dimensional flow using the Prandtl-Meyer (isentropic expansion) criteria, $\theta_{max} = 130.4^{\circ}$ for M = 1. However, as Mach number increases, this maximum angle decreases quite rapidly; at M = 10, $\theta_{max} = 28.2^{\circ}$ and at M = 20, $\theta_{max} = 14.3^{\circ}$. This simple model becomes much more complicated when entropy layers from upstream shock detachment and thick boundary layers create a region of low Mach number flow near the corner.[19] The inviscid evacuated cavity now becomes a viscous separated region, fed by the low energy fluid from the boundary layer. Of equal importance is the pressure rise due to downstream recompression.[20,21] This pressure rise will contribute to the reversal of flow back into the separated region which, in turn, influences the size of the entrained fluid region. The characteristics of the flow within the entrained fluid region are identical to those described for boundary layer separation. Analytical models describing the fluid mechanical phenomena of breakaway separation are available in references 20 through 37. Intuitively, the phenomenon may be thought to occur when the centrifugal force past the curvature (corner) cannot be supported by the radial pressure gradient. For this case, the boundary layer equations break down since one of the basic assumptions for their formulation was that the surface curvature was small, i.e., of the same order of magnitude as the boundary layer thickness. Again, the complete Navier-Stokes equations must be re-examined before any simplifying assumptions may be made for this problem.

EXAMPLES OF BREAKAWAY SEPARATION

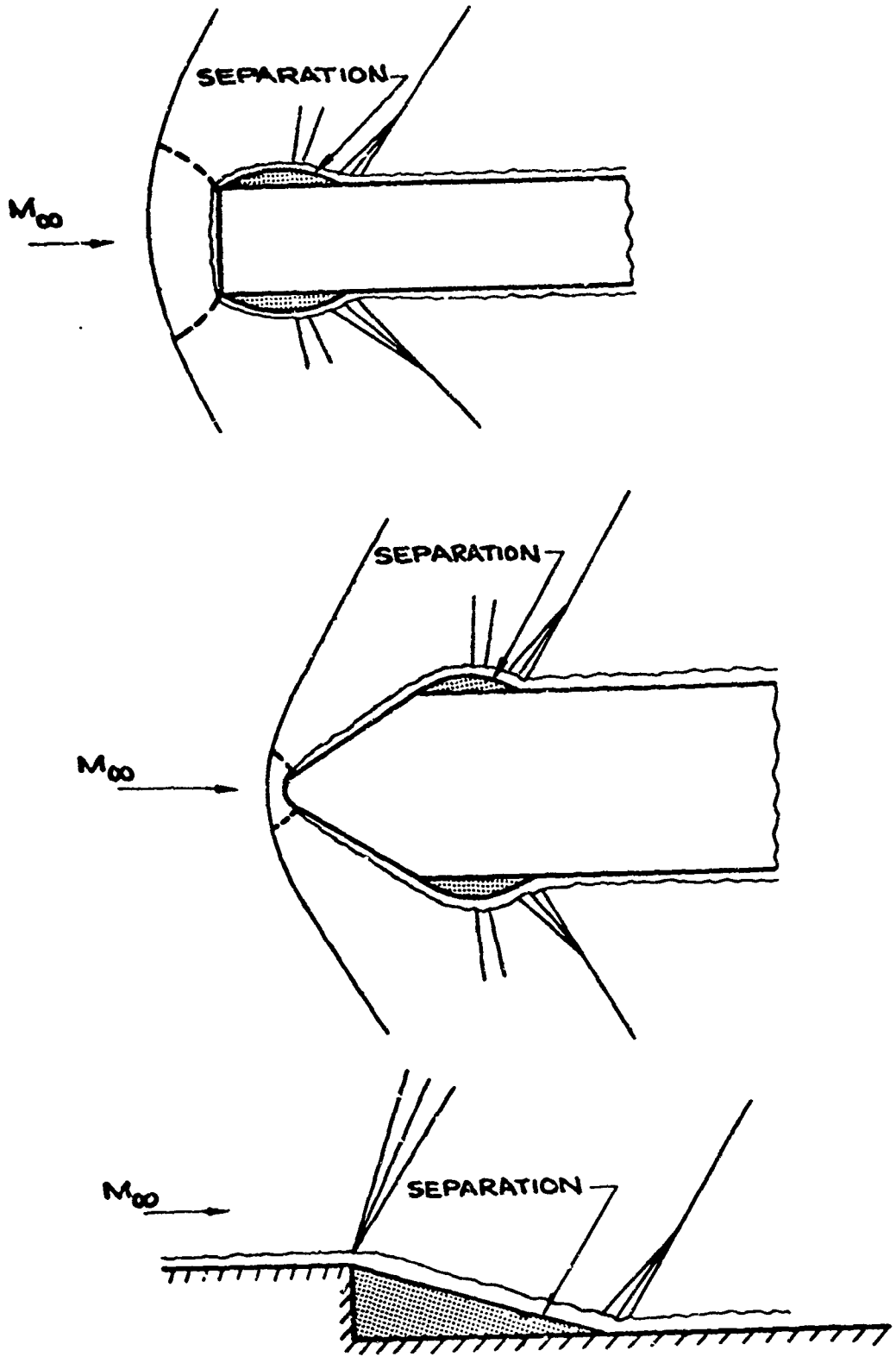

FIGURE 5

2.3 Remarks

An exact solution to the overall problem of viscous flow separation does not, at least at present, seem feasible. Because of our limited knowledge of flow in separated regions and its interrelation to the entire flow field, no simplifications of the very complex complete equations of fluid motion seem to be justified. At present, approximate analytical solutions relying partially on empirical correlations seem most promising; however, results have not been generally applicable to practical situations. Therefore, the engineer has had to resort mainly to experimental investigation to study his particular problems. To date, a substantial amount of such work has been completed. The remainder of this report deals primarily with the coverage of the highlights of these investigations and the useful, but limited, engineering tools derived from them.

3. CHARACTERISTICS OF SEPARATED FLOWS

The engineer is concerned primarily with determining the pressure, skin friction, and heat transfer distributions for the fluid motion over a specified configuration. However, before these topics are considered, much insight into the interpretation of available experimental and analytical results pertinent to separated flows may be gained by considering certain properties peculiar to these flows. Though the characteristics to be discussed are closely interdependent, they will be dealt with as discrete entities in order to isolate their significance. Some of these more prominent aspects follow.

3.1 Significant Flow Parameters

For attached flows, neglecting displacement effects of the boundary layer on the external supersonic flow, the behavior of the boundary layer depends mainly on Reynolds number, whereas conditions in the external inviscid flow are dependent primarily on Mach number. The physical significance of these two flow parameters may be explained as follows:

a. Mach Number

Mach number may be regarded as a measure of the compressibility of the fluid. In the important case of the adiabatic inviscid flow of an ideal gas, changes in pressure, temperature, and density of the flow along the body may be shown to be a function only of body shape and Mach number.

In general, as Mach number increases, the flow in the vicinity of the body becomes more complex. For example, separation normally results in multi-shock (figure 2) or expansion-shock (figure 5) flow fields. As Mach number increases, wave angles decrease and these flow processes tend to merge in the region of reattachment.

b. Reynolds Number

Reynolds number may be thought of as the ratio of the inertia force to the viscous force in the shear layer. In continuum flows, the growth of the shear layer, momentum transfer, and heat transfer are strongly dependent upon Reynolds number. This is true for both attached and separated flows.

As has been previously explained (Section 2.1.1.1), the phenomenon of flow separation is the result of a strong interaction between the viscid and inviscid flow fields. Therefore, in describing separated flows both Mach number and Reynolds number are important.

3.2 State of Flow

Experiments show that separated flows are characterized by the prevailing type of boundary layer.[37] That is to say, there are certain basic features of the flow which depend primarily on whether the boundary layer is laminar, transitional, or turbulent and which are more or less independent of other flow and geometrical parameters. Therefore, it is convenient to define the possible regimes in the following manner:

a. Pure laminar - The flow remains laminar throughout the region of separated flow; i.e., transition occurs downstream of reattachment.

b. Transitional - Transition occurs between the separation and reattachment points.

c. Turbulent - The boundary layer is turbulent throughout the entire separated region; i.e., transition occurs upstream of the separation point.

The distinct differences in flow characteristics observed between the above regimes are attributed mainly to the greater effective momentum transfer in turbulent boundary layers. Thus, the location of transition with respect to separation and reattachment is important.

3.3 Length of Separated Region

In general, for identical free stream conditions and geometry, the length of the separated region in flow with a laminar boundary layer will be considerably greater than that with a turbulent boundary layer. The reason is that the greater momentum of the fluid in the turbulent boundary layer, due to the increased effective viscosity in turbulent exchange, enables the fluid near the wall to proceed against much greater rises in pressure before the equilibrium between pressure and momentum forces is reached. Hence, separation is delayed in a turbulent boundary layer. As an example, for a forward facing step, figure 6, it has been observed for identical step height and free stream Mach numbers that the length of laminar separation was four times greater than that for the turbulent separation, even though the overall pressure rise associated with the latter case was three times greater.[38]

3.4 Shock Wave Penetration of Viscous Region

Shock waves may occur in the vicinity of separated flows due either to flow deflection caused by the separation and/or external sources (shock impingement) which may give rise to the separation. The final position that a shock wave may assume with respect to the viscous flow field is governed mainly by the state of the flow. Shock waves may, of course, occur only in supersonic streams. If the velocity profile is gradual, such as for a laminar boundary layer, the dividing line between subsonic and supersonic flow will lie farther from the surface than it would be in a turbulent boundary layer of the same thickness. Hence, a shock wave may "penetrate" a greater distance into a turbulent boundary layer. This property gives rise to the fundamental difference in shock structures observed between laminar and turbulent interactions.[3]

3.5 Compression Process

The combined characteristics of length of the separated region and shock penetration strongly influence the compression process that the

COMPARISON OF SEPARATION LENGTH FOR LAMINAR AND TURBULENT BOUNDARY LAYER

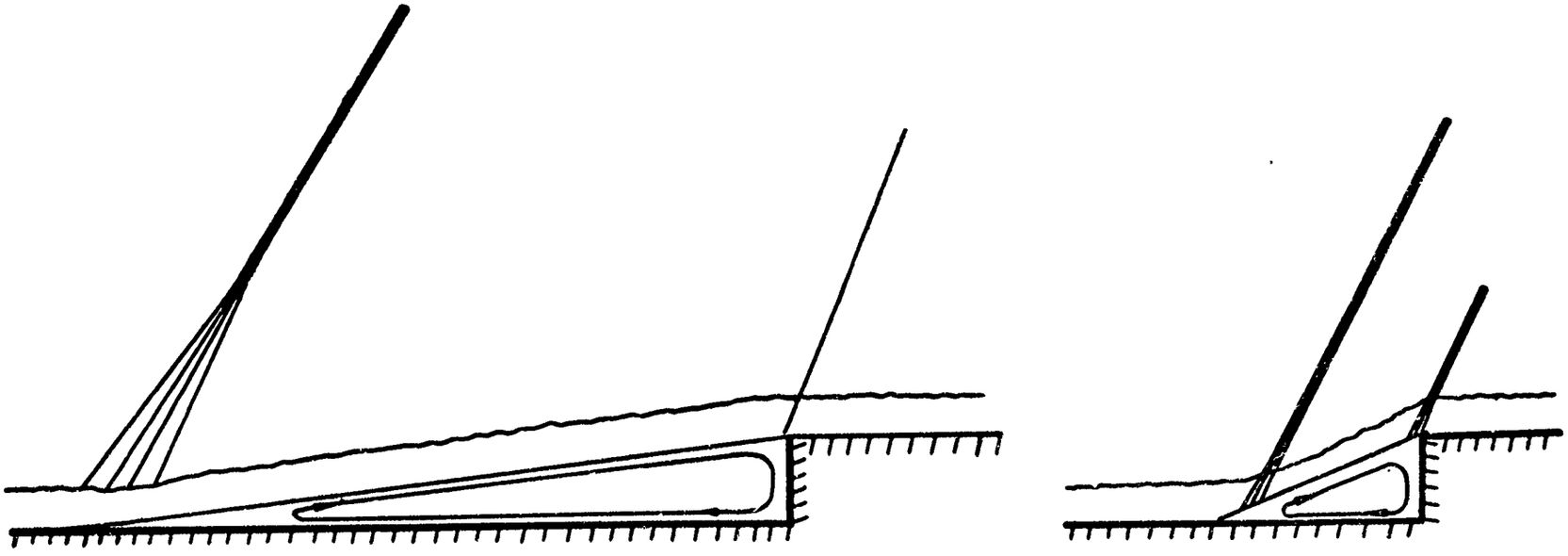

(A)
LAMINAR FLOW

(B)
TURBULENT FLOW

FIGURE 6

inviscid supersonic flow undergoes. For illustration purposes, we may use the example of flow past a step, which has been already partially discussed, refer to figure 6. For both laminar and turbulent flows, the effect of separation is to alter the effective body shape to more or less resemble a wedge with a somewhat curved approach. Because the region of separation for the laminar case is longer, the external flow is turned more gradually and through a smaller angle; hence, the resultant pressure increase is less than for the turbulent case. Compression over this geometry near the wall takes place through a series of weak waves. These wavelets then coalesce to form a shock wave some distance outside the boundary layer. For the turbulent case, the shorter separation region results in a considerably larger turning angle and a more severe approach curvature; hence, coalescence of the compression wavelets occurs closer to the surface. The combined effects of rapid coalescence of compression wavelets plus the sonic line being deeper in the boundary layer accounts for the observation that for turbulent flow the shock waves appear to emanate from a point in the boundary layer.[37]

The experimental observations cited above allow us to qualitatively discuss certain details of the flow field. First of all, for the turbulent case, since the shock wave emanates from the boundary layer, the external flow fields on each side of the shock wave would be expected to be nearly isentropic since the shock wave itself is quite straight. For the laminar case, the compression wavelets do not coalesce as rapidly and the flow field, consequently, must be examined more carefully. Near the new effective turning surface (edge of the mixing layer), the flow is turned quite gradually; hence, the process may be thought to be more or less isentropic in this vicinity. However, as we approach the region of convergence of the wavelets, the compression process occurs more rapidly; hence, an entropy gradient will occur between the effective turning surface and the shock wave. This condition would be expected to give rise to a vorticity field

in the external flow, and the extent of such an action is considerably greater for a laminar case.

The above discussion is limited to low and intermediate supersonic Mach numbers. At high (hypersonic) Mach numbers, the flow field becomes considerably more complicated. Shock wave-boundary layer interactions, caused by the rapidly growing boundary layer displacing the inviscid flow, give rise to highly curved shock waves even for compression by corners and wedges. This effect results in a non-uniform (non-isentropic) flow in the inviscid field between the shock wave and the boundary layer. Thus, an entropy gradient will exist in the inviscid flow field regardless of whether the separating boundary is laminar or turbulent.

3.6 Steadiness of the Flow

It has been found that, in general, the flow in a laminar separated region is steady, i.e., at any fixed point in the flow field the fluid motion is independent of time. On the other hand, this is not the case for the transitional and turbulent regimes. Transitional separations are normally quite unsteady in the region between the transition and reattachment points. This is to be expected since the phenomenon of transition itself is an unsteady process. Chapman's[37] experiments indicate that the unsteadiness associated with turbulent separation is considerably less than for transitional separation. This is not to say, however, that unsteadiness in turbulent separation is not significant. In fact, the experiments of Charwat[39,40] for flow over notches show that considerable mass exchange may take place between the separation cavity and the external flow when unsteadiness is present. This phenomenon appears to play a major role in the mechanism of heat transfer from the separated region.

3.7 Three-Dimensional Effects

Separated flows rarely are completely two-dimensional in either practice or experiment. In particular, it has been noted that local three-dimensional flows may exist in the separated region ahead of a

two-dimensional step whenever transition is close to the point of separation[37], and when a turbulent boundary layer flows over a notch.[39] In general, noticeable three-dimensional effects are accompanied by considerable unsteady flow activity; however, the converse is not necessarily true.

One particular three-dimensional effect that has been noticed in experiments is the existence of regularly spaced longitudinal striations at and downstream of reattachment, as indicated by sublimation and oil techniques. Ginoux reported the existence of these striations for laminar separated flows in references 40 and 42. His models included rearward and forward facing steps (both two-dimensional and axisymmetric) and two-dimensional compression corners. He found that the range of "wave lengths" (spanwise distance between striations) that existed for the rearward facing steps could be correlated with the ratio of step height to boundary layer thickness at separation. He also tentatively concluded that since similar but weaker striations were found prior to separation, these striations indicated the existence of flow phenomena that were related to the flow stability.

In references 36, 43, and 44 similar striations were found in the reattachment region behind rearward facing steps. Strack found that correlating "wavelength" and step height gave results in agreement with Ginoux's laminar data. Roshko, in reference 36, attributes these striations to Gortler-type vortices.

4. PRESSURE DISTRIBUTION

In this section, the overall effects of flow separation on the pressure distribution and the dependence of various pressure parameters on the flow are discussed. A knowledge of the wall pressure distribution is essential to the aerodynamicist in order to calculate the forces on the vehicle. However, other useful information can be obtained. To the experimenter, the wall pressure distribution gives quite an accurate picture of the separation geometry; namely, the length of the separated region and the slope of the dividing streamline separating the external flow and separated region. Pressure data have also been used to predict other properties in regions of separated flow. For example, Sayano[45] has correlated heat transfer coefficient with pressure distribution for the case of shock impingement. Such a correlation facilitates the prediction of heat transfer rates since wall pressure is considerably easier to measure.

4.1 Dependency on State of the Flow

4.1.1 Boundary Layer Separation

The experiments of Chapman, et al,[37] show that for a given geometry, the location of transition relative to the separation and reattachment points is dominant in controlling the characteristic features of the pressure distribution regardless of other flow parameters. Hence, it is proper to categorize pressure distribution characteristics in accord with the previously defined states of flow. Typical wall pressure distributions for laminar and turbulent separated boundary layers are shown in figure 7. Pertinent nomenclature of the distributions is illustrated. The distribution for the transitional case is more or less a composite of the two illustrated cases. In a general sense, the characteristics of the pressure distribution in a separated boundary layer may be described as follows.

4.1.1.1 Laminar Separation

On a relative basis, pure laminar separations usually involve relatively small pressure changes and small pressure gradients. In this

WALL PRESSURE DISTRIBUTION IN THE VICINITY OF SEPARATION

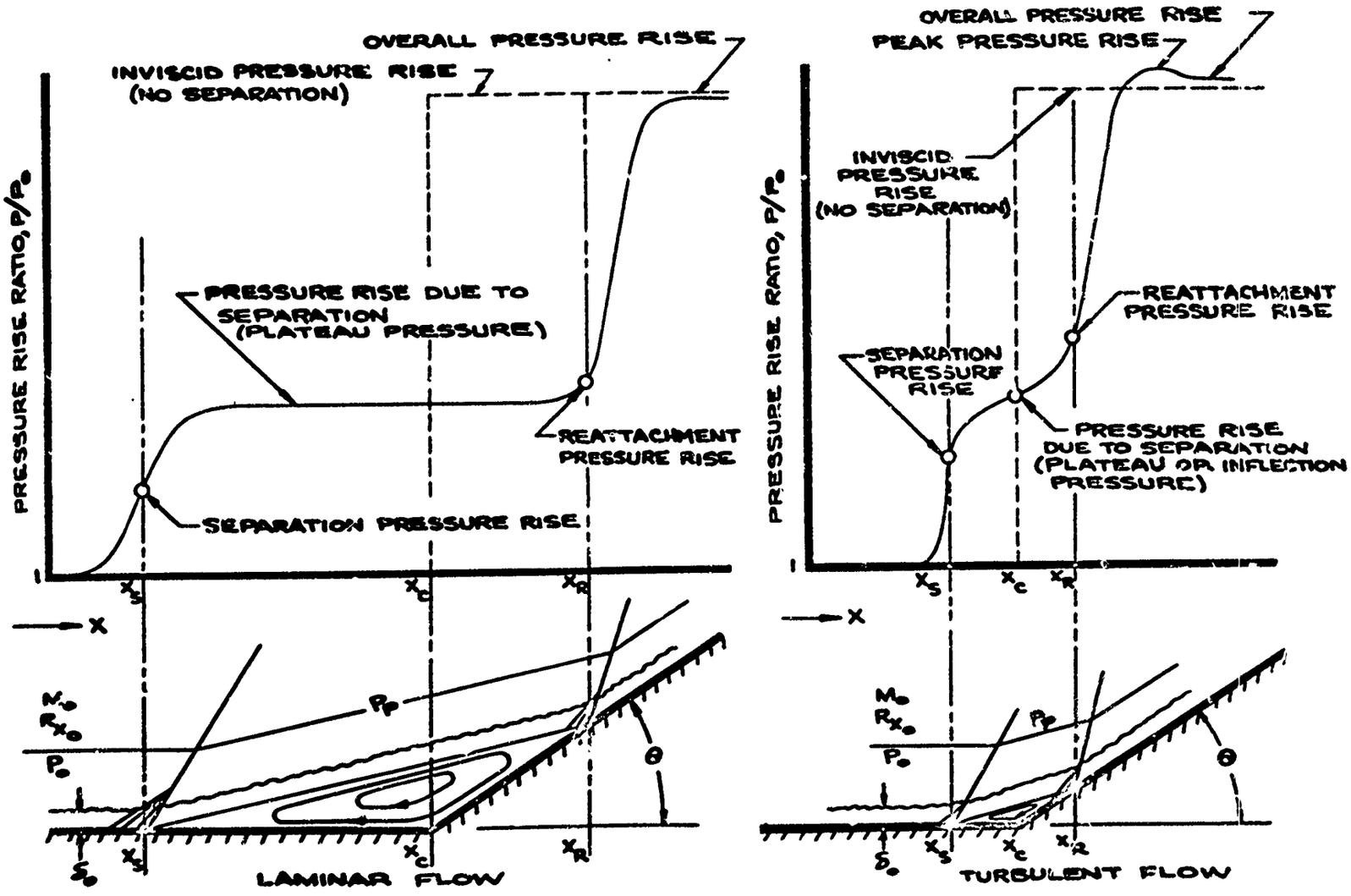

FIGURE 7

regime, the pressure rises to a plateau and remains almost constant over most of the separated flow region to reattachment. The plateau pressure is representative of the pressure in the so-called "dead air region." The remainder of the pressure distribution depends upon the flow deflection at reattachment.

4.1.1.2 Transitional Separation

At separation, the flow is still laminar, so the pressure distribution upstream of transition is quite similar to the laminar case except that the plateau pressure persists over a shorter distance. If transition occurs quite close to separation, however, there may be little or no plateau region due to the energizing of the dead-air region by turbulent exchange. This increased momentum transfer also gives rise to more severe pressure gradients after transition. An abrupt pressure rise is often found to occur at the location of transition. This is especially true when transition occurs only a short distance upstream of reattachment. However, it is not necessary that transition in a separated layer be accompanied by a rapid pressure rise or that abrupt rises in pressure necessarily indicate transition. If transition is far upstream of reattachment (near the separation point) transition may occur in the separated boundary layer (mixing layer) under conditions of nearly constant pressure. Also, if a reattaching boundary layer is very thin, a relatively rapid pressure rise (not indicative of transition) may occur. In general, it is well to compare pressure plots in all three regimes before attempting to correlate a particular phenomenon with an irregularity in a particular characteristic of the pressure distribution.

4.1.1.3 Turbulent Separation

Turbulent separations display rather abrupt pressure variations near both the separation and reattachment points. No large pressure plateau is observed for this regime; the pressure usually rises continuously to its final value. The plateau value is indicated by either an

inflection point in the pressure curve or a small plateau, depending on the length of the separated region.

4.1.2 Breakaway Separation

In general, the basic features of the pressure distribution relevant to "breakaway separation" are quite similar to those just described for "boundary layer separation". That is, the nature of the pressure gradients and relative magnitudes of the pressure changes are highly dependent on the state of the flow. The main difference between the two regimes is that, since the surface is convex, the external flow expands and, hence, for breakaway separation, a pressure decrease rather than an increase is noted in the vicinity of separation. The flow then recompresses at reattachment and approaches the value expected for attached flow.

4.2 Free Interaction

Certain properties of the pressure distribution within the separated region may be independent of the surface geometry causing the flow to separate. That is to say, such characteristics are determined only by the interaction of the oncoming flow with the adverse pressure gradient and are not dependent upon the magnitude of the overall pressure rise causing separation. Such a flow process, one which gives rise to properties independent of the geometry, is defined as a "free interaction". Two important pressure parameters may be expressed as free interaction functions; these are the pressure rise to the separation point and the pressure rise caused by separation. These parameters are discussed in detail in the following section.

4.3 Pressure Parameters

Several investigators of separated flows have found it useful, for the purposes of interpretation of data and the development of correlation formulas, to define certain parameters pertinent to specific characteristics of the pressure distribution (refer to figure 7). Some

frequently used quantities are defined as follows, together with their dependency on Mach number and Reynolds number.

The importance of the location of transition relative to separation and reattachment has already been pointed out (section 3). Therefore, we must bear in mind that any change in a flow parameter which affects transition can also directly change the pressure distribution.

4.3.1 Critical Pressure Rise

The critical pressure rise is defined as the minimum overall pressure rise required to cause separation. This quantity is usually expressed in terms of the critical pressure rise coefficient,

$$C_{p_{crit}} = \frac{p_f - p_o}{(1/2)\rho_o u_o^2} = \frac{2}{\gamma M_o^2}\left(\frac{p_f}{p_o} - 1\right) \tag{3.1}$$

Donaldson and Lange[46] have reasoned, from consideration of the physical phenomena, that the critical pressure rise should be controlled by the wall shear, τ_o, boundary layer thickness, δ_o, and stream conditions M_o, ρ_o, u_o, just prior to separation, i.e.,

$$p_f - p_o = F_1(\tau_o, \rho_o, M_o, u_o, \delta_o) \tag{3.2}$$

By the principle of dimensional homogeneity, the above relationship may be replaced by a simpler relationship in terms of dimensionless groups, namely:

$$\frac{p_f - p_o}{(1/2)\rho_o u_o^2} = F_2\left(\frac{\tau_o}{(1/2)\rho_o u_o^2}, M_o\right) = F_3(C_{f_o}, M_o). \tag{3.3}$$

Or, since skin friction depends on the local Reynolds number and local Mach number;

$$C_{p_{crit}} = F_4(R_{x_o}, M_o). \tag{3.4}$$

Recent experimental results indicate that $C_{p_{crit}}$ depends on Reynolds number in approximately the following manner.

$$\text{Laminar Flow:} \quad C_{p_{crit}} \sim R_{x_o}^{-1/4} \tag{3.5}$$

$$\text{Turbulent Flow:} \quad C_{p_{crit}} \sim R_{x_o}^{-1/10} \tag{3.6}$$

It can be seen that $C_{p_{crit}}$ is a much stronger function of Reynolds number for laminar than for turbulent boundary layers. The effect of Mach number on $C_{p_{crit}}$ is greatest for lower values, i.e., $1 < M_o < 4.0$. Experiments show that for both laminar and turbulent flows $C_{p_{crit}} \sim (M^2 - 1)^{-1/4}$. Experiments also show that $C_{p_{crit}}$ is more or less independent of the specific geometry, although this may not prove to be a general rule, especially at higher Mach numbers.

As previously discussed, the overall pressure rise required to separate a turbulent boundary layer is much greater than that required to separate a laminar boundary layer. For example, for $1.5 < M_o < 3.0$ and $R_{x_o} = 1 \times 10^6$, $C_{p_{crit(turb)}} \simeq 10 \times C_{p_{crit(lam)}}$ for an incident shock wave.

4.3.2 Separation Pressure Rise

Separation pressure rise is defined as the rise in wall pressure at the actual point of separation. As separation usually occurs under the condition of free-interaction, the pressure rise to this point is more or less independent of the mode causing it. For laminar and transitional flow, $C_{p_{sep}} \sim R_{x_o}^{-1/4}$, and the separation pressure rise for a given Mach number and Reynolds number are about equal. This is to be expected since both regimes are essentially laminar at the separation point. For turbulent flows, $C_{p_{sep}} \sim R_{x_o}^{-1/10}$. The separation pressure rise increases with Mach number; however, wave angles are usually quite small; therefore, $C_{p_{sep}}$ decreases as Mach number

increases. The separation pressure rise is usually about 1/2 and 2/3 of the plateau pressure for laminar and turbulent separations, respectively.

4.3.3 Reattachment Pressure Rise

This is the pressure rise at the point of reattachment. In laminar flow, the pressure rise to the reattachment value is approximately the same as the pressure rise to the plateau value. For turbulent flow, however, the reattachment pressure rise is usually about 1/3 to 1/2 of the peak or overall pressure rise (figure 7). The reattachment pressure is greatly dependent on the particular geometry; hence, flow properties at reattachment cannot be viewed from a free interaction basis.

4.3.4 Plateau Pressure Rise

The plateau pressure rise may be defined as that pressure rise resulting from the external flow deflection caused by separation. Because the flow within the separated region is of relatively low energy, the pressure of the deflected external flow is impressed on the separated region in much the same manner that the external pressure is impressed on an attached boundary layer. Hence, the plateau pressure and the pressure at the edge of the separated boundary layer may be considered identical. This relationship of the wall and external flow pressures is shown in figure 8 for the case of a compression corner. The gradual gradients along the wall (dotted line) are attributed to the pressure diffusion phenomenon which takes place in the subsonic portion of the flow. The indicated length, $L_{F.I.}$, represents that region in which the adverse pressure gradient reacts with the oncoming flow, i.e., the free interaction region.

COMPARISON OF PRESSURES ON WALL AND AT EDGE OF BOUNDARY LAYER

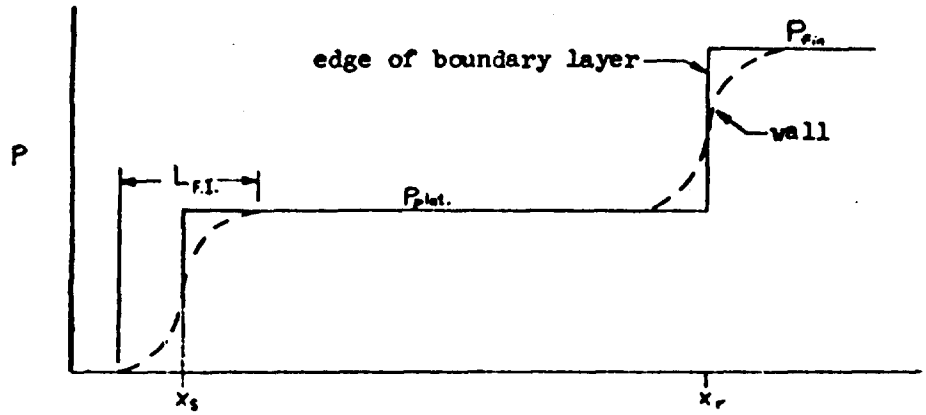

FIGURE 8

Figure 9 shows a plot of laminar flow plateau pressure data as a function of Reynolds and Mach number of the oncoming flow.[47,48] The data shows good correlation for several geometries; namely, compression corner, incident shock and forward facing step geometries, thus substantiating the argument of free interaction. The data points for $1 < M_o < 16$ may be approximated by the following empirical relationship which is indicated by the curve on figure 9.

$$C_{p_{plat_{(Laminar)}}} = 1.60 \left[R_{x_o} \quad (M_o^2 - 1) \right]^{-1/4} \qquad (3.7)$$

Certain experiments[37] indicate that the phenomenon of free interaction, as previously defined, is not generally applicable to the problem of turbulent separation. However, the correlation of a reasonable amount of experimental data[47] for the same flow model geometries considered in laminar flow shows that plateau pressure is more or less independent of these geometries for turbulent flow (see figure 10). Care must be taken in extending these data to other geometries. The following equation approximates the R_{x_o} and M_o dependency of plateau pressure coefficient for turbulent flow

PLATEAU PRESSURE-LAMINAR FLOW

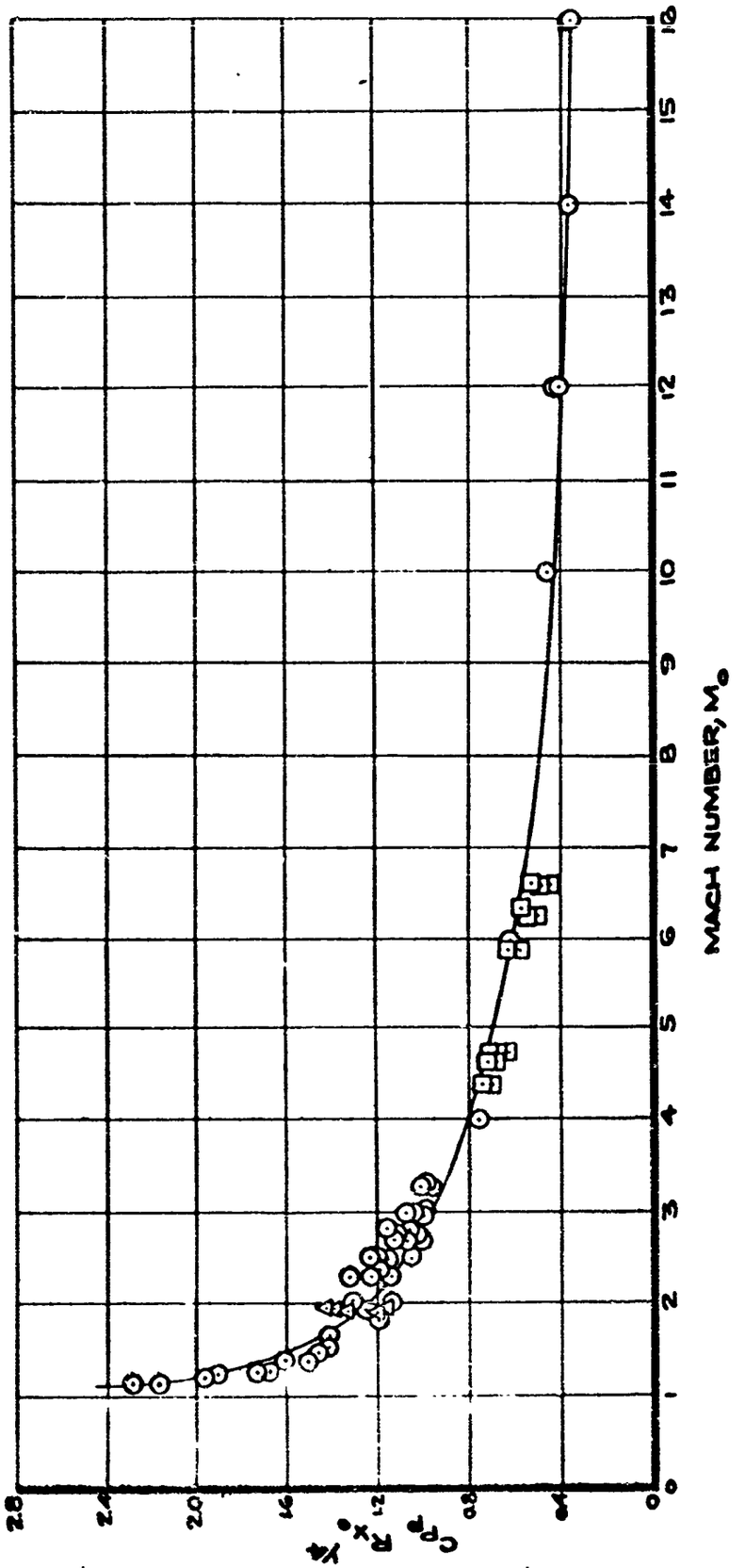

FIGURE 9

PLATEAU PRESSURE-TURBULENT FLOW

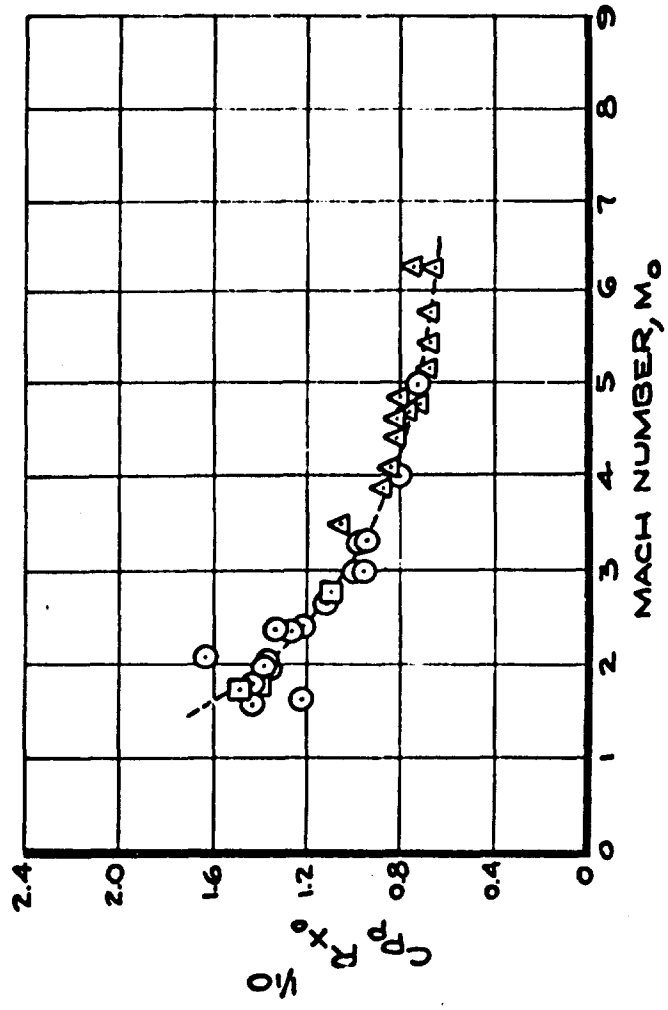

FIGURE 10

$$C_{p_{plat_{(tubulent)}}} = 1.70 \; R_{x_o}^{-1/10} \left(M_o^2 - 1\right)^{-1/4} \qquad (3.8)$$

It has been argued that the plateau and critical pressure rises are necessarily identical.[47] The basis for this argument is that the flow field resulting from a shock-boundary layer interaction can exist only in one of three possible stable conditions, namely:

a. The overall pressure rise is less than the plateau pressure rise. Hence, the flow remains attached. This may be defined as a "weak interaction".

b. The overall pressure rise is just equal to the plateau pressure rise. Here the flow still remains attached, but the interaction is completely self-induced by the mutual dependence of the viscous and inviscid flow fields. The interaction of the adverse pressure gradient with the oncoming flow is independent of the geometry.

c. If the overall pressure rise becomes greater than the plateau pressure rise, the attached flow becomes unstable. Stability is achieved by the separation of the boundary layer, resulting in a modified effective geometry giving rise to stable shock-boundary layer interaction, such as shown in figure 7. Here again, the strength of the leading shock wave is determined by mutual interaction of the viscous and inviscid flow fields and is independent of the body geometry giving rise to separation.

From the above conditions, it would appear that the plateau pressure rise and critical overall pressure rise are identical providing that initial separation is continuous and free from any hysteresis effects. Kuehn[49] made rather extensive experimental measurements to determine the critical overall pressure rise necessary to cause separation. His values for $C_{p_{crit}}$ were somewhat higher than $C_{p_{plat}}$. This is possibly

due to the difficulty in experimentally detecting the exact onset of separation. The criterion used was to assume that separation occurred when the pressure distribution curve changed from a curve with one inflection point to a curve with three inflection points, i.e., when an incipient plateau pressure developed. This technique certainly detects the onset of significant separation; however, the criterion is not necessarily unique. Hakkinen, et al.[50] conducted a similar investigation for laminar boundary layers, but in addition made wall friction measurements. These results, based on the more fundamental criteria of zero wall shear at separation, did show that the pressure rise to cause separation was of the same magnitude as the plateau pressure. Nevertheless, because of the lack of complete data, there appears to be a significant need for more detailed experimental measurements of the incipient separation for both laminar and turbulent flows, especially if the free-interaction phenomenon is to be used as a basis for analysis.

One additional piece of useful information may be developed from the plots in figures 9 and 10.[47] Since the pressure coefficient in a supersonic flow is uniquely determined by Mach number and flow deflection angle, these data may be re-arranged to show the interdependence of flow deflection angle, Reynolds number, and Mach number. This is done in figure 11 which more clearly shows the nature of free-interaction phenomenon. The result shows that for a given Reynolds number, Mach number, and state of flow, the angle of deflection of the separated flow is uniquely determined. It must, of course, be remembered that the foundation of this observation is experimental and limited to specific geometries. The result, however, is applicable to many practical aspects of separated flows, primarily in determining the extent of the separated region, especially in situations where either the separation or reattachment point is fixed.

FREE INTERACTION FLOW DEFLECTION ANGLE AS A FUNCTION OF MACH NUMBER AND REYNOLDS NUMBER

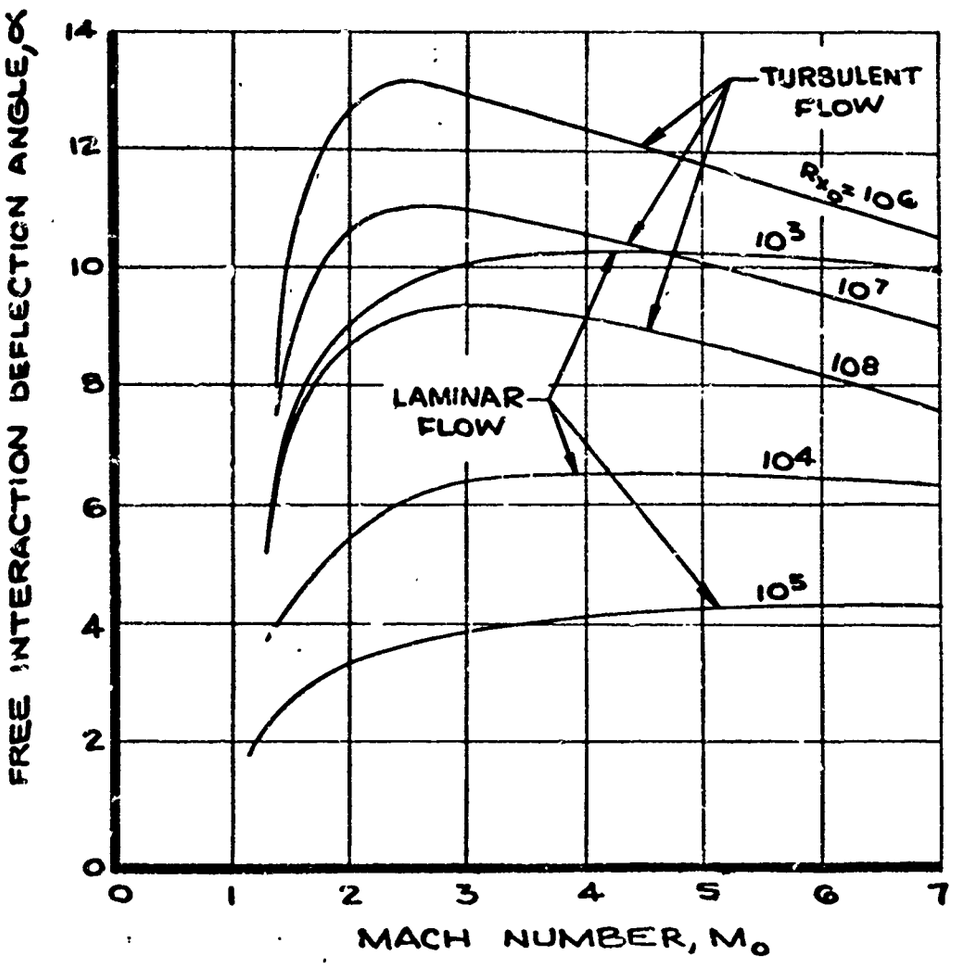

FIGURE 11

4.4 Comments Pertinent to Specific Geometries

Several representative pressure distributions for specific geometries are illustrated in figure 12. Limited analytical techniques have been developed for calculating the length of the separated region and the plateau pressure rise. These are based primarily on experimental results and are discussed under the following headings, together with properties of the pressure distribution which are peculiar to the specific geometry.

4.4.1 Compression Corners

The flow in a compression corner may exist in one of two possible equilibrium positions. If the overall pressure rise is less than the critical value, the flow remains attached. However, if the overall rise exceeds the critical value, the flow separates, modifying the effective body geometry in such a manner as to compress the flow in two stages (figure 12.1). The extent of the separated region is determined by the mutual interaction (equilibrium) of the viscous and inviscid flow fields.

Typical surface pressure distributions for separated flows over compression corners are shown in figure 12.1. The pressure rise across the first shock, i.e., pressure rise due to separation, is quite evident for laminar and transitional flows, as may be seen by the "plateau" in the pressure curve. In the turbulent case, the plateau pressure rise is characterized by an inflection point in the pressure curve. A distinct plateau is usually not observed in turbulent flow, since the length of the separated region is quite short. In both cases, the pressure approaches the inviscid value after reattachment.

If the pressure distribution is known, the geometry of the separated region, i.e., the location of the dividing streamline, may be detmined with reasonable accuracy. The separation point for laminar and transitional flows occurs about where the pressure rise is about one-half the plateau value. In turbulent flow, separation occurs where

PRESSURE DISTRIBUTION FOR SEPARATED FLOW

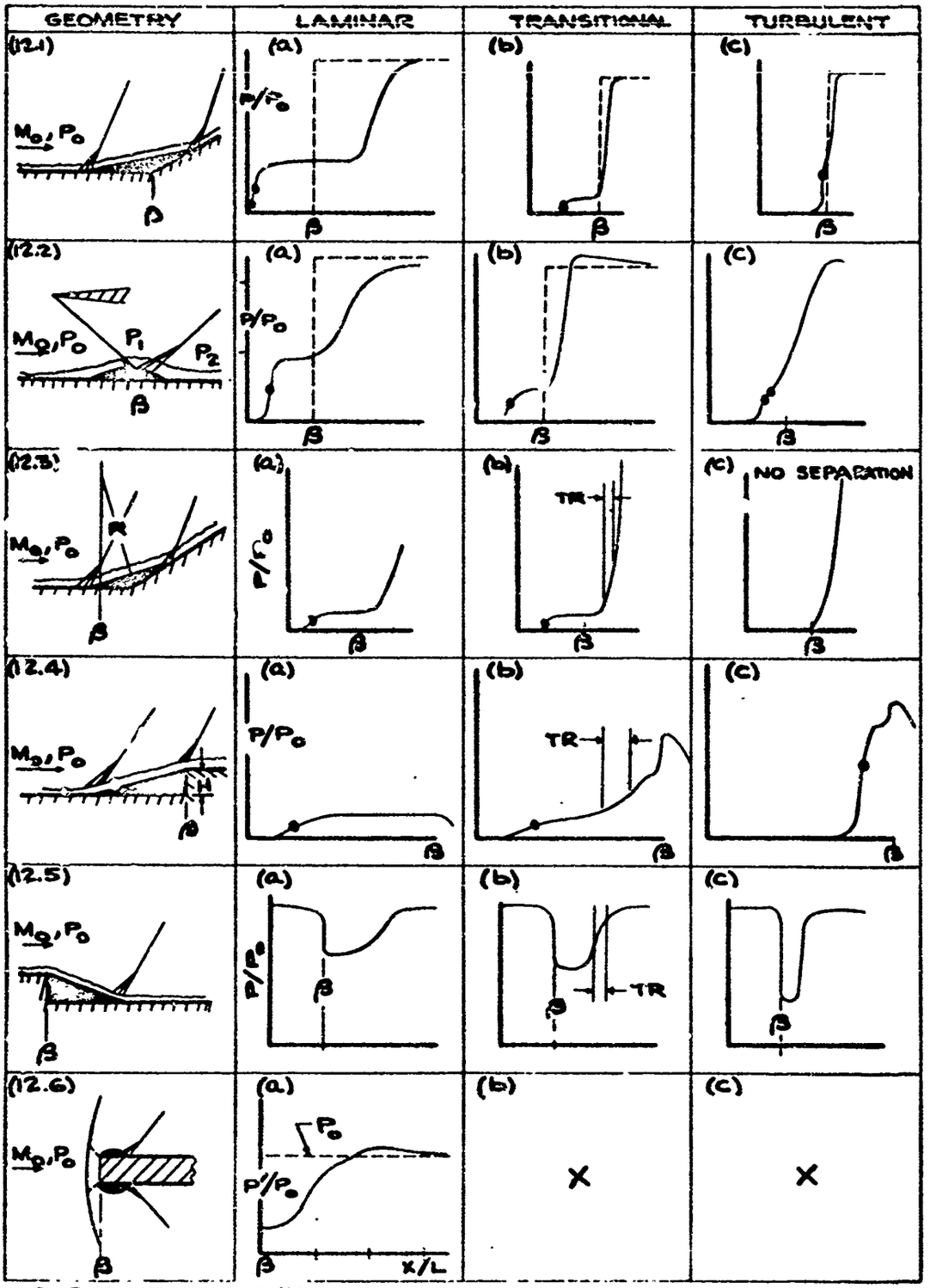

• SEPARATION POINT
TR APPROXIMATE TRANSITION REGION
β REFERENCE POINT ON BODY

FIGURE 12

the pressure rise is approximately two-thirds the value of the plateau value. Once the separation point has been established, the dividing streamline may be drawn, since its slope (the flow deflection angle) is uniquely determined, knowing M_o and the pressure rise due to separation.

Analysis of the problem of flow separation over a compression corner is somewhat complicated by the fact that neither the separation nor reattachment points are known. However, sufficient data have been made to correlate certain flow parameters which are independent of the geometry, namely:

a. The effective deflection angle formed by the separated flow as a function of Mach number and Reynolds number prior to separation (see figure 11).

b. A reference separation length as a known function of the pressure distribution, namely the initial, plateau, and final pressures.

Considering the possible ways ℓ_{sep}/δ_o can vary, the following expression can be derived.[47]

$$\frac{\ell_{sep}}{\delta_o} = \left(\frac{\ell_{sep}}{\delta_o}\right)_{ref} \cdot \frac{\alpha_{ref}}{\alpha} \tag{3.9}$$

where

$$\frac{\ell_{sep}}{\delta_{c_{ref}}} = K\left[\frac{p_f - p_p}{p_o}\right]. \tag{3.10}$$

The required quantities to complete the calculation based on experimental data for $1 < M_o < 7$ are as follows:

Laminar Flow	Turbulent Flow
$M_{o_{ref}} = 2.0$	$M_{o_{ref}} = 2.8$
$R_{x_{o_{ref}}} = 2.0 \times 10^5$	$R_{x_{o_{ref}}} = 2.0 \times 10^6$
$K = 105.0$	$K = 4.15$
Insulated wall	Insulated wall

Knowing the separation length and flow deflection angle, the separation geometry is determined.

Certain geometrical limitations exist to the above criteria. If the compression surface is too short or the turning angle, θ, too great, the flow will reattach at the end of the compression surface, the limiting case of $\theta = 90^o$ being the flow ahead of a step. For these cases, the extent of the separated region is determined solely by the effective turning angle presented in figure 11, since the reattachment point is known a priori.

4.4.2 Shock Wave Interaction

A boundary layer may separate locally as the result of the pressure rise associated with an impinging shock wave. The perturbing shock wave may be generated by a nearby body causing an oblique shock incident to the boundary layer, or by a protuberance from the plane of the boundary layer, giving rise to a swept planer type shock wave, figure 13.

Of these two types of shock induced separations, that resulting from an incident shock wave is the simplest and best understood case (references 45, 46, 48, 49, 50, 51, 52). Basically, the shock wave

SHOCK WAVE BOUNDARY LAYER INTERACTION

13.1 PLANE SHOCK WAVE BOUNDARY LAYER INTERACTION

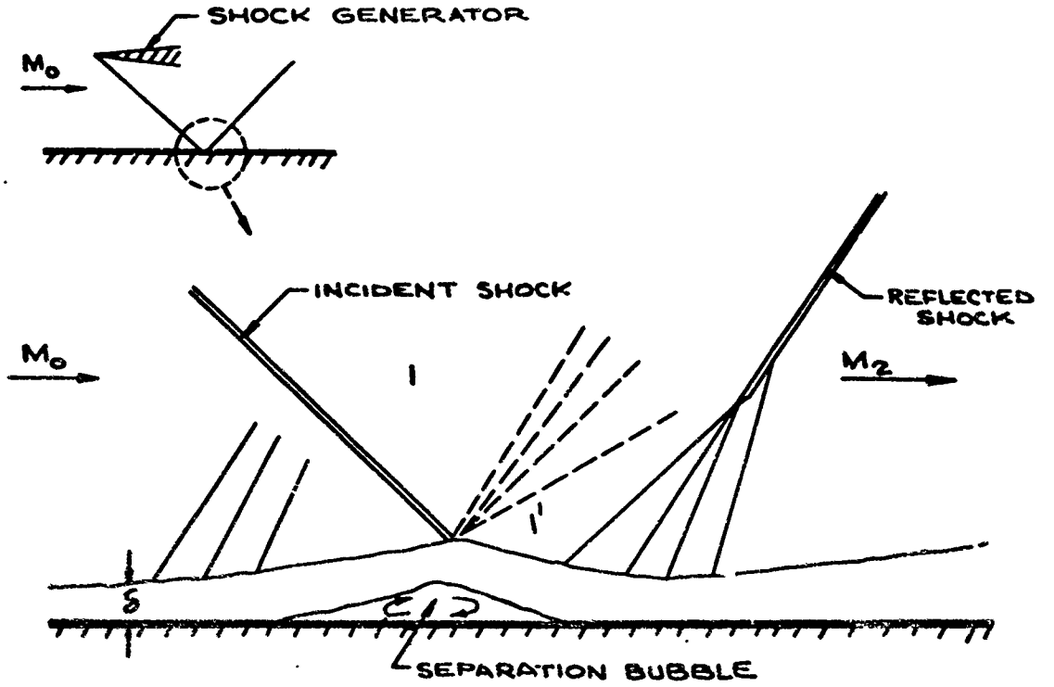

13.2 SWEPT PLANAR SHOCK WAVE BOUNDARY LAYER INTERACTION

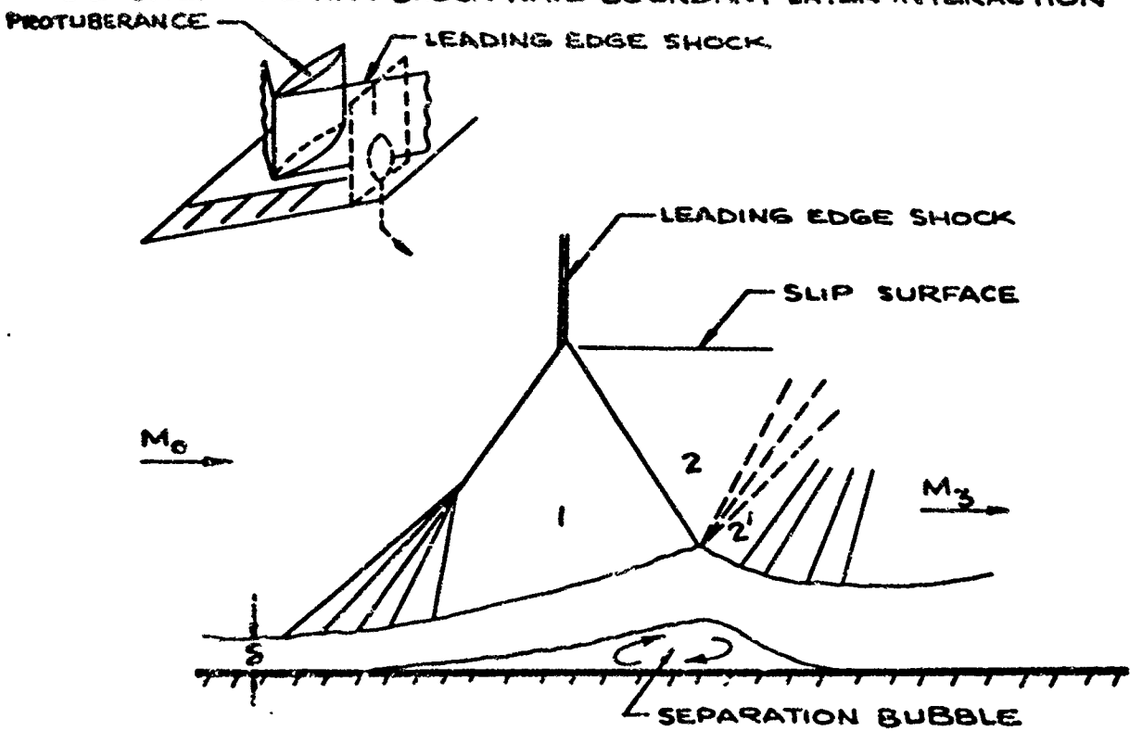

FIGURE 13

impinges on the boundary layer, establishing a jump in pressure at the surface. The low velocity subsonic portion of the boundary layer, of course, cannot support the existence of a shock wave; however, the nature of the subsonic flow does allow the high pressure behind the shock to "diffuse" forward, establishing an adverse pressure gradient. If this pressure gradient is sufficiently steep so as to overcome the momentum of the boundary layer, the flow will separate. A flow model for this type of separation is shown in figure 13.1.

The study of incident shock separation is somewhat simplified in that the location of the inviscid shock wave is not affected by the interaction, as it is for the compression corner. As in all cases of separated flow, the extent of the region affected is considerably greater for laminar than for turbulent flow. Measurements for one case showed that the total length of pressure diffusion was 100 $\delta_{o_{lam}}$, while for turbulent flow the diffusion length was about 10 $\delta_{o_{turb}}$.

Typical surface pressure distributions for incident shock separation are shown in figure 12.2. The characteristics of the pressure curves are quite similar to those observed for corner flow (see figure 12.1). In both the laminar and transitional case, the pressure rises to a plateau value, while the turbulent curve has a point of inflection. The pressure then rises to its final value. The magnitude of the critical pressure rise for separation or the plateau pressure may be determined from data correlation shown in figures 9 and 10.

One complicating factor for the case of the incident shock wave is the presence of both the incident and reflected wave. The mechanism of flow compression and expansion through the interacting shock system is quite complex, as might be inferred from the flow model shown in figure 13.1. In many instances, the pressure in the region of reattachment reaches a "peak" value and then deceases to a final value.

The following correlation has been proposed for the peak value for turbulent flow over a flat plate.[45]

$$\frac{p_{pk}}{p_o} = \left(\frac{p_1}{p_o}\right)^{1.75} \qquad -<M_o<5 \qquad (3.1?)$$

The final value is usually reasonably approximated by the inviscid value, at lease in intermediate Mach number ranges, $1<M_o<4.0$.

Much less is known about swept planar shock interactions. The problem is complicated by the fact that the boundary layer flow is three-dimensional, and that the shock wave is normal to the surface. A flow model showing the lambda shock-boundary layer interaction for luminar flow is illustrated in figure 13.2. A somewhat different interaction consisting of only a single shock limb impinging on the boundary layer would be expected for turbulent flow; the flow field resulting for the case of a uniform strength swept shock wave has been dealt with analytically.[53] This special problem may be reduced to a two-dimensional one.

4.4.3 Curved Compression Surfaces

The pressure distribution over a curved compression surface differs basically from that discussed for a compression corner in that the compression near the surface is always isentropic provided the corner is properly filleted. In any event, the pressure rise is more gradual since the inviscid pressure rise in the vicinity immediately outside of the boundary layer is continuous (figure 12.3).

Experiments show that as the extent of filleting is increased in a compression corner the flow becomes more difficult to separate. Overall pressure rises greater than the critical value for steps, corners, and shock impingement (figures 9 and 10), are observed without separation. Most investigators believe that this occurrence is due mainly to the

more gradual, continuous, compression. One other feature may be considered in the explanation of this observation. The fillet could be considered to represent an existing separation in a compression corner. The pressure rise required to separate the flow over the curve would then be of the order of magnitude required to cause an increase in separation in an already separated corner flow having a dividing streamline approximating the geometry of the fillet.

For the other geometries discussed, as the pressure ratio for incipient separation is exceeded, the flow separates slightly, and the extent of the separation increases continuously as the pressure ratio increases. For curved surfaces with large turning angles, however, it has been observed for turbulent flow that the flow may instantaneously separate over a large region when a certain pressure rise is reached. The flow accompanying such separations is usually quite unsteady.

4.4.4 Forward Facing Steps

Separation of the boundary layer is to be expected ahead of forward facing steps provided that the step height, H, is not small compared to the thickness of the oncoming boundary layer. The viscous and inviscid flow fields affect each other and reach some final equilibrium condition. The reattachment point is known since it must be at the top of the step. The separation point is free and determined by the flow conditions. The separated region gives rise to an effective geometry which may be approximated by a wedge.

As is to be expected from the nature of momentum transfer in laminar and turbulent boundary layers, the laminar boundary layer separates much farther upstream of the step. For example, it has been observed that for identical free stream conditions and step height, the laminar separation occurred about 17 step heights upstream, whereas, turbulent separation occurred about 4 step heights upstream. As a result of the relative effective body shapes, the shorter length of the turbulent

region gives rise to greater turning angles, and hence, stronger shock waves, i.e. greater pressure rises. For the present example, the turbulent pressure rise was approximately three times the rise associated with laminar flow.

Typical surface pressure distributions for the flow ahead of a step are shown in figure 12.4. For the laminar case, the plateau pressure prevails over most of the separated region. The turbulent distribution is characterized by steep pressure gradients and displays the usual inflection point prior to reattachment. A peak pressure results from the interaction of the more energetic turbulent boundary layer with the edge of the step. Transitional separation yields a flow picture and pressure distribution which are composites of the laminar and turbulent cases.

The separation point for either laminar or turbulent flow ahead of a step may be approximated as follows. The plateau pressure for the prevailing boundary layer may be found, knowing the local Mach number and Reynolds number before separation (figures 9 and 10). The turning angle is then uniquely determined by the Mach number and pressure coefficient or by use of figure 11. The separation point may then be determined by projecting the required wedge angle from the top of the step to the plane of the upstream surface, the point of intersection being the separation point.

As noted from equation 3.8, for turbulent flow, the plateau pressure is only slightly dependent upon the Reynolds number at the separation point. For the present case of forward facing steps, the following empirical equations have been developed as a function of Mach number only:

$$c_{p_{plat}} = \frac{3.2}{8 + (M_o^2 - 1)^2} \qquad 1.5 < M_o < 3.5 \qquad (3.13)$$

$H < \delta_o$

(reference 53)

$$c_{p_{plat}} = 0.13 - \frac{1.5}{M_o^2} + \frac{9.1}{M_o^3} \qquad 3.5 < M_o < 6.5 \qquad (3.14)$$

$H < \delta_o$

(reference 38)

Reynolds number variation in the experiments from which the above equations were developed was somewhat limited; $5 \times 10^6 < R_{x_o} < 5 \times 10^7$; therefore, its elimination was somewhat justified. However, this restriction to the above equations must be realized before they may be applied to more general situations.

The foregoing discussion has been limited to the case where the step height is greater than the boundary layer thickness. When this is not the case, the resultant flow no longer displays the characteristics of a free interaction. For this case, experiments show that the plateau pressure increases with step height and that the pressure gradient leading to the plateau value is quite steep. This pressure gradient decreases as step height increases.

4.4.5 Rearward Facing Steps

In contrast to the previously discussed geometries, the flow over a base comes under the classification defined as breakaway separation. The flow expands around the corner, and must recompress at the bottom of the step. The combined effects of the fluid's inability to negotiate the very sharp and large turning angle, the presence of a low momentum boundary layer, and an adverse pressure gradient created by recompression of the flow at reattachment cause the flow to separate. Experiments indicate that the separated region and external flow reach equilibrium in such a manner that separation occurs at the top of the step. The separated flow geometry and typical pressure distributions are shown in figures 1?.5. Recent data (references 36, 43, 44, and 54) have indicated that, for a given step height, as Mach number is increased, a plateau appears in the pressure distribution in the reattachment region. This plateau is very similar in appearance to that occurring in the pressure distributions for compression corners; however, its cause is not known at this time. The pressure drop due to expansion over the geometry affected by separation is greatest for the turbulent case. This is to be expected, since the

length of the separated region for turbulent flow is shortest, and consequently, the turning angle of the expansion the greatest. As for the case of the forward facing step, if the pressure distribution is known, the extent of the separated region may be approximately determined by finding the turning angle required to expand the flow to the base pressure. A line of this slope extended from the top of the step to the base plane then determines the reattachment point.

Chapman, et al,[37] has developed an analytical approach applicable to the case of laminar flow over a rearward facing step. The primary limiting assumption of the analysis is that the boundary layer is of zero thickness at the step edge. Their result for the plateau pressure is

$$\frac{p_b}{p'} = \left[\frac{1 + \frac{\gamma-1}{2} M'^2}{1 + \frac{\gamma-1}{2} \frac{M'^2}{1-u_*^2}} \right]^{\gamma/(\gamma-1)} \qquad (3.15)$$

Good agreement is obtained for the case $\delta_o = 0$ at separation. The condition $u_* =$ constant is not applicable if a boundary layer is present prior to separation. Certain analytical difficulties are encountered for this case, namely, a new value of u_* would have to be calculated solving the momentum equation. Values for u_*, when the boundary layer at separation is not zero, can be found by the methods of reference 23.

4.4.6 Bluff Leading Edge

The supersonic flow past a square-nosed flat plate involves a detached bow shock wave with a resulting region of separated flow. The boundary layer which forms on the front face of the plate is unable to negotiate the right-angle corner, and separates at the corner. Reattachment occurs some distance downstream. The flow

field around the separation bubble and typical surface pressure distribution on the plate are shown in figure 12.6.

After passing through the bow shock, the flow near the centerline is subsonic but expands to supersonic speeds; it is generally accepted that sonic speed is reached at the corner. Throughout the front portion of the separation bubble, the pressure is quite constant at the surface. A rapid rise in pressure then occurs through the recompression fan, and the pressure approaches the free stream static pressure behind the recompression shock. Experimental results for both the two and three-dimensional cases can be found in references 55 and 56, respectively. There are no transitional or turbulent data.

4.4.7 Cutouts

Traditionally, flow separation has been regarded as always disadvantageous. However, recent considerations within the hypersonic flight regime make the concept of controlled separation seem somewhat attractive. As a result, considerable effort has been expended in the investigation of flows over cutouts or notches. For this geometry, the extent of separation is quite well defined since the separation and reattachment points remain fixed. One proposed practical application of controlled separation is to employ notches as drag generating devices for re-entry vehicles. In addition, it is well known that within the separated region itself, heat transfer rates are substantially lower than for an equivalent attached flow. However, much higher local heating rates at reattachment greatly reduce the attractiveness of using controlled separation to suppress aerodynamic heating. Heat transfer in cavities is discussed in detail in Section 6.

The nature of the pressure distribution over a notch is greatly dependent upon the length to depth ratio, L/H, of the notch as well as whether the flow is laminar, transitional or turbulent. Possible

flow patterns for various L/H ratios are shown in figure 14. For short, more or less square notches, figure 14.1, a single vortex forms in the cavity as a result of the interaction with the oncoming flow. As the ratio L/H increases, i.e., the notch becomes longer, the viscous flow field becomes much more complex. The single vortex becomes more oblong and eventually an unstable condition is reached where two vortices of opposed rotation are established within the cavity (figure 14.2). The fact that the two vortices are of opposite rotation indicates that viscous influence from the primary (downstream) vortex effects the secondary (upstream) vortex development rather than momentum transfer from the external flow. As the notch becomes even longer, a point is eventually reached where the boundary layer reattaches in the central region of the cavity, again separates and reattaches at the end of the cavity (figure 14.3). Here, two vortices of like rotation develop and are maintained by momentum transfer from the external flow. This last case is similar to combined flow over a rearward facing step and flow over a forward facing step. As the length of the notches increases to the point where the central reattachment zone becomes well established, the two separated regions may be dealt with independently.

Typical floor pressure distributions resulting from flow over notches also are sketched in figure 14. Some detailed pressure measurements for such flows are presented in references 39, 40, and 57 through 60. In short notches, the floor pressure is nearly uniform. However, on the recompression (downstream) face a strong rise in pressure due to flow impact is noted near the reattachment point (point R, figure 14.1). In long notches, there is a rapid decrease in pressure due to the expansion of the external stream in the vicinity of the separation point (point S, figure 14.2). The flow recompresses on the floor to approximately zero pressure coefficient and again separates, causing a pressure rise on the floor prior to the end of the notch. For this case, the wall pressure on the downstream face remains relatively

FLOW OVER CUTOUTS

TYPICAL FLOW PATTERNS AND PRESSURE DISTRIBUTIONS

14.1 SHORT NOTCH

14.2 MEDIMUM NOTCH

14.3 LONG NOTCH

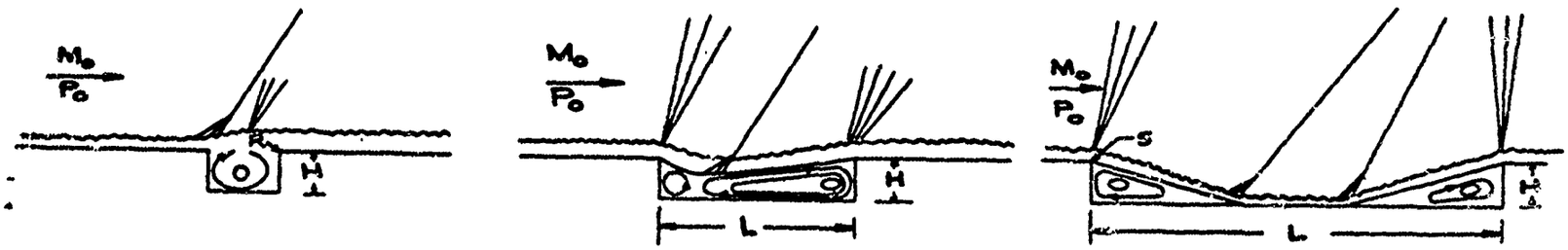

FLOW PATTERNS

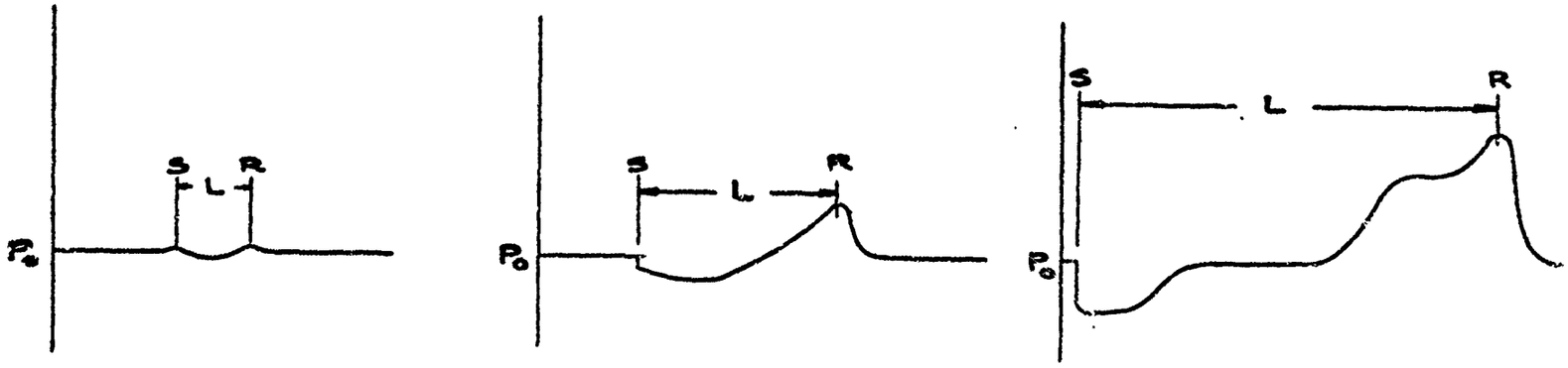

PRESSURE ON HORIZONTAL WALLS

FIGURE 14

THE RECOMPRESSION PRESSURE RISES AS FUNCTIONS OF L/H AND MACH NUMBER (AFTER CHARWAT ET. AL. REF. 39)

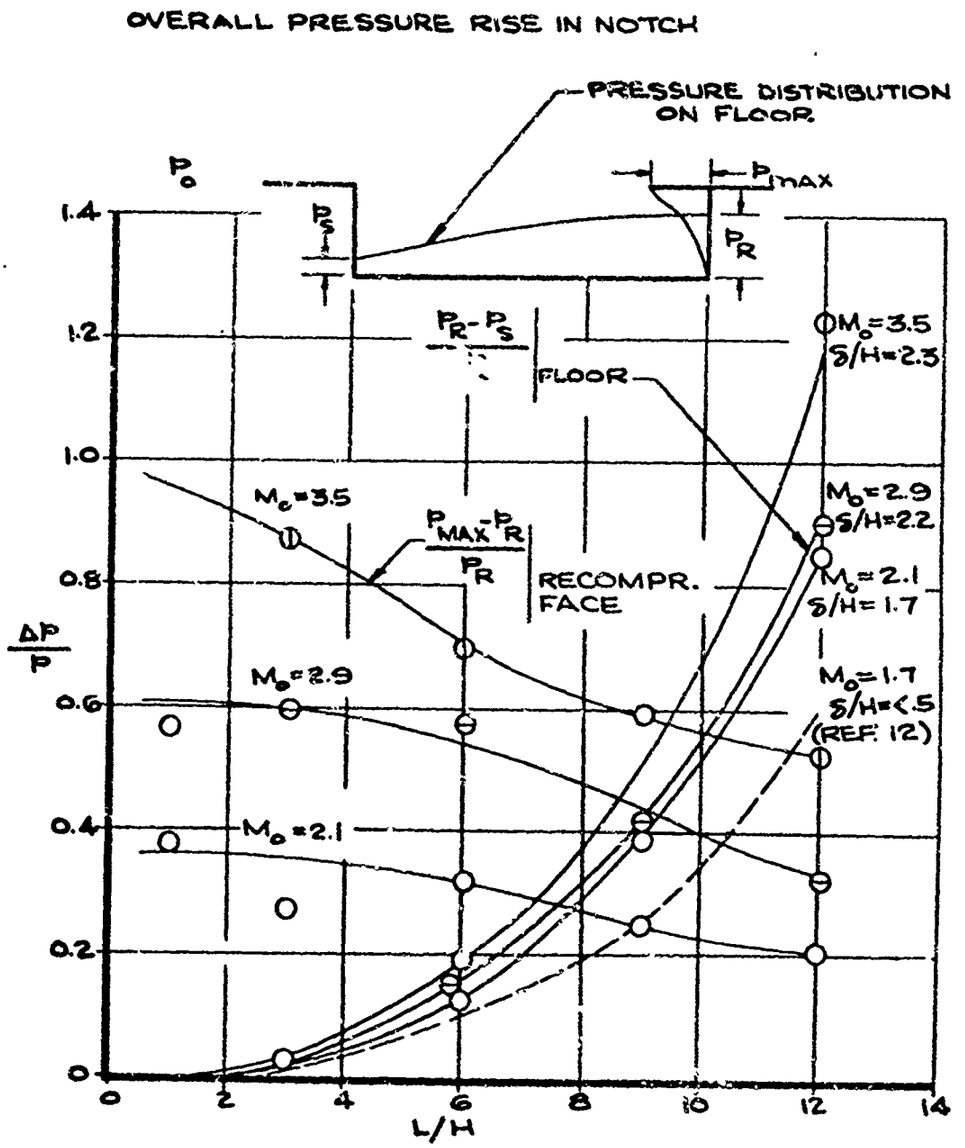

FIGURE 15

constant. A summary of floor and downstream face pressure characteristics for various notch flows are summarized in figure 15, after Charwat, et al.[39]

Because of the different possible flow patterns which may result from flows over notches, it is difficult to predict the geometry (slope) of the dividing streamline and, hence, the effect of the separated region on the inviscid flow field. One geometrical parameter, however, has been determined for such flows and this is the critical cavity length.

The critical cavity length, L_{crit}, is defined as that length which just gives rise to the limiting case illustrated in figure 14.3, i.e., the vortices of the two separated flow regions just coincide. The following equation describing L_{crit}, based on the geometry of figure 16, has been developed[39] for a turbulent boundary layer:

$$\frac{L_{crit}}{H_1} = \frac{L_1}{H_1} + \frac{H_2}{H_1} \cdot \frac{L_2}{H_2} \tag{3.16}$$

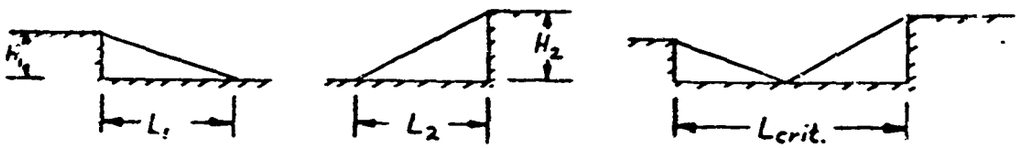

CRITICAL CLOSURE LENGTH FOR CAVITY FLOW

FIGURE 16

The data obtained for turbulent boundary layers showed that for $2.0 < M_o < 3.4$ the critical length is independent of Mach number and the shape of the recompression step.

4.4.8 Remarks

A great deal of experimental and theoretical work has been done to describe the pressure distribution within regions of separated flows. Because of the vast amount of experimental data available on the subject, many practical problems may at least be attacked from an empirical approach. Recent analytical developments seem to indicate good progress in describing the pressure distribution in laminar separated regions. However, complete solutions for the turbulent regime, the transitional regime. and three-dimensional problems have not been found.

5. SKIN FRICTION DISTRIBUTION

Very little work has been done specifically on the problem of skin friction in regions of separated flow. The primary reasons for this are the complexity of analytically describing the details of the viscous flow in the separated region and experimental difficulties encountered in the measurement of skin friction.

As has previously been explained (figure 1.b), the local skin friction coefficient vanishes at the point of separation. Since the flow is generally reversed in the separated region, the skin friction becomes negative. However, velocities in the reverse flow region are usually small as are the gradients, hence, the skin friction, although negative, would be small in magnitude. An unusual case may occur for flow over notches. Charwat, et al,[39] have shown that circulatory flows of opposed rotation may exist in the notch. Thus, for this special case, zones of both positive and negative shear may exist within the separated region.

Hakkinen, et al,[50] have made measurements of skin friction to regions of shock impingement for both attached and separated flows. Measurements were made with a Stanton tube resting on the wall. The tube was calibrated with an absolute floating element skin friction meter. Their work was limited to laminar flows, although in certain cases, transition was observed just after reattachment. Typical results are shown in figures 17, 18, and 19. Unfortunately, no reliable negative skin friction measurements could be made because of instrumentation response characteristics.

The data in figure 17 show that the shock strength is insufficient to cause separation. The skin friction prior to shock impingement is close to the value predicted by the Blasius solution for a flat plate. In the vicinity of impingement, Schlieren photographs show that the boundary layer thickened. As would be expected under this condition, velocity profiles become less steep and the wall shear

SAMPLE PRESSURE AND WALL SHEAR DISTRIBUTIONS AND VELOCITY PROFILES (AFTER HAKKINEN ET. AL. REF. 50)

$R_{x\,SHOCK} = 2.84 \times 10^5$

$P_f / P_o = 1.20$

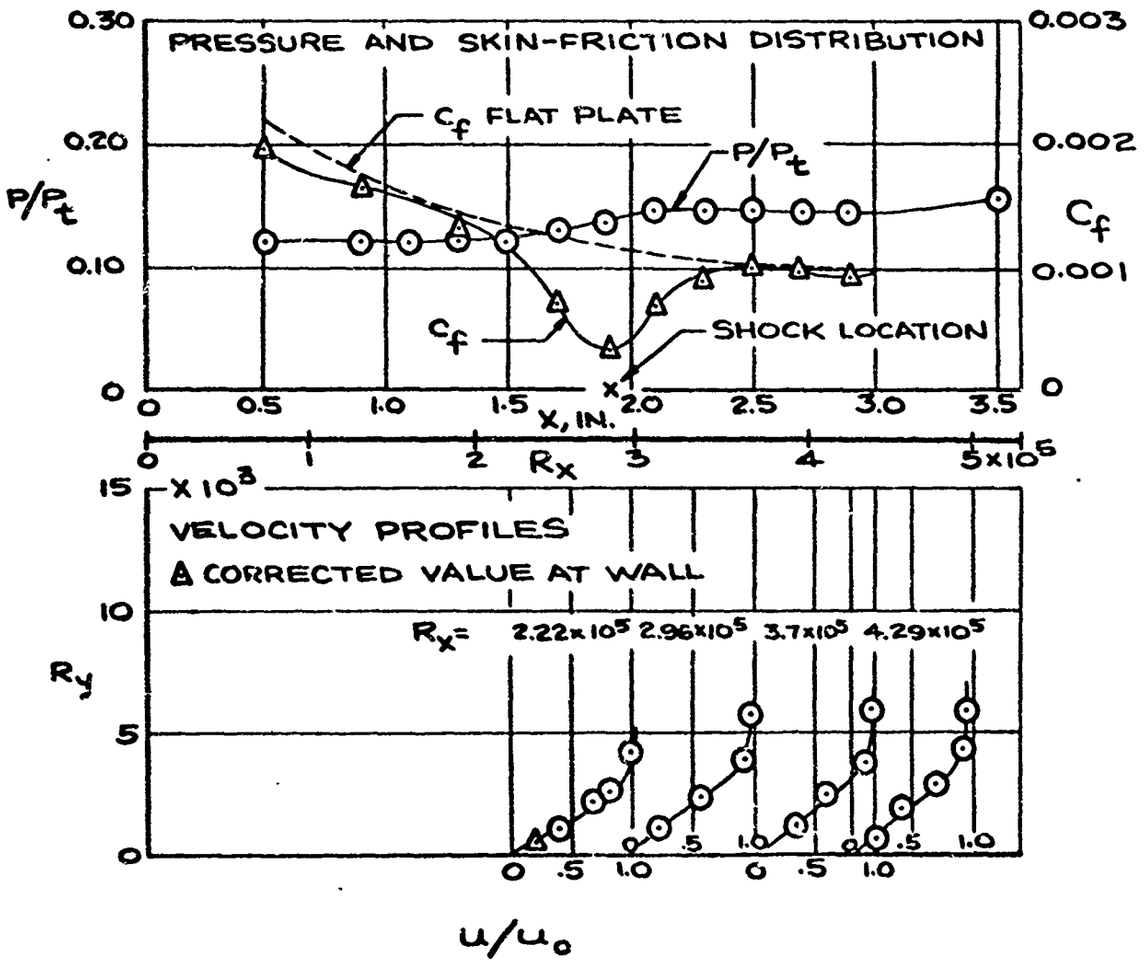

FIGURE 17

SAMPLE PRESSURE AND WALL SHEAR DISTRIBUTIONS AND VELOCITY PROFILES (AFTER HAKKINEN ET.AL. REF. 50)

$R_{x_{SHOCK}} = 2.96 \times 10^5$

$P_f/P_o = 1.40$

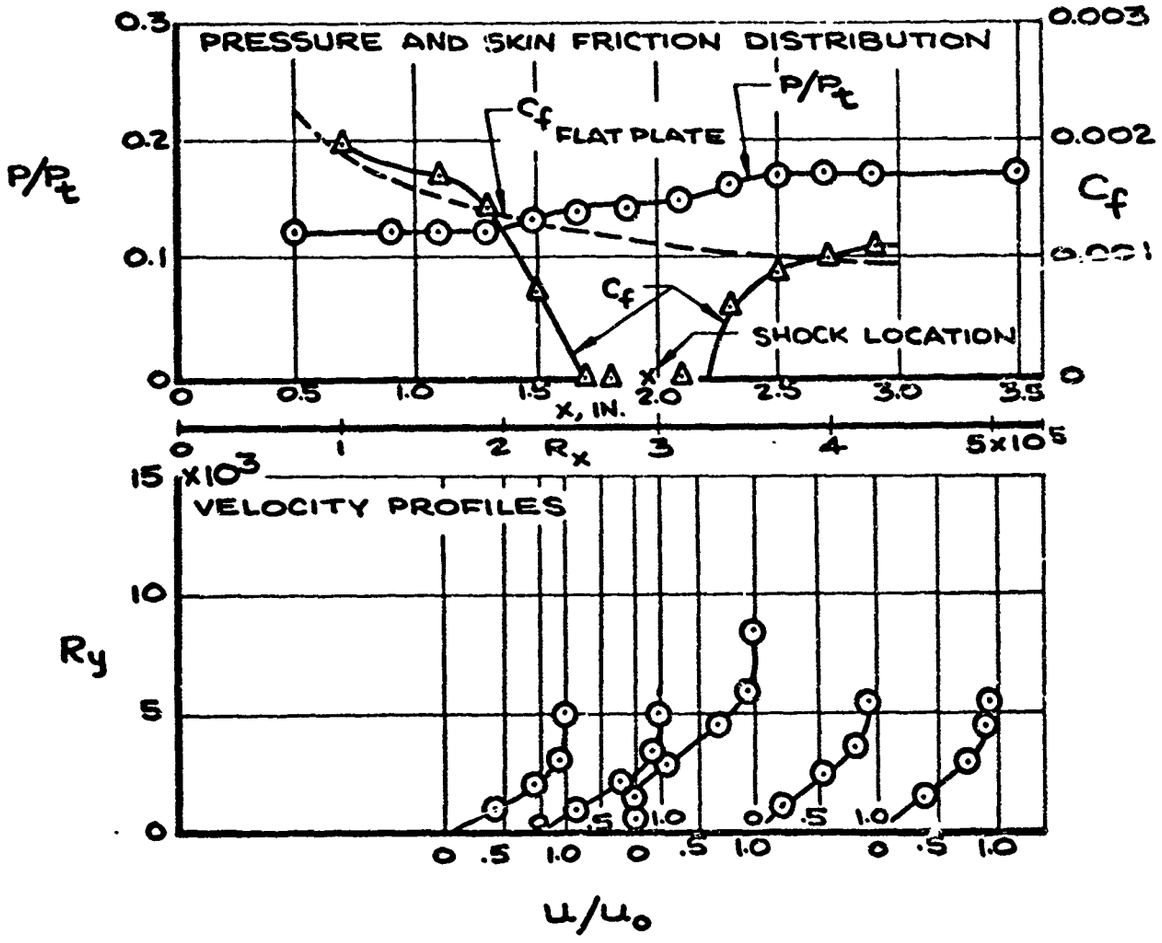

FIGURE 18

SAMPLE PRESSURE AND WALL SHEAR DISTRIBUTIONS AND VELOCITY PROFILES (AFTER HAWKINS ET. AL. REF. 50)

$R_{X_{SHOCK}} = 3.29 \times 10^5$

$P_f / P_o = 1.91$

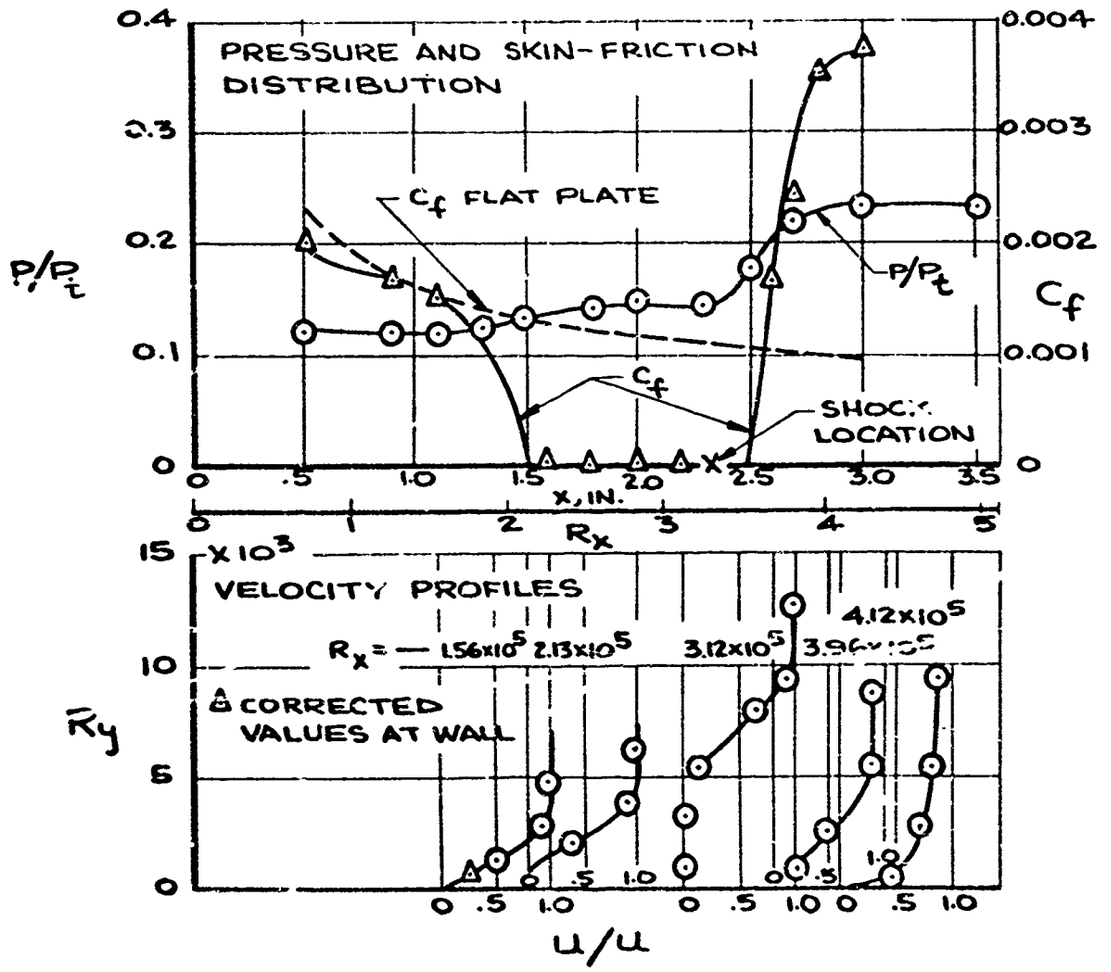

FIGURE 19

decreases but always remains positive. Downstream of impingement the boundary layer appeared to recover its normal thickness, and skin friction measurements returned approximately to the theoretical value.

In figure 18, the pressure rise associated with the incident shock system is sufficient to cause separation. The skin friction is close to that predicted by theory both upstream and downstream of reattachment. Negative values are indicated in the region of separation. Velocity profiles indicate that the flow in the mixing layer, i.e., outside of the reversal region, displays essentially the characteristics of the undisturbed constant pressure boundary layer.

The data in figure 19 also show that separation has occurred. Qualitatively, flow characteristics during the approach to separation and in the separated region itself, are similar to that shown in figure 18. However, the skin friction after reattachment is considerably greater than that predicted by laminar theory. The rather full velocity profile after reattachment indicates that the boundary layer underwent transition to turbulent flow.

The foregoing experimental results are limited only to one case - the impinging shockwave. However, the data presented do provide a qualitative insight to the general problem of skin friction in regions of separated and reattaching flows.

6. HEAT TRANSFER DISTRIBUTION

Limited work has been performed to determine the general effect of flow separation on heat transfer. Available results are difficult to compare owing to differences in geometry and flow conditions. No one has yet performed an extensive heat transfer evaluation covering a wide range of geometries and flow conditions similar to that performed on pressure distribution by Chapman, et al, reported in reference 37.

The only general remarks that can be made are as follows:

a. The local heat transfer coefficient within the separated region is usually smaller than the equivalent attached value.

b. The local heat transfer coefficient in the reattachment region normally exceeds the value for attached flow. In certain cases, the peak heating rate may approach the same order of magnitude as that at the stagnation point or leading edge, whichever analogy is most applicable to the situation.

c. The state of the flow is a critical parameter in determining the effects of flow separation and reattachment on the heat transfer rate.

The following discussion is organized by geometry with pertinent specific investigations discussed under each geometry.

6.1 Cavity Flows

There have been four main investigators of the problem of heat transfer to surfaces with cavities. There investigators were Chapman,[61] Larson,[62] Charwat, et al,[40] and Nicoll.[59] Charwat's, Larson's, and Nicoll's studies were experimental while Chapman's work was theoretical.

In all cases of interest here, the flow completely bridged the cavity and cavity dimensions were such that the lengths were large compared to the cavity depth, and depths were of the same order of magnitude as the mixing layer thickness.

6.1.1 Chapman's Theory

In reference 61, Chapman presented a theoretical analysis to determine the average heat transfer to a surface bounded by a separated flow. He assumed that the transfer properties in the mixing layer control the heat transmission, and his model consisted of a two-dimensional cavity with the flow separation and reattachment points at the upstream and downstream cavity edges, respectively. Three other major assumptions required were (1) constant pressure from separation through reattachment, (2) zero boundary layer thickness at the separation point, (3) no thermal resistance between the internal flow within the cavity and the wall, and (4) constant wall enthalpy.

After the discussion in the previous section on the pressure distribution, assumption 1 would seem grossly in error. However, close observation of the pressure distributions shown in figure 1.3 reveals that for laminar flows the reattachment region is small compared to the overall size of the separated bubble, and that the pressure is nearly constant from just after separation to just before reattachment (for forward facing steps there is no pressure rise at reattachment). Hence, the high pressure region at reattachment will, in many cases, have only a negligible effect on the average heat transfer, since the area it influences is small compared to the total area.

The second assumption is invoked in order to achieve similarity in the velocity and temperature profiles within the mixing layer. This is rather restrictive, since strictly speaking, it limits the applicability of this analysis to leading edge type problems. Some recently

obtained information (references 22 through 27) may aid in removing this assumption.

Assumption 3 is a simplification justified by the assumption that the transfer properties in the mixing layer control the energy transfer to the wall. The fourth assumption was made due to lack of pertinent experimental evidence to the contrary. If information is obtained indicating this to be a bad assumption, the method of reference 63 may be used to account for a variable wall enthalpy.

Chapman found the laminar separated heat transfer rate to be independent of Mach number and Reynolds number. Performing a heat balance by integrating around the closed contour formed by the cavity wall and the dividing streamline, he calculated a constant value of 0.56 for the ratio of the average laminar separated heat transfer rate to that for laminar attached flow. For turbulent flow, this same calculated ratio is a function of Mach number; the value at a Mach number of zero is 6.3, while at a Mach number of 1.6, this ratio is 2.8. These are the only values presented by Chapman due to a lack of information describing the rate of growth of a turbulent mixing layer, which is a critical parameter in determining the heat transfer rate.

6.1.2 Larson's Heat Transfer Experiments

By measuring the average heat transfer rate to both two-dimensional and axisymmetric cavities, Larson attempted to verify Chapman's results in a wind tunnel program described in reference 63. His experimental data support Chapman's theoretical value of heat transferred from a separated laminar boundary layer since he obtains a value of 0.5 for the previously mentioned ratio for both two-dimensional and axisymmetric flows. However, for the turbulent case, he obtained a ratio of about 0.60, this ratio being nearly independent of Mach number, but proportional to Reynolds number to the minus 1/5 power. His conclusion was that good agreement was obtained for the laminar

separation, but that the turbulent theory and experimental values approached one another only at high Mach numbers.

6.1.3 Charwat's Investigation

In reference 40, Charwat, et al, postulates that there are three basic mechanisms controlling the heat transmission from (or to) the flow in a separated region: (1) conduction through the mixing layer; i.e., Chapman's hypothesis, (2) conduction between the cavity wall and the internal flow, and (3) mass exchange between the internal and external flows. While all three of these mechanisms may exist in all separated flow geometries, one of the three may be dominant for a given geometry and set of flow conditions.

As has been pointed out, Chapman's theoretical analysis indicated that upon transition from a laminar to a turbulent mixing layer, there is an abrupt increase in the average heat transfer rate to a surface immersed in separated flow, while Larson's experimentally determined values do not verify this abrupt change. Hence, it appears that Chapman's model is incorrect for the turbulent case. Therefore, Charwat proposed an experimental study to determine if, for a turbulent mixing layer, there is significant mass exchange between the external and internal flows. A second portion of the program was concerned with determining both the distribution and the average value of the heat transfer coefficient at the cavity walls. It has already been pointed out in Section 3.6 that Charwat detected considerable mass exchange accompanying the unsteadiness of a turbulent mixing layer. In addition, it was found that the primary parameter affecting both the average heat transfer coefficient and the heat transfer coefficient distribution was the turbulent boundary layer thickness prior to separation. For the boundary layer-step height considered in the experiments it was found that the thicker the boundary layer, the greater the heat transfer coefficients.

The study revealed that regardless of the boundary layer thickness, the heat transfer coefficient dropped to a minimum value (less than the attached value) immediately downstream of the separation point. Increasing the cavity length tended to decrease this minimum further. Downstream of this minimum the heat transfer coefficient increases through recompression to a maximum at reattachment; this maximum being, in all cases shown, greater than the attached value that would exist at that point.

For thin oncoming boundary layers, increasing the cavity length appeared to sharply increase the maximum heat transfer at recompression for small values of length to depth ratio. For large values of length to depth ratio, the above affect was not observed. For thick boundary layers, increasing the cavity length appears to result in a steadily increasing maximum at reattachment regardless of the length to depth ratio.

As the thickness of the boundary layer increases, the heat transfer coefficient at each point within the cavity increases and the location of the rise in heat transfer coefficient through recompression shifts closer to the separation point. Thus, it is quite conceivable that both the total and the average heat transfer rate over the separated region could be higher than that obtained with an attached flow if the oncoming turbulent boundary layer were sufficiently thick.

In the appendix of reference 40, Charwat presents an approximate analysis of a simplified mass exchange model based on the conservation of momentum. The analysis yields the following result for the mean Stanton number:

$$\overline{St} = \frac{1}{\phi}\left(\frac{\delta s}{L}\right) \qquad (4.1)$$

where δs is the mixing layer thickness just prior to recompression, L is the cavity length, and ϕ is a function of the slope of the mixing layer velocity profile at the mean vertical location about which this mixing layer oscillates.

Several trends can be noticed from this equation:

a. The heat transfer coefficient will increase with increasing mixing layer thickness; thus, the heat transfer coefficient will increase with boundary layer thickness since these two thicknesses are proportional.

b. Since ϕ appears to be of the order of magnitude of 1 from theoretical analyses, this equation predicts that the Mach number and Reynolds number dependence is contained solely in the parameter δ_s/L.

(1) In laminar flow $(\delta_s/L)_{lam.} \sim R_x^{-1/2}$, hence

$$St_{sep.} \sim R_x^{-1/2} \sim h_{sep.} \tag{4.2}$$

and since

$$h_{f.p.} \sim R_x^{-1/2} \tag{4.3}$$

where $h_{f.p.}$ is the flat plate heat transfer coefficient,

$$\left.\frac{h_{sep.}}{h_{f.p.}}\right|_{lam} = \text{constant} \tag{4.4}$$

(2) In turbulent flow, thin boundary layer data yield the following:

$$(\delta_s/L)_{turb.} \sim R_x^{-2/5} \tag{4.5}$$

therefore,

$$St_{sep.} \sim R_x^{-2/5} \tag{4.6}$$

and since

$$St_{f.p.} \sim R_x^{-1/5} \qquad 4.7$$

$$\left.\frac{h_{sep}}{h_{f.p.}}\right|_{turb.} \sim R_x^{-1/5} \qquad 4.8$$

It is to be noted that this simplified analysis agrees with Larson's experimental data since he found for laminar flow that $h_{sep}/h_{f.p.}$ is independent of Mach number and Reynolds number and for turbulent flow $h_{sep}/h_{f.p.} = R_x^{-1/5}$, i.e. a function only of Reynolds number.

In summary then, Charwat et al have shown that the heat transfer coefficient distribution on the cavity floor for a turbulent mixing layer is dependent upon the boundary layer thickness prior to separation. The thicker the boundary layer, the higher the average heat transfer coefficient. In addition, it was shown analytically that for the turbulent case the heat transfer coefficient ratio is proportional to the boundary layer thickness, i.e. $\delta \sim R^{-1/5}$ when the mechanism controlling the heat transfer is the mass exchange between the separated region and the external flow.

6.1.4 Nicoll's Investigation

Only recently, Nicoll[59] has reported the results of an experimental study of heat transfer for laminar hypersonic flow over various annular cavities in a 20° cone, figure 20 below.

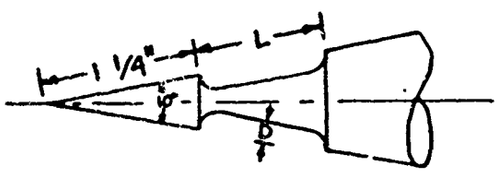

CONFIGURATIONS TESTED		
L(IN.)	D(IN.)	L/D
5/16	1/8	2.5
5/16	3/32	3.33
5/8	1/8	5.0
5/8	3/32	6.67
5/8	1/16	10.0
11/4	1/8	10.0
11/4	3/32	13.33
11/4	1/16	20.0

NICOLL'S EXPERIMENT

FIGURE 20

Measurements were made to determine the pressure, recovery factor, and heat transfer coefficient on the cavity floor and in the vicinity of reattachment. The study was conducted in a helium tunnel at a Mach number of 11. Reynolds number, cavity length-depth ratio, and reattachment region geometry were the controlled variables of the experiment.

The main results of Nicoll's investigation may be summarized as follows:

a. The recovery factory is essentially constant within the cavity and downstream of reattachment, and it is approximately equal to the value for laminar attached flow.

b. The local heat transfer coefficient is low on the cavity floor, about 10 to 20 per cent of the attached value.

c. The local heat transfer coefficient is high (several times the attached value) in the vicinity of reattachment.

d. The region of influence of significant flow disturbance due to the presenece of a cavity extends about one cavity length downstream of reattachment.

Figure 21 shows an example of a typical result of the study. The meaning of statements b, c, and d is apparent. It is important to note that although the reduction in heat transfer rate in the cavity averaged about 45% of the attached value, it was reduced to about 20% when the integration included at least one cavity length downstream. Also considered in the experiment was the effect of reattachment point geometry. Changing the shape (rounding the edge of the shoulder at reattachment) was found to have little effect on the characteristics of an open cavity laminar flow. Results of the tests were compared with the results of Chapman's theoretical analysis.[61] The integrated heat-transfer rate for a laminar cavity flow gave good agreement with experiment at least for short, deep cavities with thin boundary layers at separation.

LOCAL HEAT TRANSFER COEFFICIENT FOR CAVITY FLOW

M= 11, P_o = 700 PSIA

(AFTER NICOLL, REFERENCE 59)

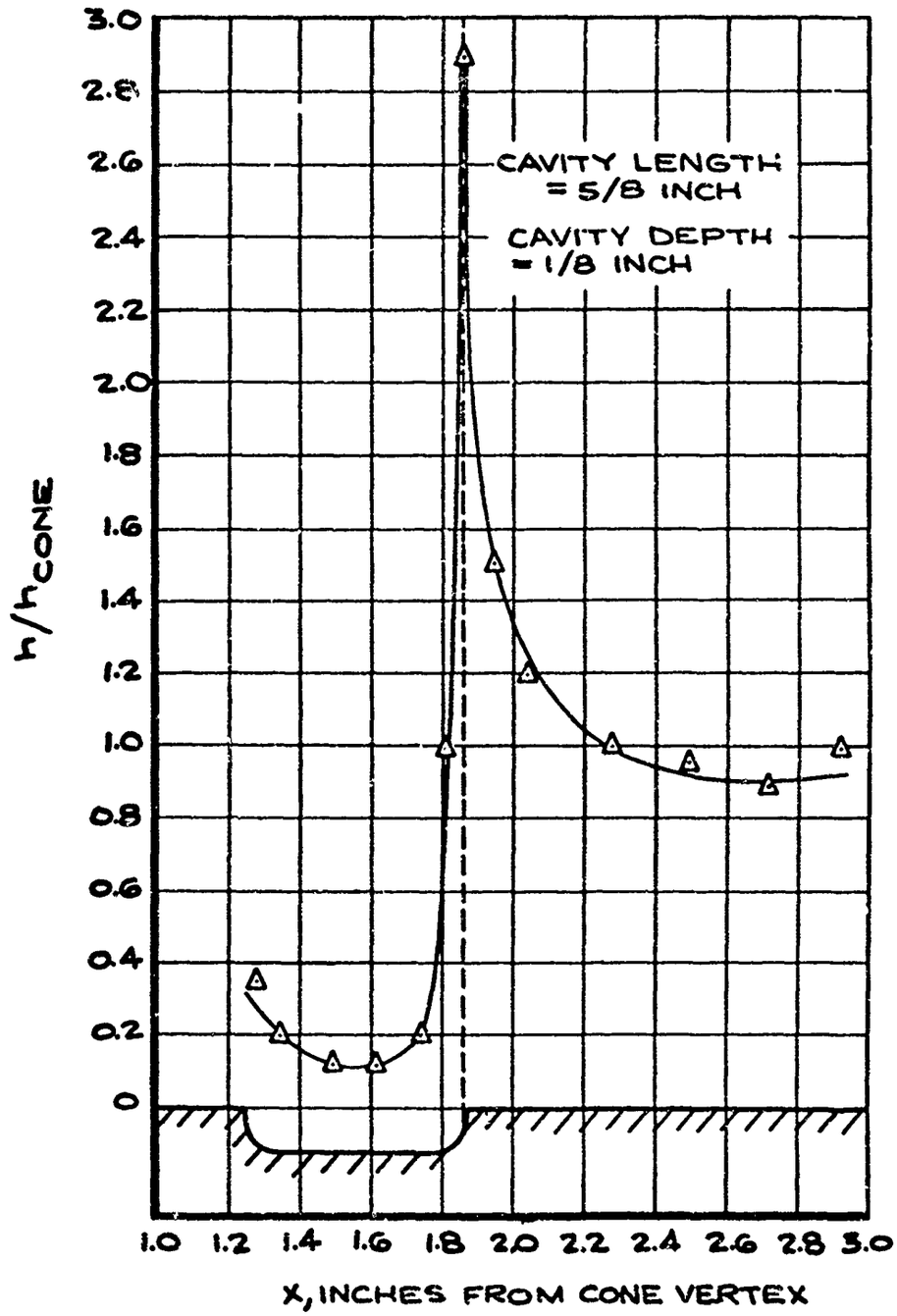

FIGURE 21

6.1.5 Centolanzi's Investigation

R. J. Centolanzi has recently published the results of a wind tunnel study in reference 64. The sketch below (figure 22) illustrates a typical configuration investigated.

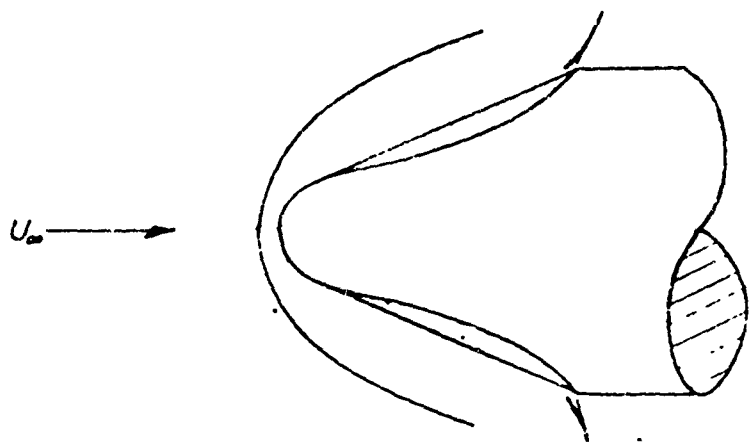

CENTOLANZI'S INVESTIGATION

FIGURE 22

As has been seen in paragraph 6.1.1, Chapman's theory[62] predicts that for a negligible boundary layer thickness at the separation point, the integrated average heat transfer rate to an open cavity with a laminar mixing layer would be reduced by approximately a factor of two. Since it would seem logical that by modifying a nose cone as shown in the sketch, one could capitalize upon this phenomenon, a study of this possibility was initiated by Ames Research Center, reference 64. There were two major results:

a. The data show that lowering the wall temperatures moves the transition point upstream, indicating that wall cooling may have a destabilizing influence on the flow. This is opposite to the effect of wall temperature on an attached boundary layer.

b. It was found that the heat transfer rate in the forward portion of the separated region was indeed below the attached value for the standard cone-sphere for all configurations. This was followed by a rise to a maximum in the reattachment region which was several times that for the standard sphere-cone.

Contrary to Chapman's theory, the total heat transferred was found to be in excess of that obtained for attached flow. This discrepancy was attributed to the geometry of the model being such that the flow reattached within the cavity. The author of reference 64 argued that better agreement would have been obtained if the limits of integration in the theory were altered to cover only that portion of the surface actually immersed in a separated flow instead of over the whole cavity. Unfortunately, this could not be done because the location of reattachment was not known. It is also evident that the region near reattachment has a larger surface area than further upstream due to the "conical" shape; hence, a high heating rate in this region would have a large effect on the total heat transferred.

6.1.6 Surface Distortions

The concept of a single cavity may be extended to include multiple adjacent cavities, or surface distortions. Two recent investigations[65,66] have been performed to determine the perturbations to the local heat transfer coefficient arising from such geometries.

6.1.6.1 AEDC Investigation

A wind tunnel program has been completed at the Arnold Engineering Development Center where the wall surface was distorted by placing spanwise hemi-cylinders normal to the oncoming flow on a flat plate at zero angle of attack. Another configuration was formed by a sine wave variation of the surface. Both sharp and blunt flat plate leading edges were tested. Selected results of this program are presented in reference 65.

6.1.6.2 NASA Investigation

A similar investigation was performed at the Langley Research Center (reference 66). The models consisted of flat plates with various wall distortions inserted, the tests were run for laminar boundary layers only. The particular wall distortion of interest in this portion of the report is the sinusoidal cavity shown in figure 23. The curve in this figure shows the following results:

a. The maximum heat transfer coefficient, i.e. that at the reattachment point, is independent of Mach number within the limit of the scatter.

b. The maximum heat transfer coefficient decreases with increasing boundary layer thickness (the laminar displacement thickness δ_o^* is proportional to the boundary layer thickness).

Both of these dependencies lend credence to Chapman's model, since:

a. His results were independent of Mach number.

b. If the maximum heat transfer coefficient decreases with increasing mixing layer thickness (mixing layer thickness is proportional to boundary layer thickness, hence, is proportional to displacement thickness), it seems logical that the transfer properties of the mixing layer are controlling the heat transmission.

6.1.7 Summary of Results on Cavities

In light of the foregoing, the following statements may be made concerning the heat transfer to a cavity:

a. If there is zero or negligible boundary layer development prior to the separation point, then the heat transfer coefficient in the separated region will be lower than the

CORRELATION OF MAXIMUM HEAT TRANSFER COEFFICIENT WITH THE LAMINAR DISPLACEMENT THICKNESS TO CAVITY HEIGHT FOR FLOW OVER A SINE WAVE CAVITY (AFTER BERTRAM AND WIGGS REF. 66)

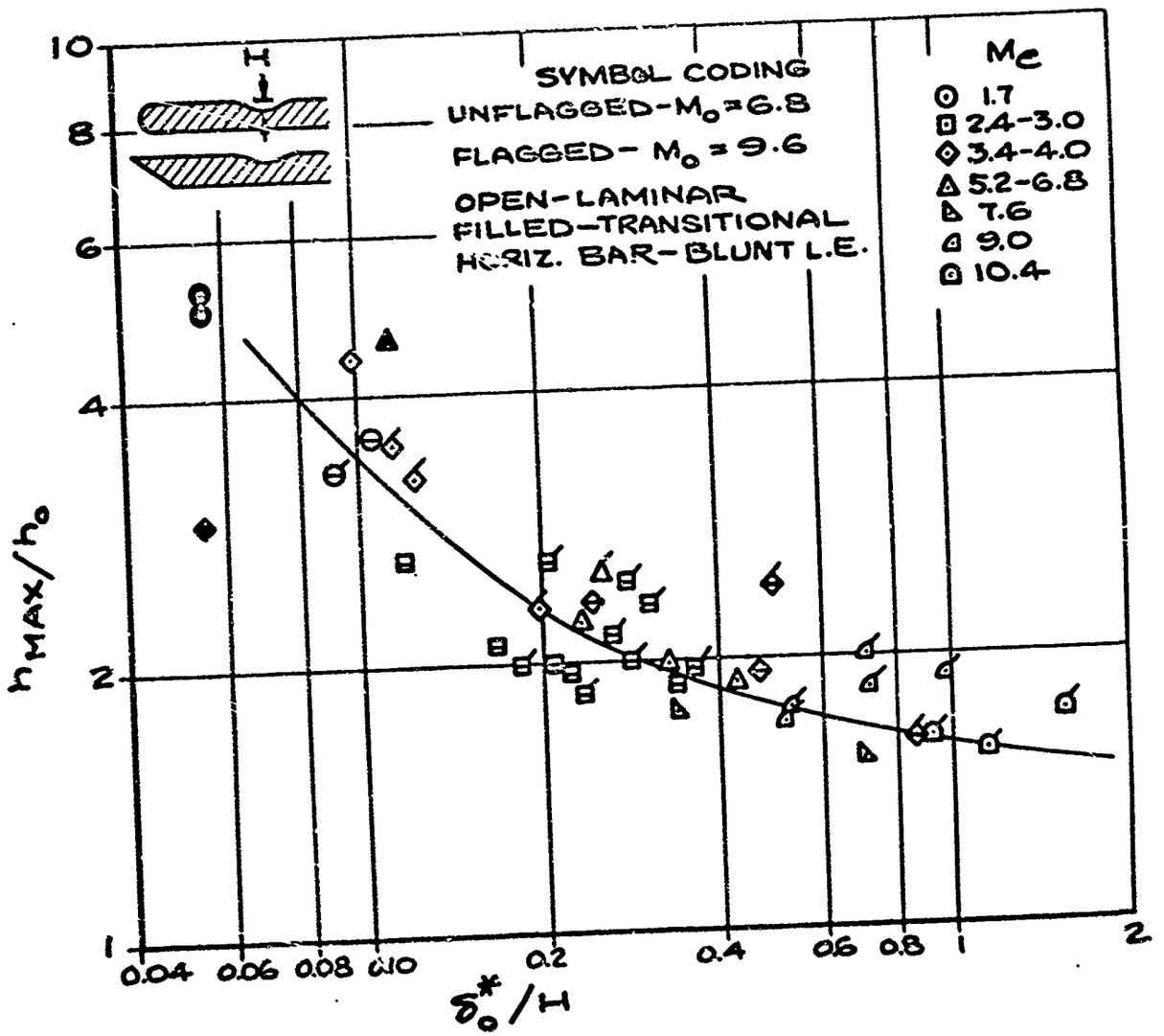

FIGURE 23

attached value and can be predicted using Chapman's theoretical model. However, care must be exercised when attempting to obtain the average and/or total heat transfer to the cavity wall to insure that the high heat transfer rates at the reattachment point and some distance downstream are adequately accounted for.

b. If a boundary layer does exist at the separation point, then the state of flow becomes critical in determining the heat transfer:

(1) If the flow is laminar throughout the separated length, heat transfer will be controlled by the transfer properties within the mixing layer. This will result in an inverse dependence of heat transfer coefficient on oncoming boundary layer thickness.

(2) If the flow is turbulent throughout the separated length, the heat transfer will be controlled by the mass exchange between the internal and external regions. This will result in the heat transfer coefficient being directly dependent on the oncoming boundary layer thickness.

6.2 Two-Dimensional Compression Corner

D. S. Miller, et al, in reference 48, have presented some of the results of a high Mach number heat transfer investigation conducted in the Boeing Hot-Shot Facility. The data they presented were for a two-dimensional compression corner with laminar separation taking place. Figure 24 is taken from this reference. The pressure distribution is shown for comparison purposes.

Both curves follow the undisturbed flow variation up to the beginning of interaction. At this point (where the pressure gradient is first

PRESSURE AND HEAT TRANSFER DISTRIBUTION FOR LAMINAR SEPARATION AT A TWO-DIMENSIONAL COMPRESSION CORNER (AFTER MILLER, HIJMAN AND CHILDS REF. 48)

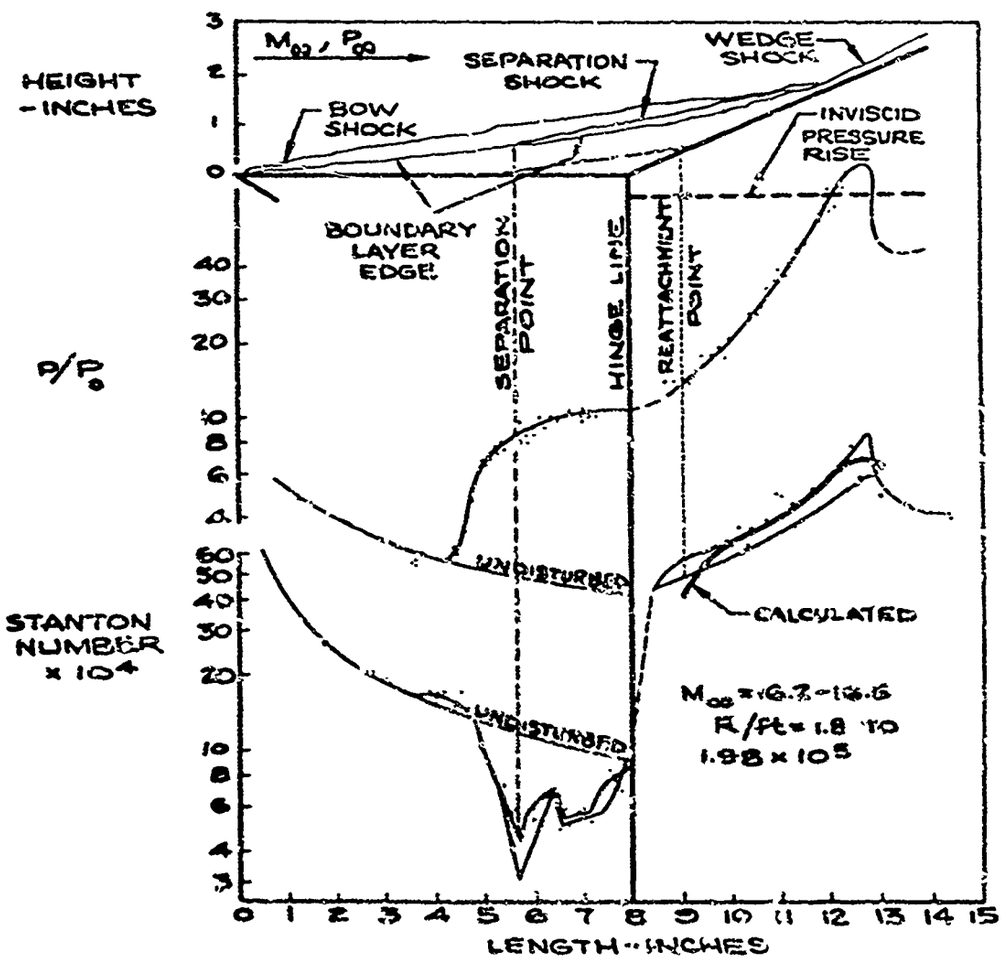

FIGURE 24

observed by the flow), there is a slight rise in Stanton number, this rise possibly being due, according to Miller, to the formation of a spanwise vortex at the separation point, similar to the vortex found at separation by Charwat.[39,40] Immediately after this slight rise, the Stanton number drops tc about 0.50 of the attached value in the region signified by the plateau pressure. The Stanton number then rises through reattachment, this rise appearing to correlate well with the pressure increase, i.e., the maximum heat transfer coefficient occurring at peak pressure. Note that this maximum value of Stanton number is higher than that measured near the leading edge of the flat plate (it is not clear from the reference why two curves are shown for the heat transfer distribution). There appears to be good agreement between the experimental rise in heat transfer coefficient and the calculated curve obtained using the method of Bertram and Feller from reference 67. This method is applicable to those problems where pressure varies as the length raised to some positive or negative power, and consists of correcting the heat transfer coefficient for both the gradient and the local value of the pressure.

6.3 Axisymmetric Compression Corner

NASA has sponsored two experimental programs investigating the pressure and heat transfer distributions along the wall of an axisymmetric compression corner. The two programs differed in Mach number but had similar model shapes and unit Reynolds number.

6.3.1 Becker and Korycinski

Becker and Korycinski have presented the results of a wind tunnel program in reference 68. The models were basic ogive-cylinder with either a 10° or 30° flared skirt. The nose was a von Karman minimum drag shape of fineness ratio 5 with a 10° half-angle cone at the tip. The cylindrical section was also 5 diameters long. The data includes all three regimes; i.e., laminar, turbulent, and transitional. Typical results of the study are shown in figures 25, 26, and 27.

PRESSURE COEFFICIENT AND HEAT TRANSFER DISTRIBUTION FOR PURE LAMINAR SEPARATION AT AN AXI-SYMMETRIC FLARED SKIRT (AFTER BECKER AND KORYCINSKI REF. 67)

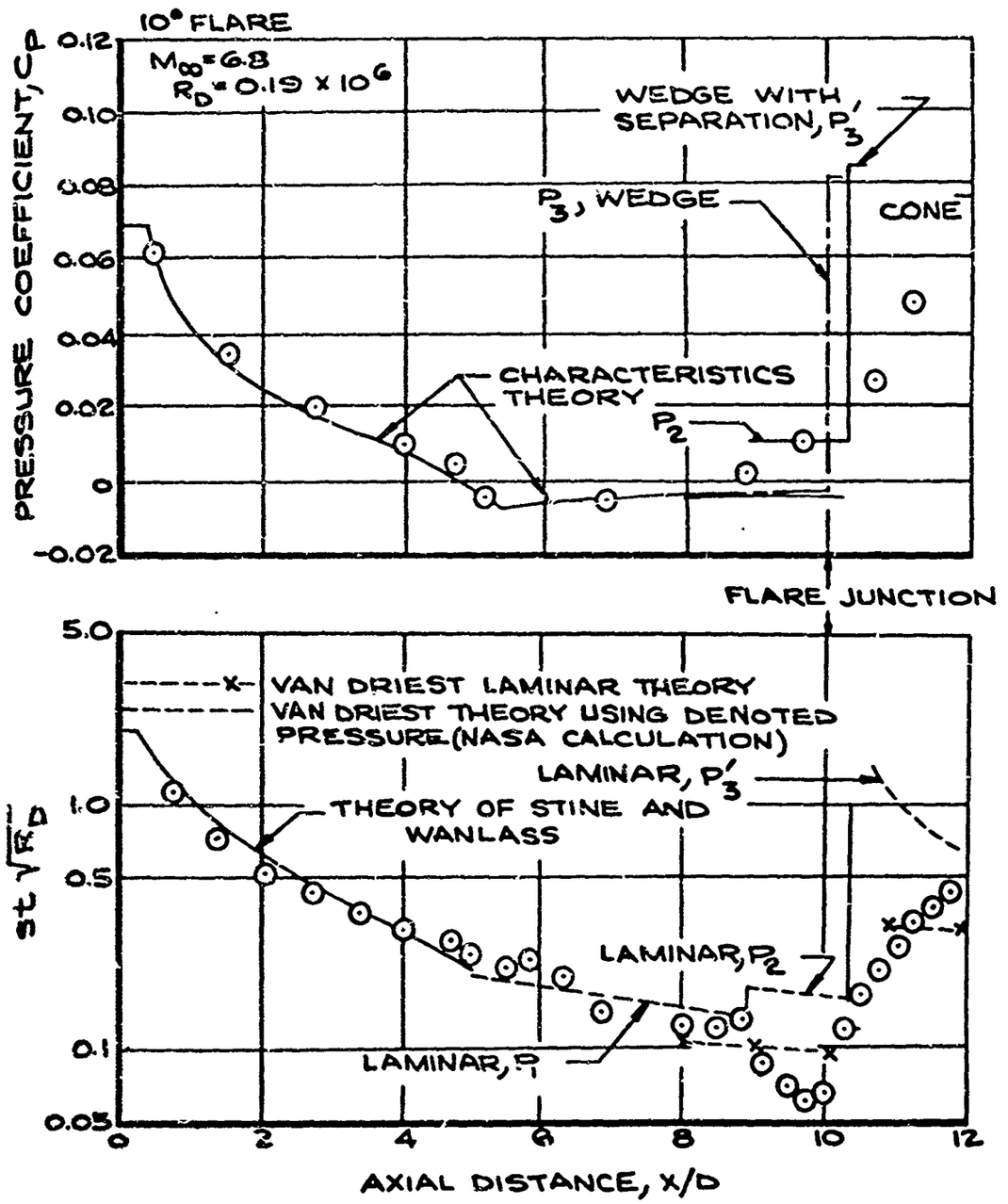

FIGURE 25

PRESSURE COEFFICIENT AND HEAT TRANSFER DISTRIBUTION FOR TRANSITIONAL SEPARATION AT AN AXI-SYMMETRIC FLARED SKIRT (AFTER BECKER AND KORYCINSKI REF. 67)

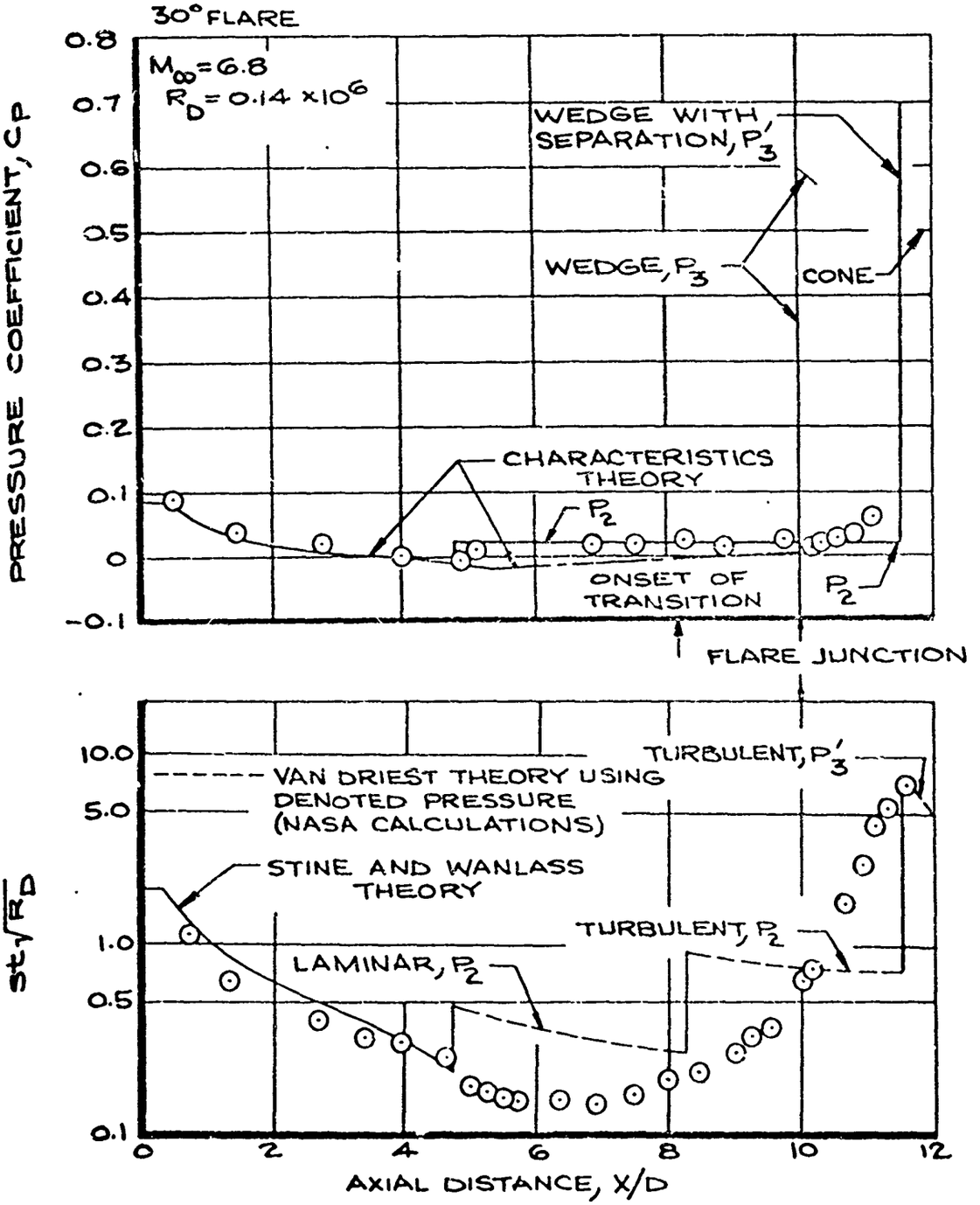

FIGURE 26

PRESSURE COEFFICIENT AND HEAT TRANSFER DISTRIBUTION FOR TURBULENT SEPARATION AT AN AXI-SYMMETRIC FLARED SKIRT (AFTER BECKER AND KORYCINSKI REF. 67)

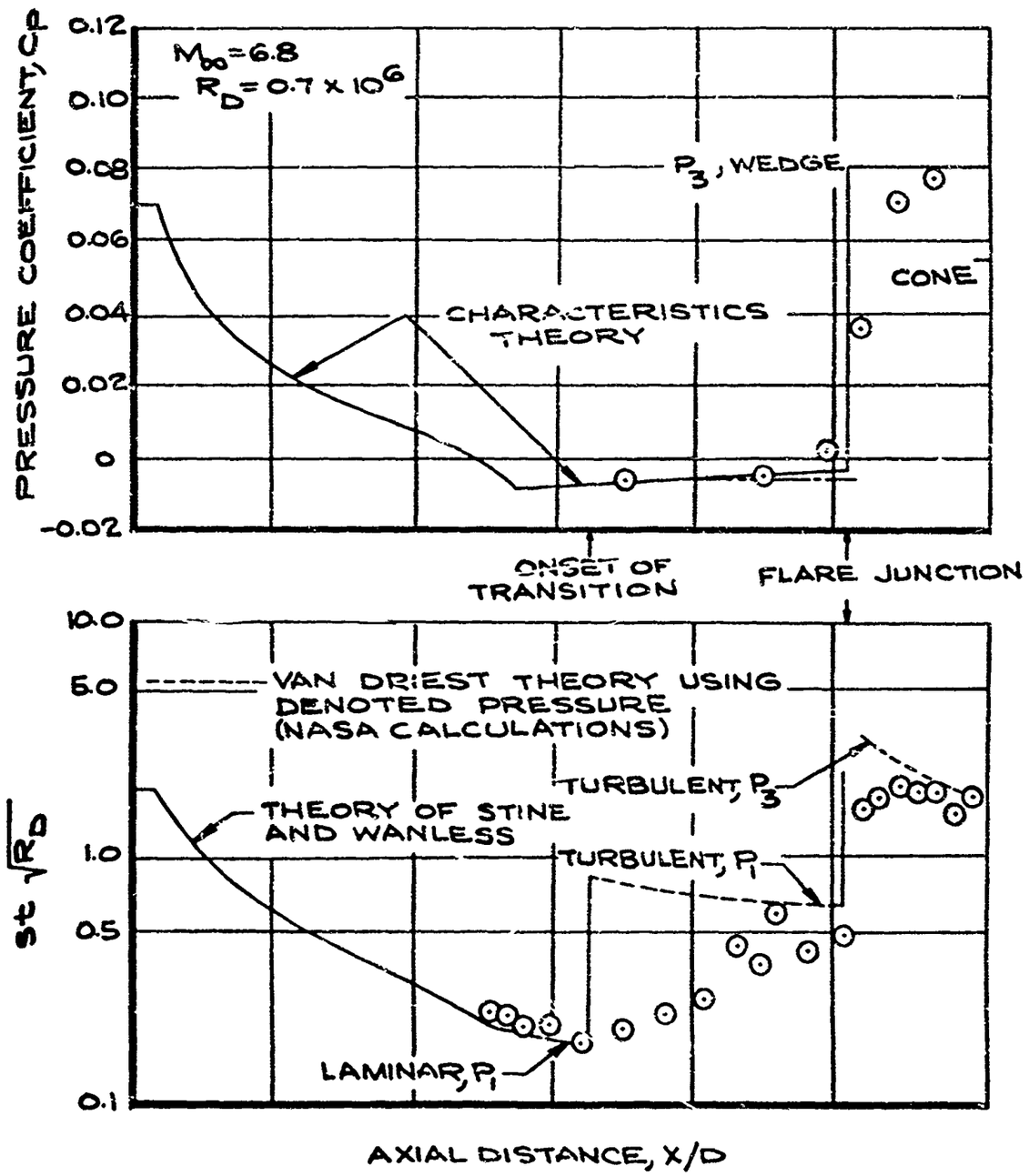

FIGURE 27

For comparison purposes, theoretical calculations using the method of van Driest[69] and pressures corrected to account for the presence of flow separation. The pressures used are defined as follows:

a. P_1 is the pressure on the cylinder as computed by characteristics theory.

b. P_2 is the estimated plateau pressure that exists for the laminar case and for the transitional case when transition is near reattachment.

c. P_3 is the inviscid two-dimensional (wedge) pressure at the flare body juncture calculated by starting with P_1 on the cylinder.

d. P_3' was calculated by starting with the plateau pressure P_2 and taking the flow deflection at reattachment as the flare body angle minus the inclination angle of the "wedge" formed by the separated region. In this case, the measured separation "wedge" angles were 3° for the 10° flare and 7° for the 30° flare.

In calculating the heat transfer distribution on the cylinder, it was assumed that the boundary layer started at the nose. The heat transfer distribution calculated for the flare utilizes the reattachment point as the origin of the boundary layer.

6.3.1.1 Laminar Case

Figure 25 presents the data gathered for the laminar case. As can be seen, the experimental points follow the theoretical curve down to the beginning of the interaction of the boundary layer with the pressure gradient. Immediately downstream of this point, the experimental values of the parameter $St\sqrt{R_D}$ drop to about one-half of the attached value, then increases through reattachment to about 1/4 of the nose value.

At the beginning of the flow interaction with the pressure gradient, the NASA's theoretical predictions (dashed curve without X's) indicate an increase in the heat transfer due to the increase in pressure to the plateau value. Of course, this calculation is invalid since it is based on van Driest[69] attached flow theory while in actuality, this is the separated region; thus, the discrepancy between experimental and theoretical values. At reattachment, the theoretical curve is based on P_3' and the origin of the running length for the laminar van Driest[69] theory is taken at the reattachment point. This results in the curve labeled "laminar P_3'" in figure 25 and, as can be seen, the theoretical and experimental values appear to approach one another.

6.3.1.2 Transitional Case

Again, the experimental heat transfer distribution follows the theoretical curve until the interaction point, as illustrated in figure 26. At this location, there is a slight hump in the heat transfer distribution, then the experimental values of $St\sqrt{R_D}$ drop below the attached value at the separation points, although not quite to half of it. This condition exists until transition takes place, where there is a rise, this rise becoming steeper until reattachment is accomplished where the heat transfer parameter is about 3.5 times that at the nose. (Note that the flare angle in this case is 30°.) Comparison with the pressure distribution shows good agreement at the separation point. However, the pressure data do not indicate the abrupt rise characteristic of transition and do not extend all the way to reattachment.

Similar theoretical calculations were for the transitional case. Again in the separated region, the theory ("laminar P_2" in the figure) based on the increased plateau pressure yields an increase instead of a decrease in the heat transfer coefficient. At the transition point, the theory is shifted from laminar to turbulent, still using P_2, since there is no evidence of a pressure increase due to transition. This

curve crosses the experimental points as they rise through reattachment, but only predicts a value for the heat transfer coefficient of about 0.10, the final value at reattachment. The theoretical value at the reattachment point based on P_3' appears to agree quite well except that it is decreasing with running length much faster than the data. Thus, this method could lead to over-optimistic predictions at points downstream of reattachment.

6.3.1.3 Turbulent Case

Figure 27 is for a completely turbulent mixing layer and may be directly compared to the laminar flow situation, since all conditions are the same except the Reynolds number. The experimental data are not complete prior to separation; however, the previous figures indicate that there should be good agreement between theory and experiment in this region. The value for $St\sqrt{R_D}$ begins to increase at the beginning of transition; however, it is not a step rise because transition from laminar to turbulent flow is accomplished over a finite distance. This rise continues through reattachment to a value equal to that at the nose, this maximum occurring at maximum pressure.

The calculated heat transfer distribution uses laminar flow theory up to the point where the beginning of transition was detected. Downstream of this point, turbulent flow theory was used. The theoretical attached flow pressure distribution on the cylinder was used up to the cylinder-flare junction because the separated region was too small to cause any gross distortions of the pressure distribution. However, the last experimental pressure point on the cylinder is higher than the attached value, indicating that a pressure gradient does indeed exist. In any case, the heat transfer parameter in the transitional regime approaches the turbulent theory as transition tends toward completion. Since the separated region is small, the position of reattachment was not discernable; therefore, the origin of the running length was taken at the flare-cylinder junction. In this case, the theory and experimental points appear in fairly good agreement,

converging to the same value downstream of reattachment. The theory used for the flare in this case was based on the attached flow wedge pressure since the flow separation "wedge" angle could not be defined.

6.3.2 Ferguson and Schaefer

Ferguson and Schaefer[70] have presented the results of an investigation very similar to the preceding one, the main differences being the test Mach number and that a cone-cylinder instead of the ogive-cylinder was used. Also, only the pure laminar and transitional cases were investigated.

Figures 28 and 29 are from this reference and, as can be seen, there is no decrease in heat transfer within the separated region for either case. A possible explanation for this in the transitional case is that transition occurred very near the separation point, thus producing a much more energetic separated region. The reason no decrease appeared in the laminar case is not apparent. The pressure coefficient on the cylinder is zero in figure 28 because of a fault in the experimental apparatus.

In both figures, theoretical calculations are shown. The solid curves are Douglas calculations by the theory of reference 69, and the dotted and dot-dashed curves are NASA calculations using the theory of references 71 and 72.

In figure 28, the laminar van Driest[69] theory compares well with that of Reshotko[71] on the cylinder up to the junction. On the flare, the NASA calculations take into account the pressure gradient; hence, they show an increase in heat transfer coefficient with running length, whereas the constant pressure van Driest calculations show a decrease. In both cases, the running length is taken from the nose. It is interesting to note the temperature labels on the two NASA laminar curves. The present authors feel that there has been a misprint and that the labels should be reversed since the Stanton number decreases with increasing wall temperature (see reference 69, figure 6).

PRESSURE COEFFICIENT AND HEAT TRANSFER DISTRIBUTION FOR A LAMINAR SEPARATION AT AN AXI-SYMMETRIC FLARED SKIRT (AFTER FERGUSON AND SCHAEFER REF. 70)

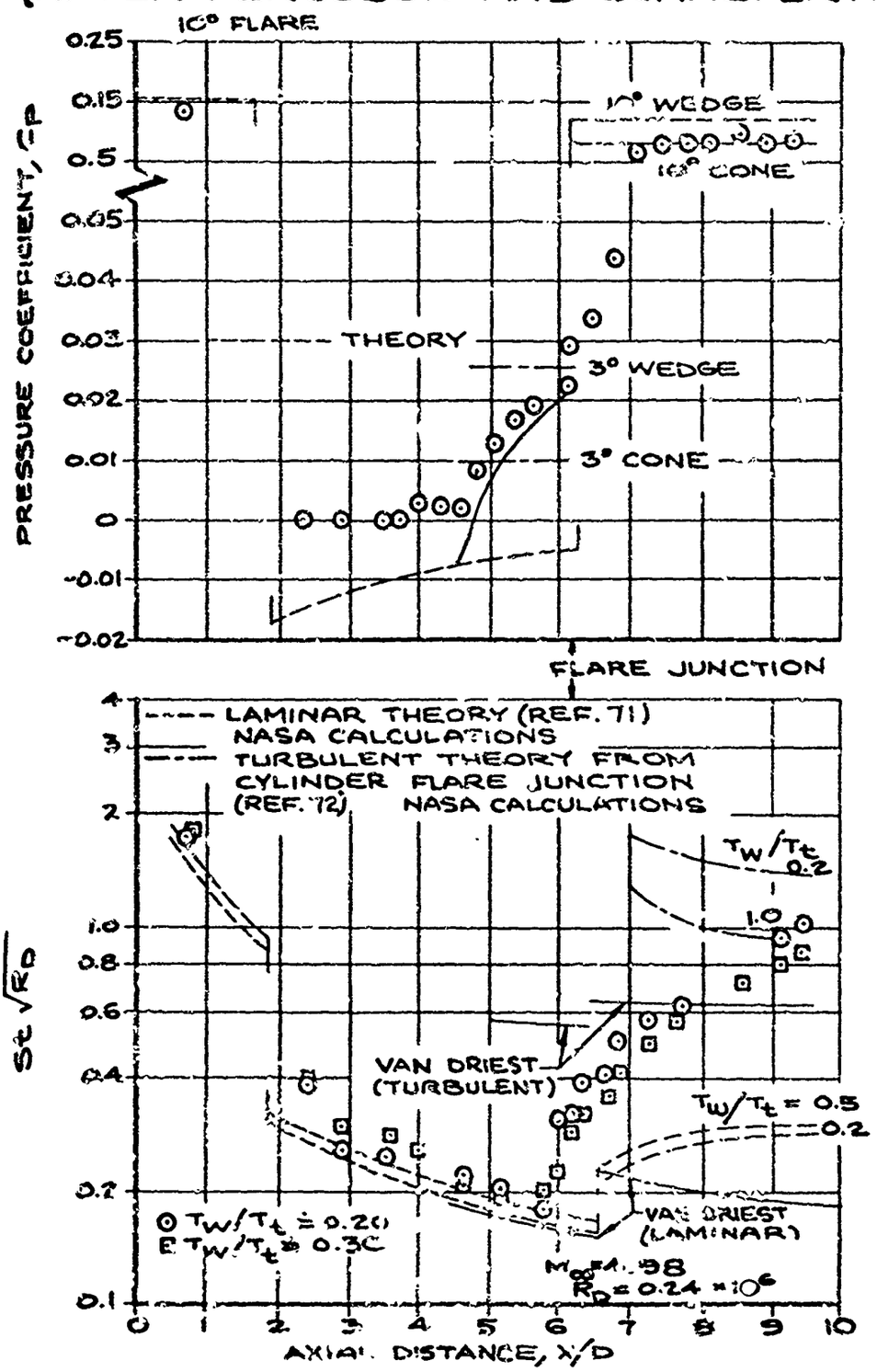

FIGURE 28

PRESSURE COEFFICIENT AND HEAT TRANSFER DISTRIBUTION FOR TRANSITIONAL SEPARATION AT AN AXI-SYMMETRIC FLARED SKIRT (AFTER FERGUSON AND SCHAEFER REF. 70)

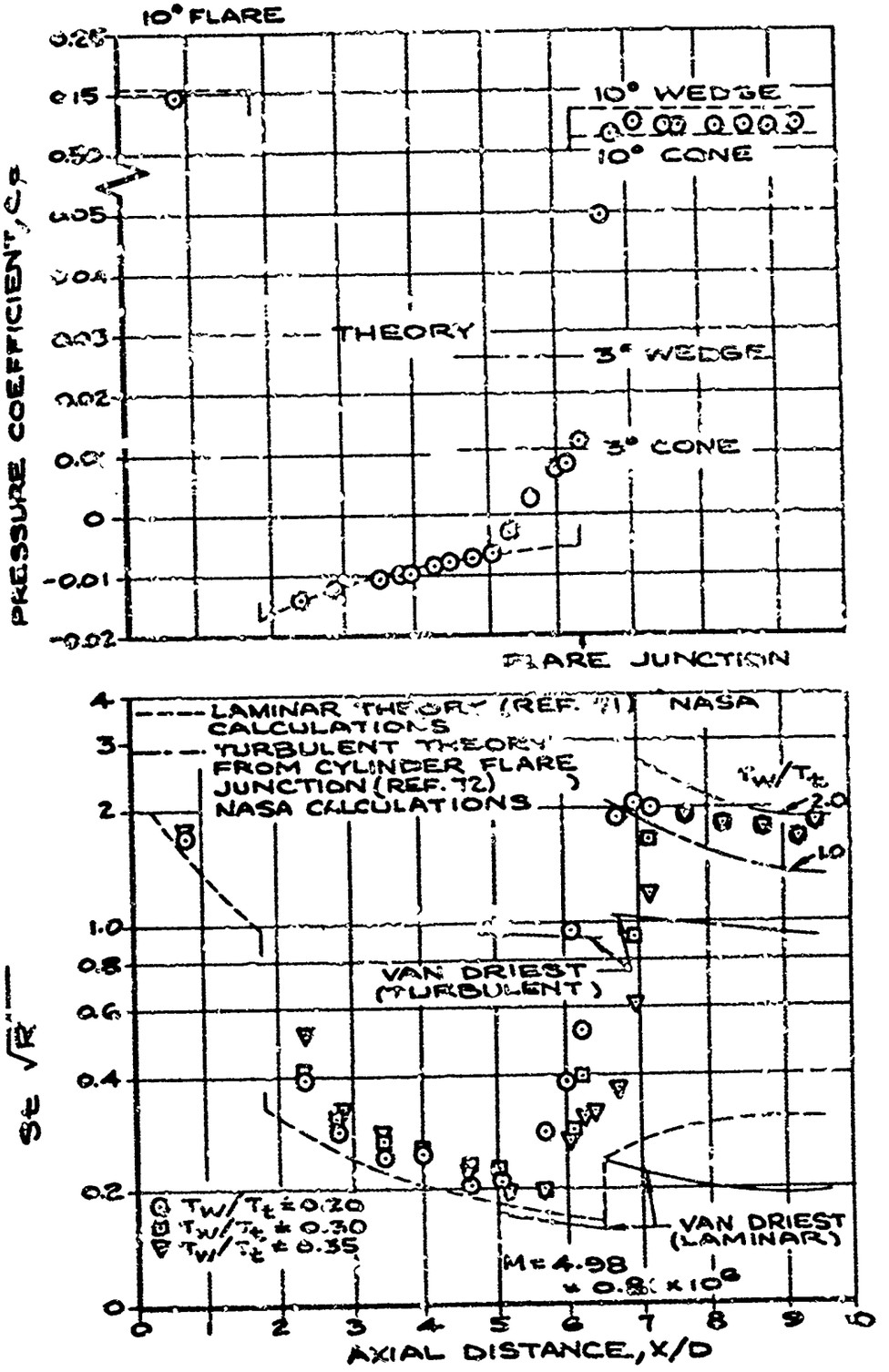

FIGURE 29

In figure 28, downstream of separation the laminar theory appears to be invalid and the turbulent theory based on the nose as the running length origin (solid lines) predicts a value low by about 40 per cent. The turbulent theory calculations with running length from the cylinder-flare junction appear to give better agreement with the data.

Similar comments apply to figure 29.

6.3.3 Summary of Results on Axisymmetric Compression Corners

When the flow is turbulent at recompression, applying running length modifications to turbulent theory appears to predict maximum values of $St\sqrt{R_D}$ that are close to the experimental data as shown in figures 27, 28, and 29. Additional data from these two references (68 and 70) verify this observation. Also, while it is readily discernible from these data that for turbulent flow, the maximum value of $St\sqrt{R_D}$ increases with increasing flare angle, it is not evident how this heat transfer parameter varies with Mach and Reynolds number at a given deflection angle. With this latter fact in mind, the present authors constructed figure 30 by plotting the maximum experimental values of Stanton number at reattachment, divided by the theoretical value of the Stanton number that would exist at that point according to the theory of reference 69, versus the maximum experimental value of the overall pressure rise from separation through reattachment. This figure is to be considered merely representative since there are only a few data points. It does indicate, however, that as the maximum pressure rise increases the departure of the Stanton number from the theoretical value increases.

One can summarize as follows:

a. For laminar flow, the $St\sqrt{R_D}$ increases over the theoretical attached flow value at reattachment can be significant,

CORRELATION OF THE RATIO OF MAXIMUM EXPERIMENTAL STANTON NUMBER AT REATTACHMENT TO THE VAN DRIEST VALUE AT THAT POINT WITH THE MAXIMUM EXPERIMENTAL PRESSURE RISE

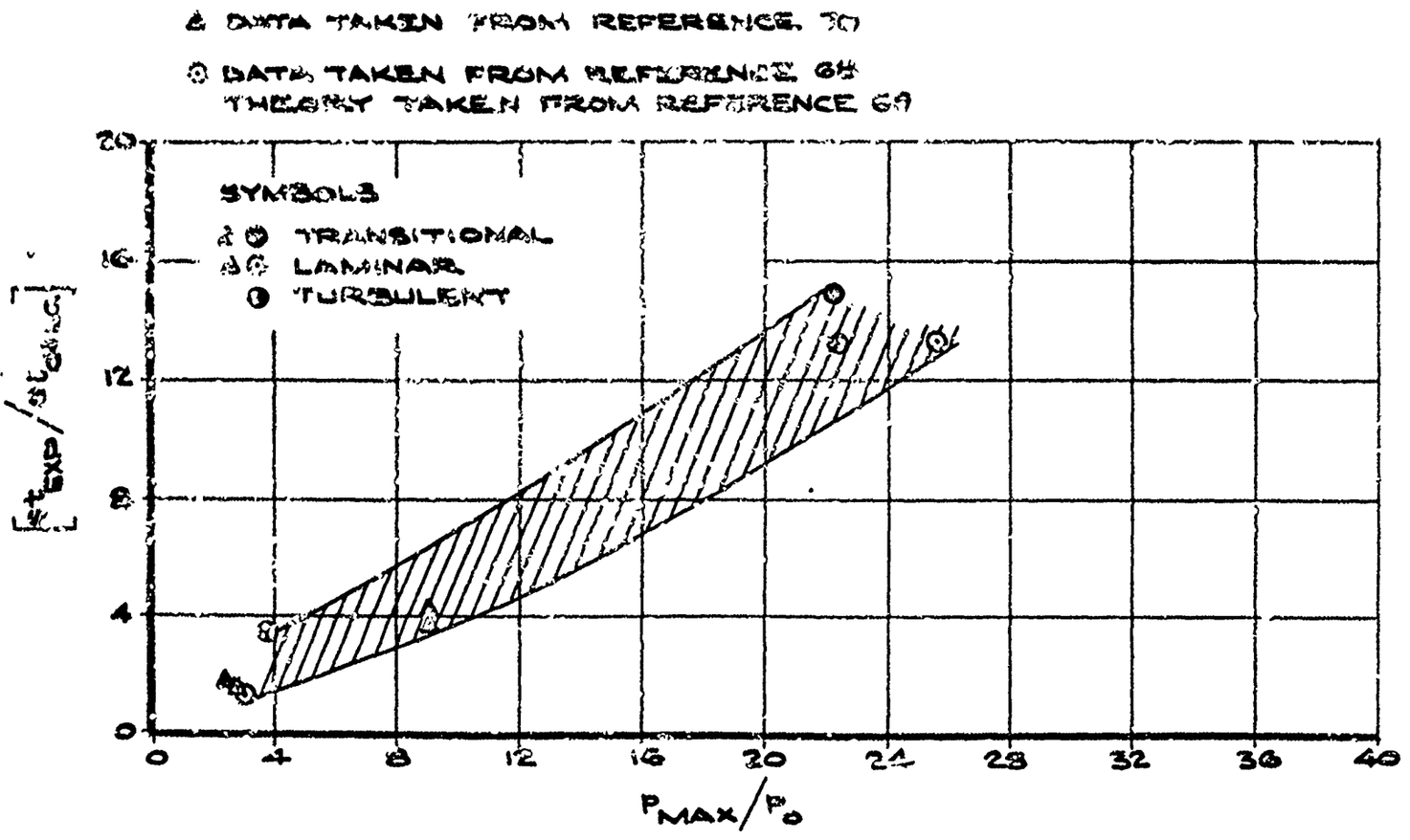

FIGURE 29

however, further data are required to define the Reynolds and Mach number dependence of this parameter.

b. For turbulent and transitional flow, the $St\sqrt{R_D}$ increase over the theoretical attached flow value at reattachment is significant. Also, the maximum value of $St\sqrt{R_D}$ appears to correlate with the maximum overall pressure rise; however, further data are needed to better define the Reynolds and Mach number effects.

c. Use of attached flow theory and a foreshortened running length does not adequately describe reattachment heating for laminar flow. Turbulent flow data give better agreement with this modified theory. This poor correlation may be attributed to the lack of knowledge of the boundary layer thickness at reattachment. It would appear that for laminar flow the boundary layer is thinner, but definitely not zero since the rise in $St\sqrt{R_D}$ is slow and there is no sharp peak. In the turbulent case, this thinning is much more pronounced as evidenced by the sharper rise and higher peak value of the $St\sqrt{R_D}$ in figures 26, 27, and 28. For the present, it appears that for laminar flow using the reattachment point as the running length origin will give conservative results. For turbulent flow over moderate flare angles ($\leq 20^{\circ}$) the cylinder-flare junction may be used for the running length origin, while for larger flare angles the reattachment point should be used.

6.4 Shock Wave Impingement

Of the two types of impinging shock waves noted in Section 4.4.2, only the oblique type will be considered in detail. The swept planar shock interaction has not been investigated extensively; therefore, the treatment shall not be in great depth. Discussions are limited to turbulent boundary layers since only data for this regime are available.

6.4.1 Oblique Shock Impingement

There have been two extensive programs for the investigation of the heat transfer in a separated region generated by the impingement of an oblique shock on a turbulent boundary layer, one by Douglas Aircraft Company and one by North American Aviation.

6.4.1.1 Douglas Study

The results of an Air Force funded investigation by the Douglas Advanced Missile Technology Department are reported in references 45, 73, and 74. The impinging oblique shock waves were produced by wedges of various half-angles, and hence were two-dimensional; however, the boundary layer generators considered were both two-dimensional and axisymmetric. By varying chamber conditions and wedge angle, a wide range of shock strengths, Reynolds number and Mach number were attained.

6.4.1.1.1 Impingement on a Flat Plate

Figure 31, which is from reference 73, shows some of the pressure and heat transfer data gathered using a flat plate as the boundary layer generator. As can be seen, the pressure distribution exhibits a very definite inflection point; in fact, it is almost a plateau. This is not unexpected since the shock strength is high, thus giving a large separated region; at lower shock strengths this plateau degenerates to an inflection point. The heat transfer coefficient increases from the undisturbed value to a higher value in the separated region where it appears to remain constant. Further downstream, the heat transfer coefficient increases to a maximum value at reattachment, then begins to drop back to the local zero pressure gradient value. Note that the maximum value of the heat transfer coefficient is about 4.5 times the attached zero-pressure gradient value prior to the interaction.

The distribution of the ratio of recovery temperature to total temperature is plotted in figure 32. The variance of this ratio can be

OBLIQUE SHOCK IMPINGEMENT ON A TWO-DIMENSIONAL TURBULENT BOUNDARY LAYER (AFTER SAYANO, BAUSCH AND DONNELLY REF. 73)

SHOCK GENERATOR ANGLE –
FREESTREAM MACH NUMBER–

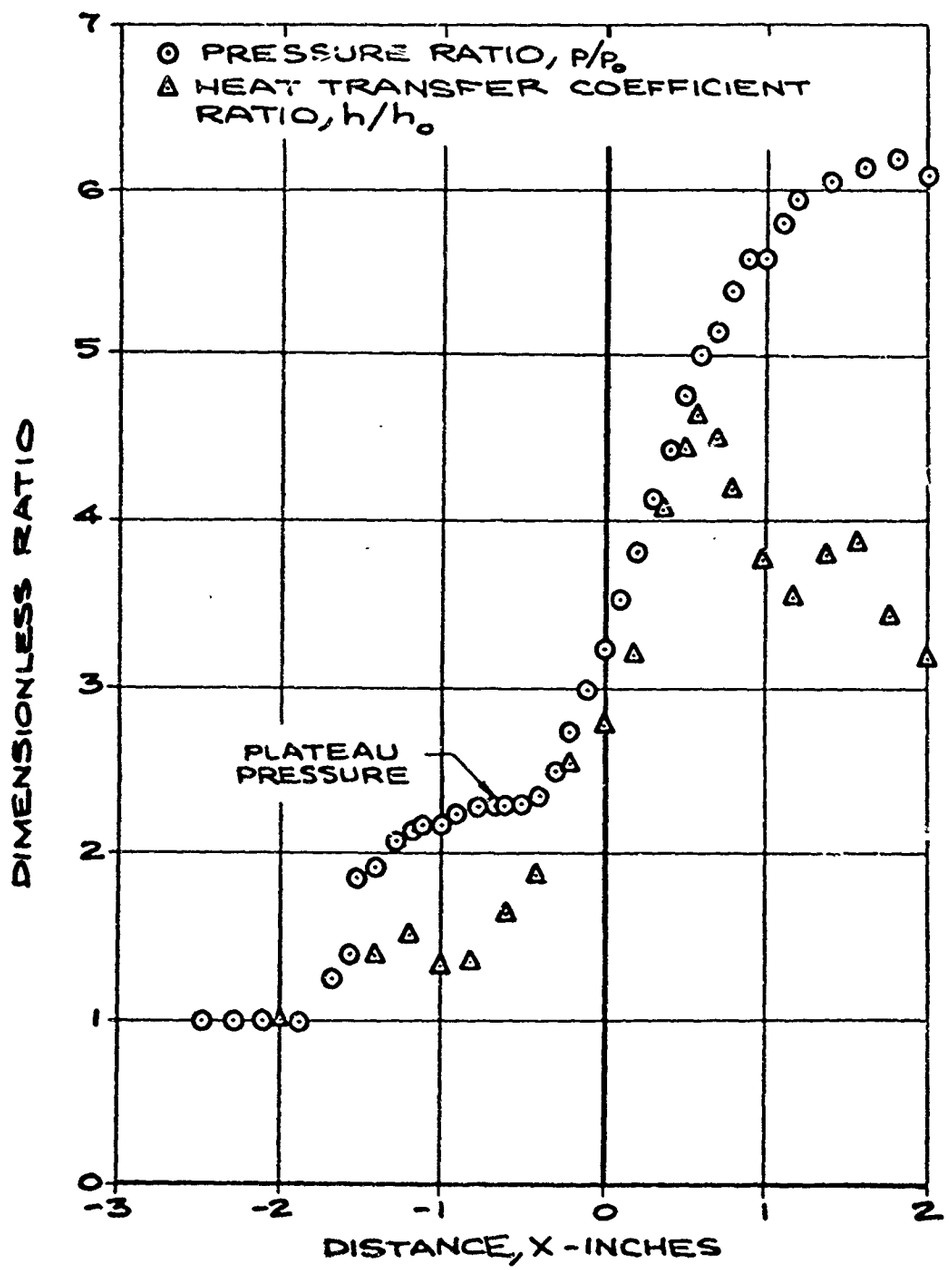

FIGURE 31

RECOVERY TEMPERATURE IN SHOCK WAVE BOUNDARY LAYER INTERACTION (AFTER SAYANO, BAUSCH AND DONNELLY REF. 73)

SHOCK GENERATOR ANGLE - 15°
FREESTREAM MACH NUMBER - 3.0

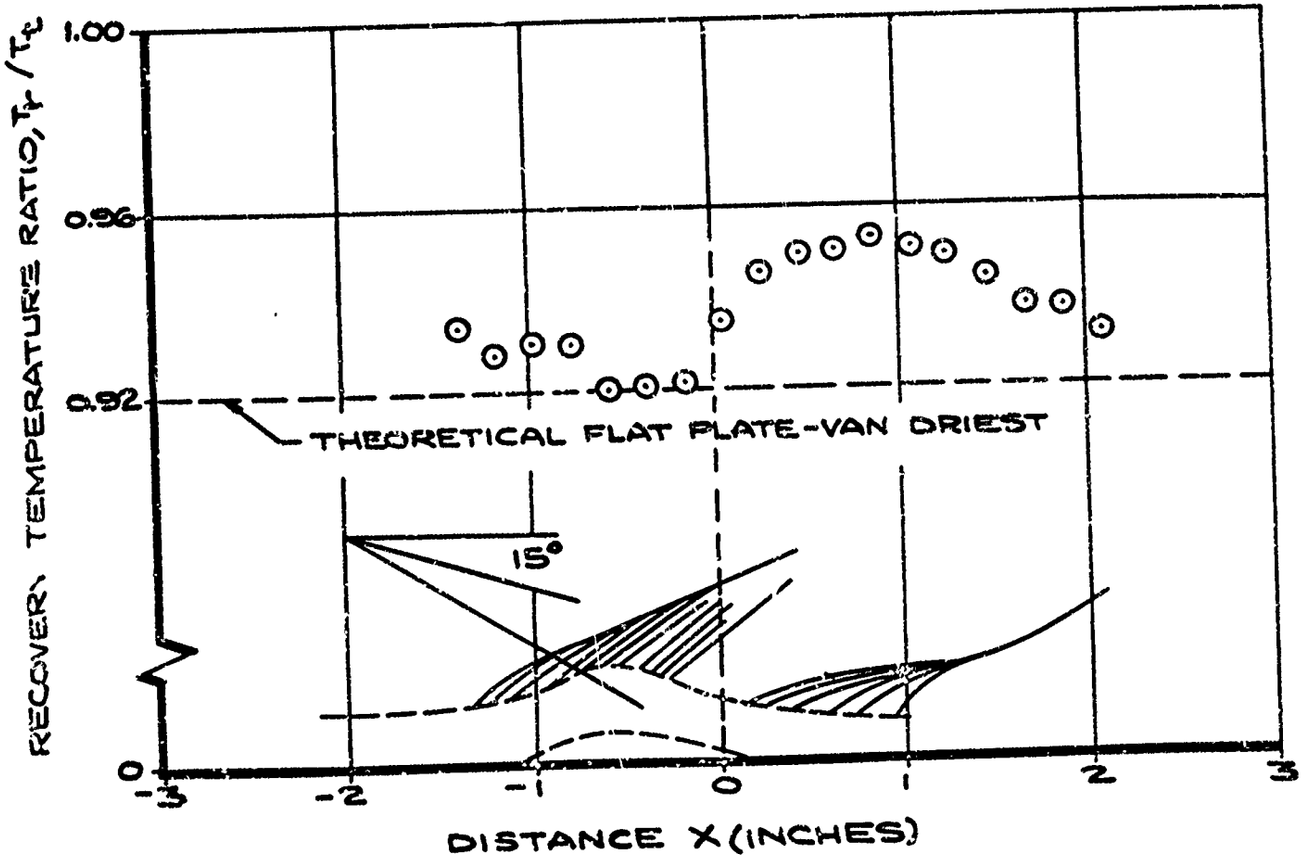

FIGURE 32

due only to a variation in recovery temperature since total temperature is a constant. As can be seen, this figure indicates a recovery temperature about 3% higher than the Van Driest value in the reattachment region.[69]

6.4.1.1.2 Impingement on a Cylinder

Figure 33, from reference 74, presents some of the data gathered with an axisymmetric boundary layer generator. These data were obtained at nearly identical conditions as those above, the only difference being a slightly higher stagnation temperature.

Comparison of figure 33 with that for a flat plate (figure 31) reveals that the overall pressure rise is greater in the latter case. This is reasonable since a favorable pressure gradient exists around the cylinder from the shock impingement point; thus the fluid may escape the pressure rise across the impinging shock by flowing around the body in a cross-flow pattern. This reasoning also explains why there is only incipient separation on the cylinder (as indicated by the very slight changes in curve slope)as indicated while a rather large region of separated flow exists on the flat plate. The other data from these references also indicate that when both types of boundary layers are subjected to the same overall pressure rise, under the same free stream conditions, the separated region for the axisymmetric case is always much less extensive than that for the two-dimensional case.

The heat transfer coefficient distribution follows the pressure curve as it does with the flat plate. A change in slope appears to occur at approximately the same location as that in the pressure distribution. Downstream of this slope change, the heat transfer coefficient increases to a maximum of between 3 and 3.5 times the undisturbed value, then decreases to the local zero pressure gradient value.

The recovery temperature shows similar characteristics only not so pronounced as for the flat plate boundary layer generator.

OBLIQUE SHOCK IMPINGEMENT ON AN AXI-SYMMETRIC TURBULENT BOUNDARY LAYER (AFTER SAYANO AND BAUSCH REF. 74)

SHOCK GENERATOR ANGLE - 15°
FREESTREAM MACH NUMBER - 3.01

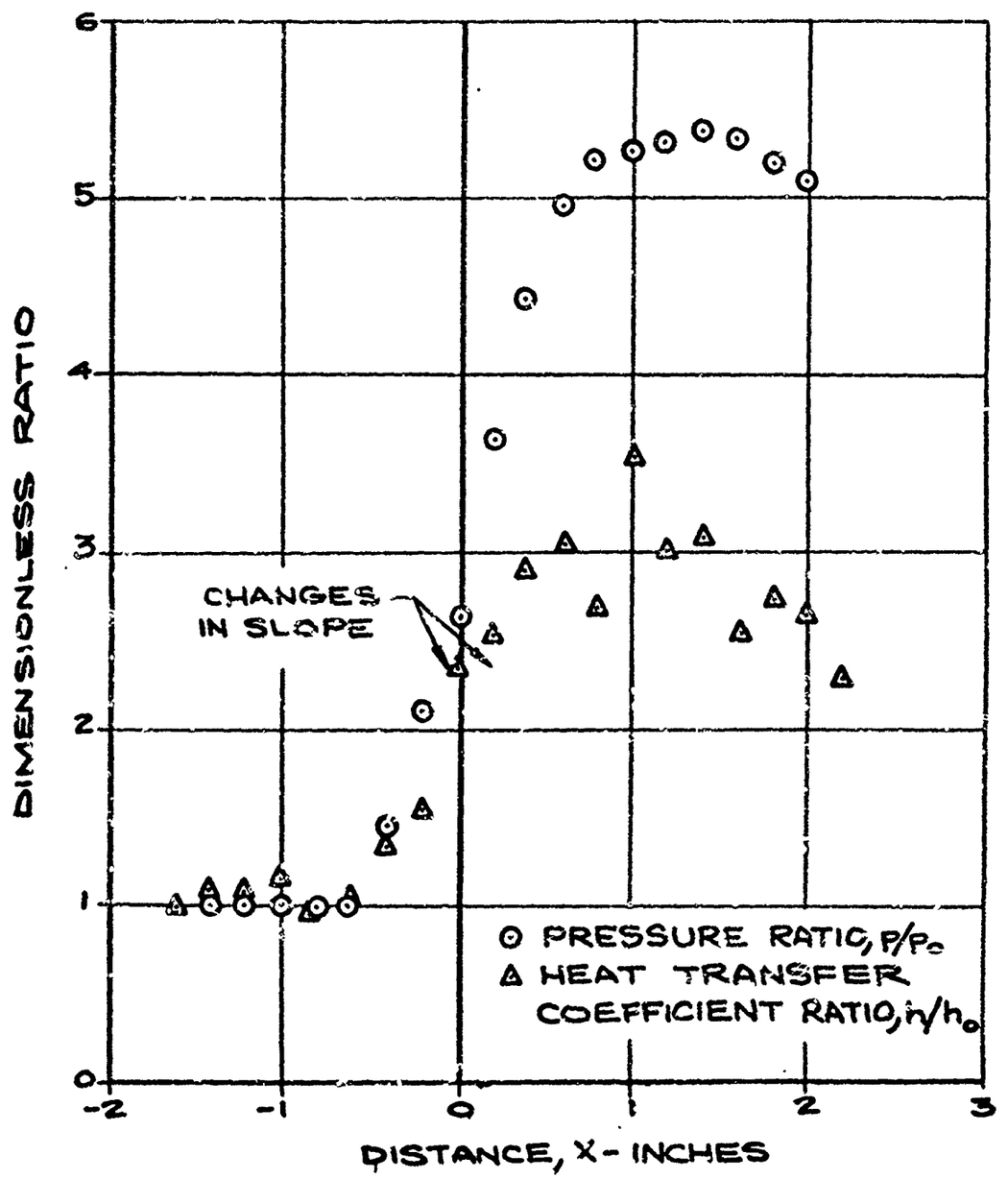

FIGURE 33

6.4.1.2 North American Aviation Study

Reference 75 presents the results of a Navy funded study performed by North American Aviation. The model consisted of a two-dimensional shock impinging upon a flat plate. A row of orifices was placed near the leading edge of the plate leading to a plenum chamber in which air was stored. This air could be injected into the boundary layer to thicken it and/or to initiate transition.

The data from this reference show similar qualitative characteristics for both the pressure and heat transfer distribution; the same trend of correlation between pressure and heat transfer also is evident. The increase in recovery temperature in the reattachment region was found to be similar.

6.4.1.3 Correlation of Pressure and Heat Transfer

Sayano has presented in reference 45 a compilation of the data reported in references 73 and 74. In one of the figures he plots maximum rise in heat transfer coefficient against the maximum rise in pressure. This figure is reproduced in this report as figure 34, with additional data from reference 75. As can be seen, there appears to exist a definite correlation between the rise in heat transfer coefficient and the rise in pressure, from which the following relation was determined:

$$\frac{h_{max}}{h_o} = \left(\frac{p_{max}}{p_o}\right)^Q$$

where h_o and p_o are the heat transfer coefficient and the pressure existing just prior to the shock wave interaction, respectively, and Q is the slope of the curve which may or may not increase with increasing boundary layer thickness. Combining this with a correlation between the measured maximum pressure rise and the theoretical pressure rise across the incident shock gives an expression of the maximum heat transfer coefficient as a function of theoretical pressure rise

CORRELATION OF MAXIMUM RISE IN HEAT TRANSFER COEFFICIENT WITH THE MAXIMUM RISE IN PRESSURE FOR OBLIQUE SHOCK WAVE IMPINGEMENT ON A TURBULENT BOUNDARY LAYER

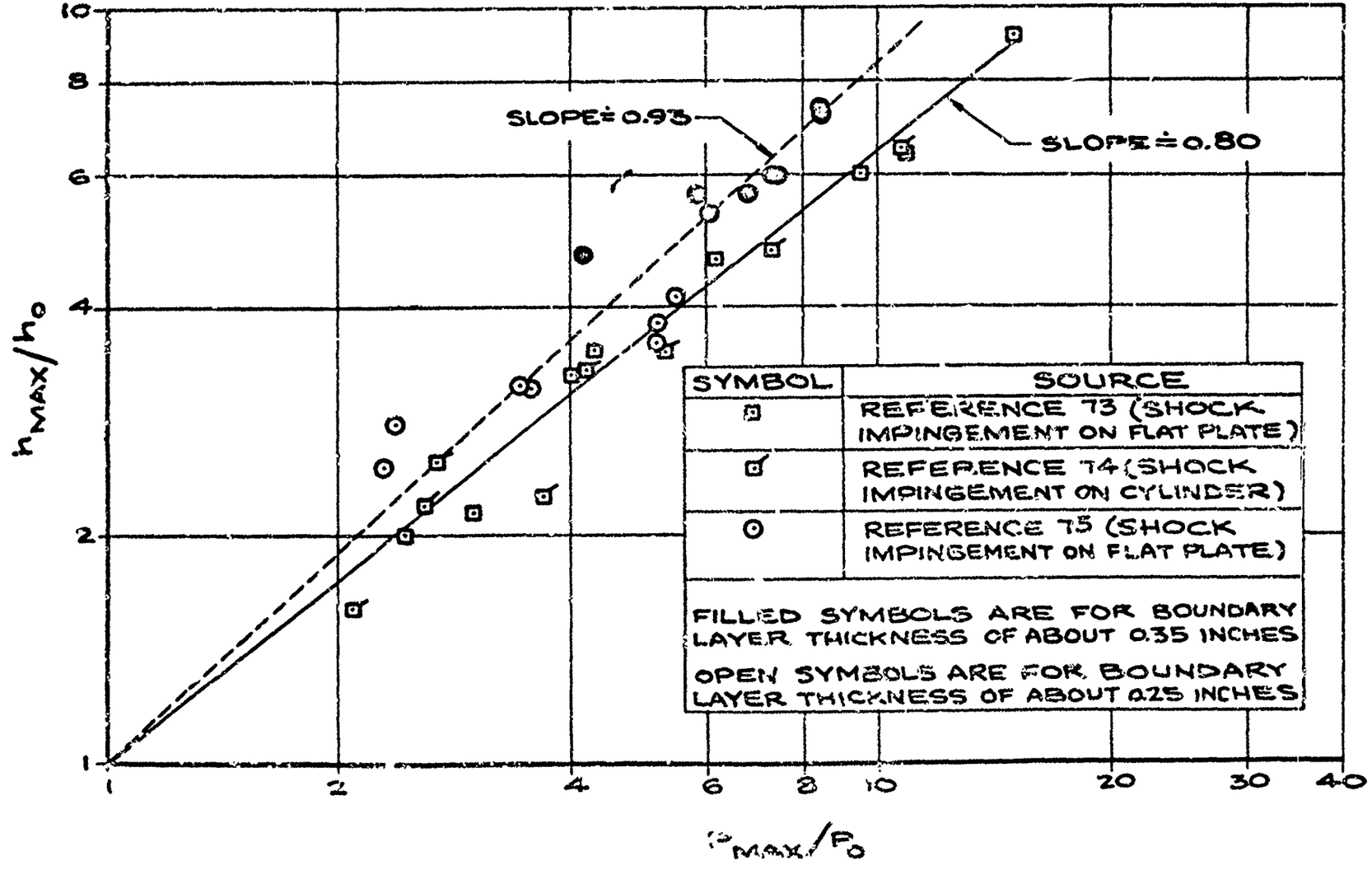

FIGURE 34

across the incident shock gives an expression of the maximum heat transfer coefficient as a function of theoretical pressure rise (p_1/p_o), across the incident shock of the following form:

$$\frac{h_{max}}{h_o} = \left(\frac{p_1}{p_o}\right)^{QN}$$

where N is the exponent from

$$\frac{p_{max}}{p_o} = \left(\frac{p_1}{p_o}\right)^{N} .$$

From reference 45, N = 1.75 for $2 < M_o < 4_x$ and $7.95 \times 10^6 < R/ < 2.56 \times 10^6$.

It should be emphasized that these correlations are strictly representative of a trend and should be used in any design calculations with extreme care since the exponent appears to be a function of the boundary layer thickness. Further discussion of extending the applicability of this curve is contained in Section 8.

In summary, both the Douglas and North American investigations have indicated that shock impingement on a turbulent boundary layer can result in excessive heating at the reattachment point. It is also evident that the rise in heating for the axisymmetric boundary layers is less severethan that for a two-dimensional boundary layer due to the existence of the cross-flow.

The maximum heat transfer coefficient appears to correlate well with the theoretical inviscid pressure rise across the incident shock wave; however, further data are needed to accurately define the effect of boundary layer thickness.

6.4.2 Swept Planar Shock Impingement

In reference 70, Miller, et al, report the results of an investigation of the interaction of a surface boundary layer with a shock wave produced by the leading edge of a fin perpendicular to the surface. The authors of this reference do not state flow separation actually occurs, but the heat transfer distribution shows a significant rise as seen in figure 35.

6.5 Rearward Facing Steps

There have been two recent investigations of the heat transfer distribution in high speed flow aft of a downstream facing step. One by S. L. Streck at Boeing Airplane Company, reported in references 43 and 77, and one by A. Naysmith at the Royal Aircraft Establishment (Britain), reported in references 78 and 54.

6.5.1 Boeing Study

In references 43 and 77, S. L. Strack of Boeing reports the results of some rather recent experimental work performed to determine the heat transfer distribution aft of a downstream facing step. The Mach numbers were nominally 3.0 and 6.0, and the boundary layer was turbulent prior to separation in all cases. The model was such that a range of boundary layer thickness to step height ratios of 0.12 to 1.2 was possible. Figure 36 presents two curves that are representative of the Boeing data, differing only in Mach number; i.e., the ratios of boundary layer thickness to step height and the free stream unit Reynolds number are nearly the same. The ratio of the experimentally determined heat transfer coefficients under separated flow conditions to those determined for a flat plate are shown as a function of axial distance measured in step heights. As can be seen, the two curves differ quite significantly. From the Mach 3 data, there appears to be about a 30 per cent increase in the heat transfer in the reattachment region. This percentage increase decreases with increasing boundary layer thickness to step height ratio. From the Mach 6 data, while there appears to be a peak in the heat transfer distribution; this peak has a maximum value

PLANAR SHOCK WAVE INTERACTION WITH A TWO-DIMENSIONAL BOUNDARY LAYER

(AFTER MILLER ET. AL. REF. 76)

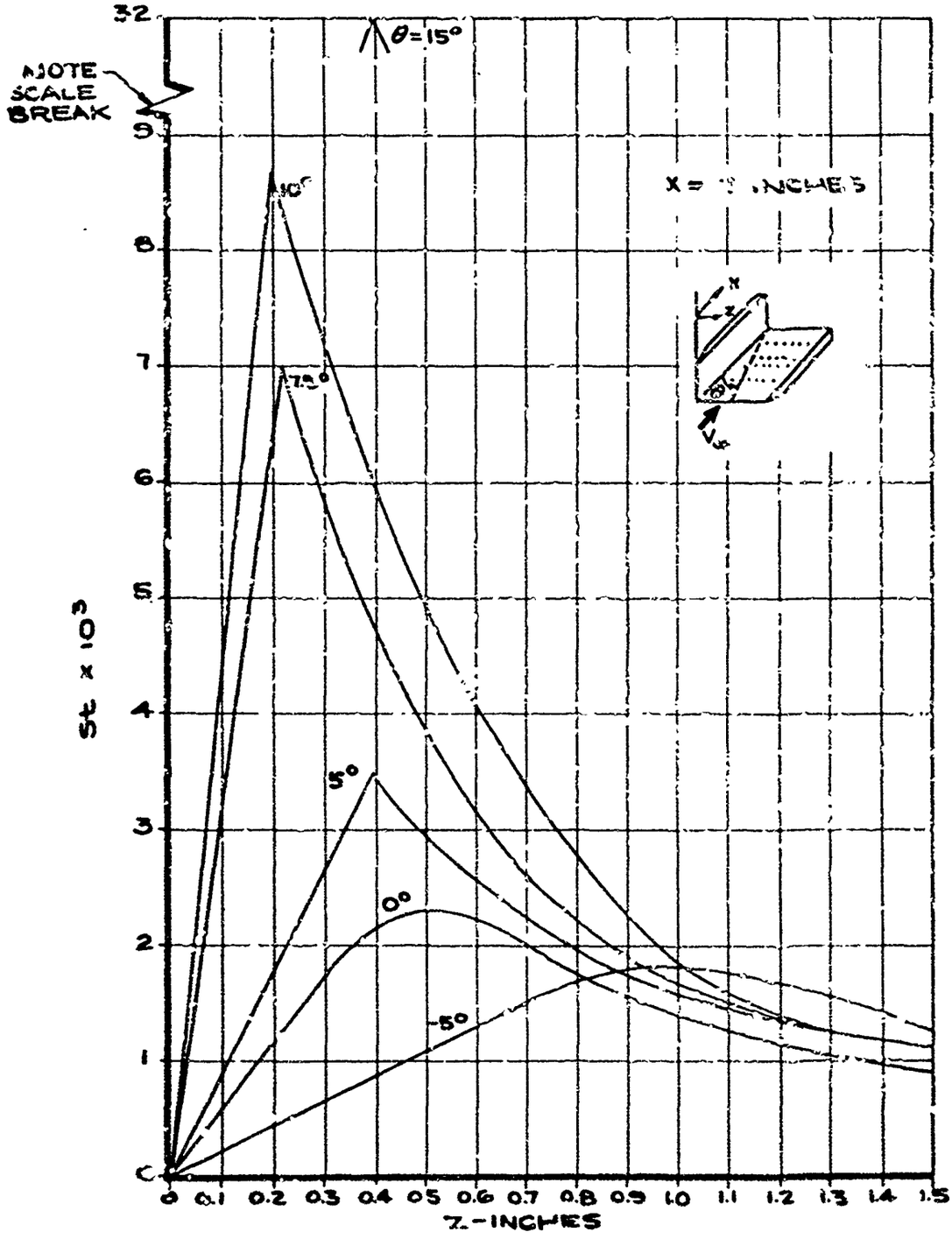

FIGURE 35

HEAT TRANSFER DISTRIBUTION AFT OF A DOWNSTREAM-FACING STEP WITH A TURBULENT BOUNDARY LAYER (AFTER STRACK AND STRACK AND LORENZ REF. 77 & 43)

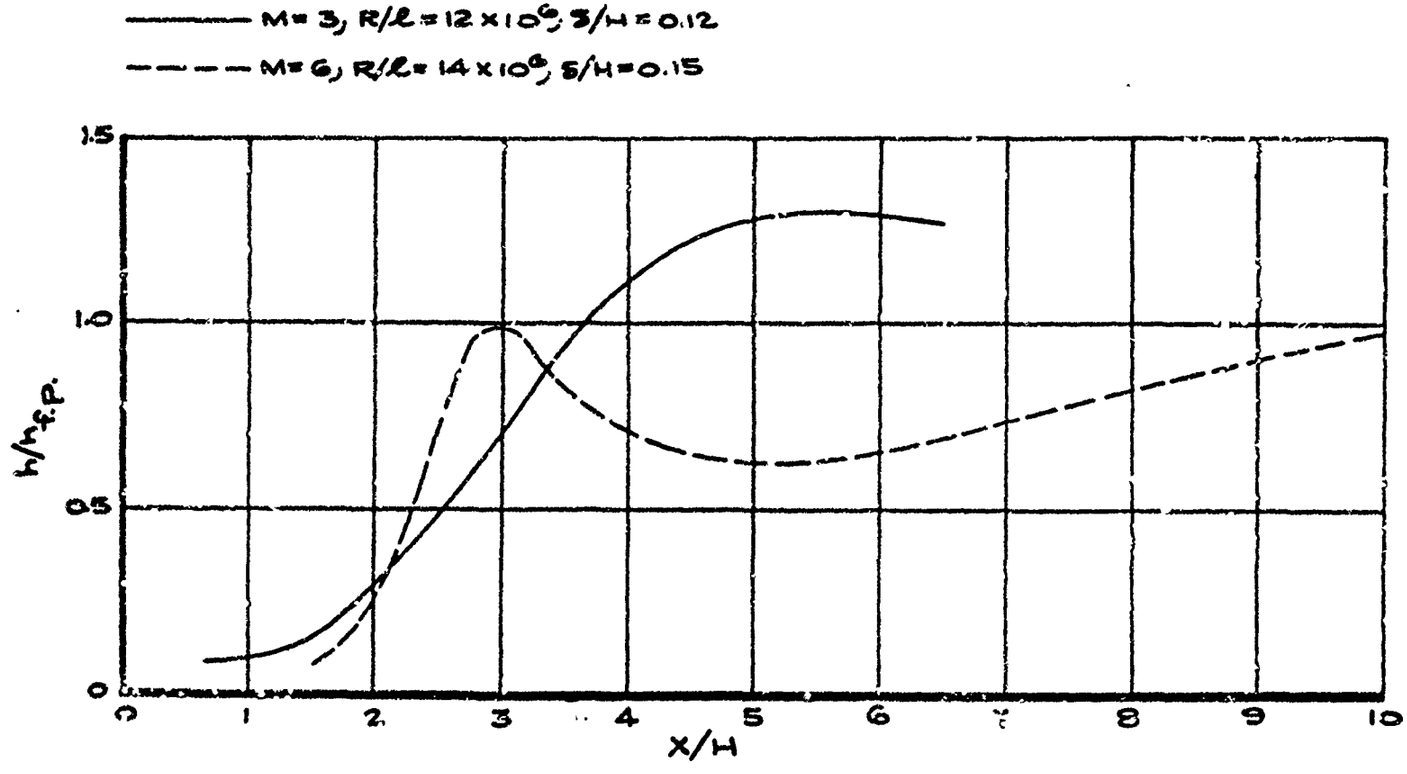

FIGURE 36

FIGURE 36

that is less than the value that would exist at that same point on a flat plate. This peak is followed by a dip in the curve and a subsequent increase that appears to approach the flat plate value. The shape of these distributions and the fact that the flat plate value of heat transfer coefficient was nowhere exceeded for Mach number equal to 6 was evident in all the data.

From the Mach 3 data it appeared that the maximum heat transfer occurred considerably downstream of the impingement point of the dividing streamline. The impingement point was determined by using standard oil flow techniques. However, the location of maximum heat transfer was found to occur upstream of the point where the pressure had recovered its flat plate value. This latter trend was evident from the Mach 6 data also.

6.3.2 Naysmith's Work

Naysmith has reported some experimental data in references 54 and 78 on the heat transfer distribution aft of a downstream facing step for both a two-dimensional and an axisymmetric body. The two-dimensional model consisted of a wedge placed on top of a flat plate, and the axisymmetric model consisted of a cone-cylinder with the base diameter of the cone exceeding the diameter of the cylinder. The boundary layer was turbulent for the two-dimensional model and laminar for the axisymmetric model.

Figure 37 presents the data resulting from the above experimental investigation for both configurations along with some free-flight data reported in reference 79 obtained on a model very similar to Naysmith's axisymmetric model. However, these free-flight data were obtained with a turbulent boundary layer prior to separation, whereas the data from Naysmith for this configuration were for a laminar boundary layer upstream of the separation point.

The data indicate for a laminar boundary layer upstream of the separation point there is a drop in heat transfer coefficient behind the step

HEAT TRANSFER DISTRIBUTION AFT OF A DOWNSTREAM-FACING STEP (AFTER NAYSMITH REF. 78)

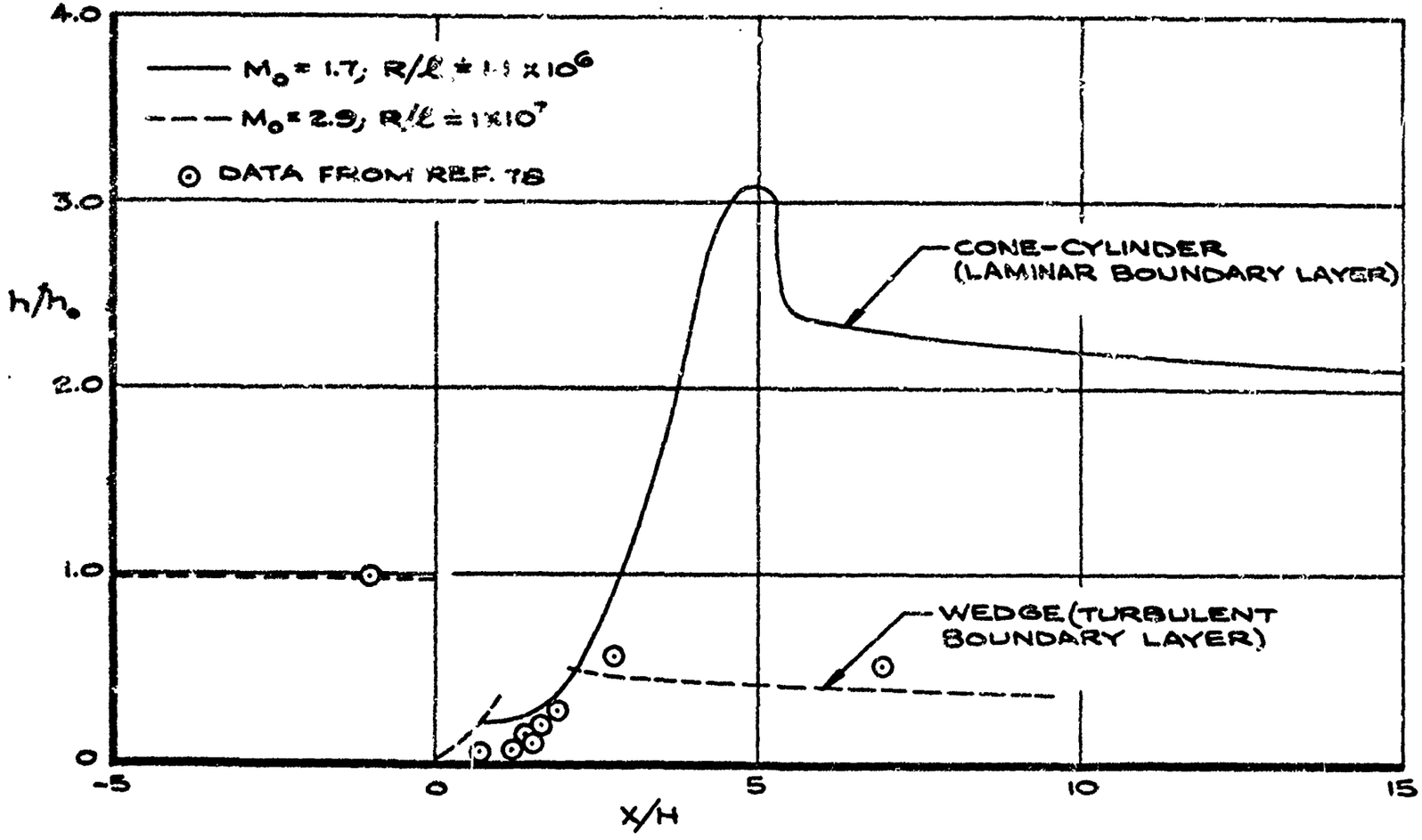

FIGURE 37

then a rise to a peak value of about 3 times the heat transfer coefficient at the cone shoulder (separation point). This peak is followed by a subsequent drop that appears to approach a value of about 2 times the value of heat transfer coefficient at the cone-shoulder. The reason for this rather high value of heat transfer coefficient downstream of reattachment was that transition occurred after separation (this may also be the reason for the rather high value of the ratio of h/h_o at reattachment).

For a turbulent boundary layer there is no evident peak in the data, which was probably due primarily to the heat transfer instrumentation being too widely spaced to pick up the peak. The data for both models appear to agree quite well. Note should be taken, however, that the data are normalized by the heat transfer coefficient that existed at the cone or ramp shoulder. This value is much higher than the flat plate value that would exist along the plate. Thus, the fact that downstream of reattachment the ratio of heat transfer coefficients is less than 1 does not necessarily indicate a low heat transfer coefficient. In other words, the heat transfer downstream of reattachment may still be greater than an equivalent flat plate value.

6.6 Summary of Results on Heat Transfer

a. The heat transfer mechanism may be strongly dependent upon the state of flow:

   (1) For laminar separation, the transfer properties of the mixing layer appear to control the heat transfer to the wall.

   (2) For turbulent flows, the continual flushing of the wall with new fluid from the external flow may control the heating.

   (3) For transitional flows, no conclusions can be drawn due to lack of data; however, the location of

transition relative to the separation and reattachment points will probably determine which of the above mechanisms would predominate along with the degree of flow steadiness.

b. From the above, it is logical to state that the distribution of heat transfer will also depend upon the flow regime encountered:

(1) For laminar flow, there is sometimes a rise in heat transfer at the separation point due to the existence of a separation vortex. Downstream of this location the heat transfer will generally drop to about 1/2 of the equivalent attached value; however, if the separated region is small, this drop may not be severe, and in fact may not occur at all. Aft of this minimum, the heating increases throughout reattachment to a value greater than the laminar attached flow value.

(2) Transitional flows do not exhibit so pronounced a minimum and may, if transition is close to the separation point, exhibit no drop in heat transfer within the separated region. At the transition point, the heat transfer begins to increase and continues to do so throughout the reattachment region reaching a maximum value which may be greater than either the laminar or turbulent attached flow values.

(3) Turbulent flows generally exhibit no drop in heat transfer due to the energetic separated fluid and small extent of the region. The rise throughout reattachment region is rapid and the maximum heat transfer is of the same order of magnitude as that near the leading edge or stagnation point.

c. The heat transfer distribution appears to be dependent upon the oncoming boundary layer thickness:

(1) For laminar separation, the local heating would decrease with increasing mixing layer thickness (proportional to boundary layer thickness) if 6.6.a.1 is correct; however, the data do not indicate that this dependence exists.

(2) The data definitely indicate that the local heating for turbulent separation increases with increasing mixing layer thickness if the mass exchange governs the transfer of energy from the free stream.

(3) For transitional separations, no remarks can be made.

d. The above statement (c) may also be applied to the average and total heating rates. The turbulent data definitely show a direct dependence upon mixing layer thickness, whereas, the laminar data show no dependence.

e. The data indicate, at least for cavities, that the total heat transfer from a laminar mixing layer is about one-half of the attached value. The value for turbulent mixing layers may or may not be less than the attached value, depending upon the oncoming boundary layer thickness.

f. It is felt that three-dimensional geometries will generally suffer less severe heating at reattachment if the possibility of a cross-flow exists to relieve the high pressure at reattachment.

g. The recovery temperature may increase within the separated region; however, more data are needed to verify this observation.

h. The use of a modified pressure and a foreshortened running length with attached flow theory for calculating the heating rate at reattachment can lead to the following errors unless extreme caution is exercised:

(1) grossly conservative results for laminar separation,

(2) optimistic or conservative results for turbulent separation, and

(3) erroneous distributions downstream of reattachment that can give either optimistic or conservative estimates.

i. There appears to be a correlation between the maximum pressure rise and the maximum rise in heat transfer coefficient for axisymmetric compression corners and incident shock waves when the flow is turbulent.

j. More analytical and experimental work is needed to determine the natures of the separated flow, boundary layer downstream at reattachment, and of the mixing layer.

7. CONCLUDING REMARKS

The problems associated with flow separation in high speed flight are qualitatively understood. On the other hand our quantitative knowledge of the subject, both analytical and experimental, is deficient due mainly to its lack of generality. The purpose of this section is to synthesize the information in the preceding sections and to point out areas where further knowledge is needed.

7.1 Variables Describing the Problem

Separated flows are appropriately classified according to the state of flow, i.e., whether the flow in the separated region is completely laminar, completely turbulent, or whether the flow undergoes transition between separation and reattachment. The main variables governing the nature of the flow are free stream properties such as pressure, temperature, density, viscosity and velocity and also the geometry and thermal nature of the surface being considered. Once these factors are stipulated, the behavior of the flow can be described by three variables; namely, Reynolds number, Mach number, and fluid to wall temperature ratio. The above factors may be considered the pertinent independent variables for the problem of separated flow.

The information required when considering the problem of flow separation in vehicle design is:

a. when and where flow separation will occur,

b. what the extent and shape of the separated region will be,

c. what the pressure and heat transfer distributions throughout the separated and reattachment region will be, and

d. whether or not the flow in the separated region will be steady, and if not, what is the nature of the unsteadiness.

These latter points dictate the dependent variables which must be considered. The dependent variables are not only functions of the independent variables but, as in most real processes, they are also interrelated. Some of the more pertinent dependencies are:

a. Separation Geometry

The extent of the separated region is of substantial design importance. The quantities of primary interest are the separation and reattachment points and the slope of the dividing streamline. These quantities may be directly determined experimentally by measurement of the skin friction, from optical measurements, or from the pressure distribution. Analytically, the separation point and extent of separation are dependent primarily upon the magnitude of the pressure rise causing separation, geometry of the body, state of the flow, wall to free stream temperature ratio, and Reynolds and Mach numbers prior to separation.

b. Pressure Distribution

The pressure distribution is a function of essentially the same variables listed above for separation geometry; hence, it is plainly a dependent variable. If known, however, the pressure distribution is very useful as a dependent variable. This has proved to be a quite powerful tool in separated flow analysis since the pressure distribution is probably the most simple experimental measurement to make. A knowledge of the pressure distribution itself provides a good description of the extent and shape of the separated region. It may also be used to predict reattachment heating rates through correlation criteria. Similar schemes can probably be used to predict skin friction also. Obviously, the pressure distribution is of utmost importance in ascertaining any perturbations to the load distribution or drag characteristics caused by flow separation.

c. Heat Transfer Distribution

In order to conduct a detailed design analysis, the local heat transfer coefficient, recovery factor, and initial wall temperature distribution must be known. Certain studies have shown the recovery factor to be relatively constant throughout the separated region and approximately equal to the attached flow value. Since the initial wall temperature distribution is known beforehand, the local heat transfer coefficient is the main unknown to be determined in order to complete the calculation of the heat transfer rate. The major flow parameters influencing the local heat transfer coefficient throughout separation and reattachment are the boundary layer thickness prior to and at separation, the rate of growth of the mixing layer, the mass exchange between the separation cavity and the external flow, and the boundary layer thickness at reattachment and during redevelopment after reattachment. A knowledge of these parameters appears to be of fundamental importance in establishing an accurate analytical model for heat transfer in separated and reattaching flows.

d. Steadiness of the Flow

One of the properties of separated flows whose significance is often overlooked is flow steadiness. The stability of the free shear layer is inherently connected with the state of the flow and extent of separation along with many other flow parameters such as Reynolds number, Mach number, and stream to wall temperature ratio. Of primary importance for design purposes are the magnitude and frequence of the pressure fluctuations within the separated region, the variation of the extent of separation due to the fluctuations, and the detailed behavior of the fluid in the viscous flow region so that shear and heat transfer trends may be predicted.

The problem of separated flow is thus defined.

7.2 Solution of the Problem

There are two approaches for solution to any engineering problem; namely, analytical and experimental. In many cases, a direct analytical solution is sufficient due either to the simplicity and/or lack of significance of the problem. Unfortunately, viscous flow separation is an extremely complex problem in fluid motion and its effects cannot be indiscriminately ignored. To date, no analytical model has been developed which lends itself to an entirely satisfactory solution. On the other hand the scope of the problem is so vast that a complete experimental description of the problem is not practical. Well balanced analytical-experimental approaches appear most rewarding, although recently purely theoretical advances have made some gain in the area of laminar separated flows.

7.3 Present Status of the Problem

Additional work is needed in all areas of investigation of separated flows, particularly in the higher (hypersonic) speed range. Some areas which yet warrant special attention follow:

a. Analytical

(1) Most of the more sophisticated analytical approaches are centered around the use of the boundary layer equations. However, it is known that strictly speaking, several of the boundary layer assumptions may be violated by the occurrence of separation. The importance of these violations should be definitely established.

(2) The better theoretical and semi-empirical analytical methods should be generalized to include the heat transfer, real gas effects, and hypersonic interaction phenomena.

(3) An analytical criterion for the stability of the separated shear layer should be established and tested to assist in the determination of vehicle dynamics.

b. Experimental

(1) Additional experimental research for pressure and heat transfer distributions is needed (especially in higher Mach number ranges, $M>4$) for most geometries and for both laminar and turbulent flow.

(2) A detailed knowledge of the behavior of the flow in the free shear layer, viscous separation region, and reattachment zone is needed not only to have a better qualitative understanding of separated flow, but also to provide correlation parameters for semi-empirical analytical efforts.

(3) Additional stability data are required, primarily information which establishes the conditions under which oscillations will occur and the nature of the resultant oscillations. A detailed understanding of the interrelation of the parameters giving rise to instability is also needed.

(4) The importance of three-dimensional effects, especially those which occur on supposedly two-dimensional geometries and which would not be accounted for in a two-dimensional analysis, should be determined.

The foregoing comments point out only a few (those felt to be most important) aspects of separated flows requiring detailed attention. Obviously, a great deal of work is yet required to provide the design engineer with sufficient tools to handle the general problem.

8. LIST OF REFERENCES

1. Prandtl, L., "Uber Flussigkeitsbewegung Bei Sehr Kleiner Reibung", Verhandlungen Des Dritten Internationalen Mathematikar Kongresses, Heidelberg: 484-491, 1904.

2. Vatsykin, A. B., "On the Separation of Magnetohydrodynamic Boundary Layers", Journal of Applied Mathematics and Mechanics, Vol. 27, No. 2: 495-501, October 1963.

3. Schlichting, H., Boundary Layer Theory (4th Edition), McGraw Hill Book Co., Inc., New York, 1960.

4. Crocco, L. and L. Lees, "A Mixing Theory for the Interaction Between Dissipative Flows and Nearly Isentropic Streams", Journal of the Aeronautical Sciences, Vol. 19, No. 10: 649-676, October 1952.

5. Crocco, L., "Considerations on the Shock-Boundary Layer Interaction", Proceedings on the Conference on High-Speed Aeronautics, p. 75, Polytechnic Institute of Brooklyn, New York, 1955.

6. Cheng, S. I. and I. D. Chang, On the Mixing Theory of Crocco and Lees and its Application to Shock Wave-Laminar Boundary Layer Interaction - Part II, Princeton University Aeronautical Engineering Report 376, 1957.

7. Bray, K. N. C., G. E. Gadd, and M. Woodger, Some Calculations by the Crocco - Lees and Other Methods of Interaction Between Shock Waves and Laminar Boundary Layers Including Effects of High Temperatures and Suction, Aeronautical Research Council Report 21, 834, FM 2937, April 1960.

8. Glick, H. S., Modified Crocco-Lees Mixing Theory for Supersonic Separated and Reattaching Flows, Guggenheim Aeronautical Laboratory, California Institute of Technology, Hypersonic Research Project, Memorandum No. 53, May 1960.

9. Lees, L., and B. L. Reeves, Supersonic Separated and Reattaching Laminar Flows: I. General Theory and Applicatin to Adiabatic Boundary Layer-Shock Wave Interactions, AIAA Preprint No. 64-4, AIAA Aerospace Sciences Meeting, New York, New York, January 20-22, 1964.

10. Thwaites, B., "Approximate Calculation of the Laminar Boundary Layer", Aeronautical Quarterly, Vol. 1, Part III: 245-280, November 1950.

11. Curle, N. and S. Skan, "Approximate Methods for Predicting Properties of Laminar Boundary Layers", Aeronautical Quarterly, Vol. 8, Part 3: 257-268, 1957.

LIST OF REFERENCES (Continued)

12. Lachmann, G. V., Boundary Layer and Flow Control, Vols. I and II, Pergamon Press, New York, 1960.

13. Maskell, E. C., Flow Separation in Three-Dimensions, Royal Aircraft Establishment, Report No. Aero 2565, London, England, November 1955.

14. Oswatitsch, K., "Die Ablosungsbedingung von Grenzschichten, Sonderdruck aus Gronzschichtforschung", Symposium Freiburg, p. 357, August 1957.

15. Sears, W. R., "Boundary Layers in Three-Dimensional Flow", Applied Mechanics Reviews, Vol 7, No. 7: 281-285, July 1954.

16. Moore, F. K., "Three-Dimensional Boundary Layer Theory", Advances in Applied Mechanics, Academic Press, Inc., New York: 159-228, 1956.

17. Oman, R. A., The Three-Dimensional Laminar Boundary Layer Along a Corner, Sc.D. Thesis, Massachusetts Institute of Technology (ASTIA AD211216), June 1959.

18. Cooke, J. C., and M. G. Hall, Boundary Layers in Three-Dimensions, Royal Aircraft Establishment, Report No. 2635, AD235751, London, England, 1957.

19. Kaufman, L. G., S. A. Hartofilis, W. J. Evans, R. A. Oman, L. H. Meckler, and D. Weiss, A Review of Hypersonic Flow Separation and Control Characteristics, United States Air Force, Aeronautical Systems Division, TDR 62-168, March 1962.

20. Love, E. S., Base Pressure at Supersonic Speeds on Two-Dimensional Airfoils and on Bodies of Revolution With and Without Fins Having Turbulent Boundary Layers, NACA TN 3819, January 1957.

21. Ferrari, C., Airfoil Pressures at Supersonic Speeds Under Separated Flow Conditions, Applied Physics Laboratory, The Johns Hopkins University, August 1957.

22. Denison, M. R., and E. Baum, "Compressible Free Shear Layer With Finite Initial Thickness", AIAA Journal, Vol. 1, No. 2: 342-349, February 1963.

23. Baum, E., Effect of Boundary Layer Blowing on the Laminar Separated Shear Layer, Electro-Optical Systems, Research Note No. 9, April 1963.

24. King, H. H., and E. Baum, Enthalpy and Atom Profiles in the Laminar Separated Shear Layer, Electro-Optical Systems, Research Note No. 7, March 1963.

LIST OF REFERENCES (Continued)

25. Reller, J. O. Jr., and F. M. Hamaker, An Experimental Investigation of the Base Pressure Characteristics of Nonlifting Bodies of Revolution at Mach Numbers from 2.73 to 4.98, NACA TN-3393, March 1955.

26. King, H. H., and E. Baum, Effect of Base Bleed on the Laminar Base Flow, Electro-Optical Systems, Research Note No. 10, May 1963.

27. Baum, E., Effect of Boundary Layer Distortion at Separation on the Laminar Base Flow, Electro-Optical Systems, Research Note No. 16, October 1963.

28. Korst, H. H., "Comments on the Effect of the Boundary Layer on Sonic Flow Through an Abrupt Cross-Sectional Area Change", Journal of the Aeronautical Sciences, Vol. 21, No. 8: 568-569, August 1954.

29. Korst, H. H., R. H. Page, and M. E. Childs, A Theory for Base Pressure in Transonic and Supersonic Flow, University of Illinois, ME TN 392-2, OSR TN 55-89, March 1955.

30. Korst, H. H., "A Theory for Base Pressures in Transonic and Supersonic Flow", Journal of Applied Mechanics, Vol. 23, No. 4: 593-600, December 1956.

31. Kirk, F. N., An Approximate Theory of Base Pressure in Two-Dimensional Base Flow at Supersonic Speeds, Royal Aircraft Establishment, TN Aero 2377, London, England, March 1954.

32. Nash, J. F., An Analysis of Two-Dimensional Turbulent Base Flow Including the Effect of the Approaching Boundary Layer, Aeronautical Research Council, R&M, No. 3344, 1963.

33. Mueller, T. J., H. H. Korst, and W. L. Chow, On the Separation Reattachment, and Redevelopment of Incompressible Turbulent Shear Flow, American Society of Mechanical Engineers, Paper No. 63-AHGT-5, 1963.

34. Rom, J., "Theory for Supersonic, Two-Dimensional Laminar, Base-Type Flow Using the Crocco-Lees Mixing Concepts", Journal of the Aerospace Sciences, Vol. 29, No. 8: 963-968, August 1962.

35. Love, Eugene S., The Base Pressure at Supersonic Speeds on Two-Dimensional Airfoils and Bodies of Revolution (With and Without Fins) Having Turbulent Boundary Layers, NACA RM L53C05, April 29, 1953.

36. Roshko, A., and G. J. Thomke, Flow Separation and Reattachment Behind a Downstream-Facing Step, Douglas Aircraft Company Report SM-43056-1, January 1964.

37. Chapman, D. R., D. M. Kuehn, and H. K. Larson, Investigation of Separated Flows in Supersonic and Subsonic Streams with Emphasis on the Effect of Transition, NACA Report 1356, 1958.

LIST OF REFERENCES (Continued)

38. Sterrett, J. R., and J. C. Emery, Extension of the Boundary-Layer Separation Criteria to a Mach Number of 6.5 by Utilizing Flat Plates with Forward Facing Steps, NASA TN D-618, December 1960.

39. Charwat, A. F., J. N. Roos, F. C. Dewey, and J. A. Hitz, "An Investigation of Separated Flows", Part I, Journal of the Aerospace Sciences, Vol. 28, No. 6: 457-470, June 1961.

40. Charwat, A. F., J. N. Roos, F. C. Dewey, and J. A. Hitz, "An Investigation of Separated Flows", Part II, Journal of the Aerospace Sciences, Vol. 28, No. 7: 513-527, July 1961.

41. Ginoux, J. J., "Separated Supersonic Flows", Proceedings of the 1960 Heat Transfer and Fluid Mechanics Institute, Stanford University Press, Stanford, California: 179-191, 1960.

42. Ginoux, J. J., The Existence of Three-Dimensional Perturbations in the Reattachment of a Two-Dimensional Supersonic Boundary Layer After Separation, North Atlantic Treaty Organization, Advisory Group for Aeronautical Research and Development, Report 272, 1960.

43. Lorenz, G. C., and S. L. Strack, Heat Transfer at Reattachment of a Turbulent Boundary Layer at M=6, Boeing Airplane Company, Document No. D2-23058, March 23, 1964.

44. Thomke, G. J., Separation and Reattachment of Supersonic Turbulent Boundary Layer Behind Downstream Facing Steps and Over Cavities, Douglas Aircraft Company Report No. SM-43062, March 1964.

45. Sayano, S., Heat Transfer in Shock Wave-Turbulent Boundary Layer Interaction Regions, Douglas Aircraft Company Report No. SM-42567, November 1962.

46. Donaldson, C. duP., and R. E. Lange, Study of the Pressure Rise Across Shock Waves Required to Separate Laminar and Turbulent Boundary Layers, NACA TN 2770, 1952.

47. Erdos, J., and A. Pallone, Shock-Boundary Layer Interaction and Flow Separation, AVCO Corp. Technical Report R.A.D. TR-61-23, August 15, 1963.

48. Miller, D. S., R. Hijman, M. E. Childs, Mach 8 to 22 Studies of Flow Separations Due to Deflected Control Surfaces, American Institute of Aeronautics and Astronautics, AIAA Paper No. 63-173, June 1963.

49. Kuehn, D. M., Experimental Investigation of the Pressure Rise Required for the Incipient Separation of Turbulent Boundary Layers in Two-Dimensional Supersonic Flow, NASA Memorandum 1-21-59A, February 1959.

LIST OF REFERENCES (Continued)

50. Hakkinen, R. J., I. Greber, L. Thrilling, and S. S. Abarbanel, The Interaction of an Oblique Shock Wave with a Laminar Boundary Layer, NASA Memorandum 2-18-59W, March 1959.

51. Liepman, H. W., A. Roshko, and S. Dhawan, On Reflection of Shock Waves from Boundary Layers, NACA Report No. 1100, 1952.

52. Love, E. S., Pressure Rise Associated with Shock Induced Boundary Layer Separation, NACA TN 3601, December 1955.

53. Martellucci, A., and P. A. Libby, Supersonic Flow About General Three-Dimensional Blunt Bodies, Vol. II. Heat Transfer Due to the Interaction Between a Swept Planar Shock Wave and a Laminar Boundary Layer, United States Air Force, Aeronautical Systems Division, Report No. ASD-TR-61-727, Vol. II, October 1962.

54. Naysmith, A., Heat Transfer and Boundary Layer Measurements in a Region of Supersonic Flow Separation and Reattachment, Royal Aircraft Establishment, TN Aero 2558, London, England, May 1958.

55. Sharp, A. W., "The Supersonic Flow Past a Leading Edge Separation Bubble", Journal of Fluid Mechanics, Vol. 5, Part 3: 445-459, April 1959.

56. Burbank, P. B., and R. L. Stallings, Jr., Heat Transfer and Pressure Measurements on a Flat-Face Cylinder at a Mach Number Range of 2.49 to 4.44, NASA TM X-19, August 1959.

57. Roshko, A., Some Measurements of Flow in a Rectangular Cutout, NACA TN 3488, August 1955.

58. Johannesen, N. H., "Experiments on Supersonic Flow Past Bodies of Revolution with Annular Gaps of Rectangular Section", Philosophical Magazine (7), Vol. 46, No. 372: 31-39, January 1955.

59. Nicoll, K. M., "A Study of Laminar Hypersonic Cavity Flows", AIAA Journal, Vol. 2, No. 3: 1535-1541, September 1964.

60. McDearmon, R. W., Investigation of the Flow in a Rectangular Cavity in a Flat Plate at a Mach Number of 3.85, NASA TN D-523, September 1960.

61. Chapman, D. R., A Theoretical Analysis of Heat Transfer in Regions of Separated Flow, NACA TN-3792, 1956.

62. Larson, H. K., "Heat Transfer in Separated Flows", Journal of the Aerospace Sciences, Vol. 26, No. 11: 731-738, November 1959.

LIST OF REFERENCES (Continued)

63. Chapman, D. R., and M. W. Rubesin, "Temperature and Velocity Profiles in the Compressible Laminar Boundary Layer with Arbitrary Distribution of Surface Temperature", Journal of the Aeronautical Sciences, Vol. 16, No. 10: 547-565, September 1949.

64. Centolanzi, F. J., Heat Transfer to Blunt Conical Bodies Having Cavities to Promote Separation, NASA TND-1975, July 1963.

65. Rhudy, R. P., and J. D. Magnan, Investigation of Heat Transfer and Pressure Distributions in Regions of Surface Distortion on a Flat Plate (U), Arnold Engineering Development Center (AEDC) TDR-62-238, January 1963. CONFIDENTIAL.

66. Bertram, M. H., and M. M. Wiggs, Effects of Surface Distortions on the Heat Transfer to a Wing at Hypersonic Speeds, Institute of the Aerospace Sciences, IAS Paper No. 62-127, IAS National Summer Meeting at Los Angeles, California, June 19-22, 1962.

67. Bertram, M. H., and W. V. Feller, A Simple Method for Determining Heat Transfer, Skin Friction, and Boundary-Layer Thickness for Hypersonic Laminar Boundary-Layer Flows in a Pressure Gradient, NASA Memo 5-24-59L, June 1959.

68. Becker, J. V., and F. F. Korycinski, Heat Transfer and Pressure Distribution at a Mach Number of 6.8 on Bodies with Conical Flares and Extensive Flow Separation, NASA TND-1260, April 1962.

69. Van Driest, E. R., "The Problem of Aerodynamic Heating", Aeronautical Engineering Review: 26-41, October 1956.

70. Ferguson, H., and J. W. Schaefer, Heat Transfer and Pressure Distribution on Cone-Cylinder-Flare Configuration with Boundary-Layer Separation, NASA TND-1436, October 1962.

71. Reshotko, E., Simplified Method for Estimating Compressible Laminar Heat Transfer with Pressure Gradient, NACA TN-3888, 1956.

72. Reshotko, E., and M. Tucker, Approximate Calculation of the Compressible Turbulent Boundary Layer with Heat Transfer and Arbitrary Pressure Gradient, NACA TN-4154, 1957.

73. Sayano, S., H. P. Bausch, and R. J. Donnelly, Aerodynamic Heating Due to Shock Impingement on a Flat Plate, Douglas Aircraft Company Report No. SM-41331, August 16, 1962.

74. Sayano, S., and H. P. Bausch, Aerodynamic Heating Due to Shock Impingement on a Cylinder, Douglas Aircraft Company Report No. SM-41420, August 16, 1962.

LIST OF REFERENCES (Continued)

75. Levin, V., and T. J. Fabish, Thermal Effects of a Shockwave Turbulent Boundary Layer Interaction at Mach Numbers 3 and 5, North American Aviation Report No. NA624-795, November 12, 1962.

76. Miller, D. S., R. Hijman, E. Redeker, W. C. Janssen, and C. R. Mullen, "A Study of Shock Impingements on Boundary Layers at Mach 16", Proceedings of the 1962 Heat Transfer and Fluid Mechanics Institute, Stanford University Press, Stanford, California: 255-278, 1962.

77. Strack, S. L., Heat Transfer at Reattachment of a Turbulent Boundary Layer, Boeing Airplane Company, Document No. D2-22430, April 30, 1965.

78. Maysmith, A., "Measurements of Heat Transfer in Bubbles of Separated Flow in Supersonic Air Streams", International Developments in Heat Transfer, p. 378, 1961.

79. Hicken, J., Free-Flight Measurements of Pressure and Heat Transfer in Regions of Separated and Reattached Flow at Mach Numbers up to 4, British Ministry of Aviation Report. (Unpublished)